OULU 2018
D 1448

ACTA UNIVERSITATIS OULUENSIS

Heli Härönen

COLLAGEN XIII AS A NEUROMUSCULAR SYNAPSE ORGANIZER

ROLES OF COLLAGEN XIII AND ITS TRANSMEMBRANE FORM, AND EFFECTS OF SHEDDING AND OVEREXPRESSION IN THE NEUROMUSCULAR SYSTEM IN MOUSE MODELS

UNIVERSITY OF OULU GRADUATE SCHOOL;
UNIVERSITY OF OULU,
FACULTY OF BIOCHEMISTRY AND MOLECULAR MEDICINE;
BIOCENTER OULU;
CENTER FOR CELL MATRIX RESEARCH

ACTA UNIVERSITATIS OULUENSIS
D Medica 1448

HELI HÄRÖNEN

COLLAGEN XIII AS A NEUROMUSCULAR SYNAPSE ORGANIZER

Roles of collagen XIII and its transmembrane form, and effects of shedding and overexpression in the neuromuscular system in mouse models

Academic dissertation to be presented with the assent of the Doctoral Training Committee of Health and Biosciences of the University of Oulu for public defence in Auditorium F101 of the Faculty of Biochemistry and Molecular Medicine (Aapistie 7), on 12 January 2018, at 1 p.m.

UNIVERSITY OF OULU, OULU 2018

Acta Univ. Oul. D 1448, 2018

Supervised by
Professor Taina Pihlajaniemi
Doctor Anne Heikkinen

Reviewed by
Associate Professor Hiroshi Nishimune
Assistant Professor Tadafumi Hashimoto

Opponent
Docent Juha Hulmi

ISBN 978-952-62-1800-7 (Paperback)
ISBN 978-952-62-1801-4 (PDF)

ISSN 0355-3221 (Printed)
ISSN 1796-2234 (Online)

Cover Design
Raimo Ahonen

JUVENES PRINT
TAMPERE 2018

Härönen, Heli, Collagen XIII as a neuromuscular synapse organizer. Roles of collagen XIII and its transmembrane form, and effects of shedding and overexpression in the neuromuscular system in mouse models

University of Oulu Graduate School; University of Oulu, Faculty of Biochemistry and Molecular Medicine; Biocenter Oulu; Center for Cell Matrix Research

Acta Univ. Oul. D 1448, 2018

University of Oulu, P.O. Box 8000, FI-90014 University of Oulu, Finland

Abstract

Collagen XIII is a transmembrane protein consisting of intracellular, transmembrane and extracellular domains. The latter can be cleaved by proteases of the furin family at the plasma membrane and in the trans-Golgi network. Both the transmembrane and shed collagen XIII are expressed at the neuromuscular junctions of mice and humans. Such motor synapse passes the contraction signal from the central nervous system to the muscles and brings about all voluntary movements. Loss of both forms of collagen XIII in mice and loss-of-function mutations in the *COL13A1* gene in humans leads to congenital myasthenic syndrome characterized by decreased neuromuscular transmission and muscle weakness.

To study the roles of the two collagen XIII forms, a novel mouse line was engineered to harbor only the transmembrane collagen XIII by mutating the furin cleavage site. Transmembrane collagen XIII was discovered to be sufficient to prevent adhesion defects, Schwann cell invagination, the ineffective vesicle accumulation and dispersion of both acetylcholinesterase and acetylcholine receptors, phenotypes seen in the complete lack of collagen XIII. On the other hand, lack of shedding led to acetylcholine receptor fragmentation, aberrantly increased neurotransmission and presynaptic complexity. Remarkably, *in vivo* and *in vitro* interaction of collagen XIII and acetylcholinesterase-anchoring ColQ was detected. Furthermore, muscle and neuromuscular junction phenotype in the lack of both forms of collagen XIII closely resembled those in the human patients harboring mutations in the *COL13A1* gene and these mice were validated as a good model for studying the human disease. Misexpression of collagen XIII was studied with mice exhibiting transgenic overexpression of the protein. Overexpression of collagen XIII was detected to be mostly extrasynaptic in the muscles of such mice. Exogenous collagen XIII was found at the myotendinous junctions, tenocytes and fibroblast-like cells, in addition to some localization in the near vicinity of the neuromuscular junctions. Collagen XIII expression was found, for the most part, to be normal at the neuromuscular junctions, although some were devoid of collagen XIII. The neuromuscular junction phenotype resembled in many ways the findings made in the lack of collagen XIII. Furthermore, acetylcholine receptor and nerve pattern was discovered to be widened.

Keywords: acetylcholine receptor, acetylcholinesterase, collagen XIII, ColQ, congenital myasthenic syndrome, fibroblast, myotendinous junction, neuromuscular junction

Härönen, Heli, Kollageeni XIII hermolihasliitoksen komponenttina. Kollageeni XIII:n solukalvo- ja soluvälitilamuodon roolit sekä yli-ilmentymisen vaikutukset hermolihasliitoksessa hiirimalleilla

Oulun yliopiston tutkijakoulu; Oulun yliopisto, Biokemian ja molekyylilääketieteen tiedekunta; Biocenter Oulu; Center for Cell Matrix Research

Acta Univ. Oul. D 1448, 2018
Oulun yliopisto, PL 8000, 90014 Oulun yliopisto

Tiivistelmä

Kollageeni XIII on solukalvoproteiini, jonka rakenne koostuu solunsisäisestä, solukalvon läpäisevästä ja solun ulkoisesta osasta, joka pystytään entsymaattisesti irrottamaan solukalvoilta. Täten se esiintyy kahdessa eri muodossaan; solukalvomuotoisena ja soluvälitilan lihasperäisenä proteiinina hiirten ja ihmisten hermolihasliitoksessa. Tässä motorisessa synapsissa keskushermostosta peräisin oleva lihaksen supistumiskäsky välittyy lihakseen ja aikaan saa tahdonalaiset liikkeet. Molempien kollageeni XIII:n muotojen puute hiirillä ja *COL13A1* geenin mutaatiot ihmisillä johtavat synnynnäiseen myasteeniseen oireyhtymään, jossa heikentynyt hermolihasliitoksen toiminta johtaa lihasheikkouteen.

Kollageeni XIII:n eri muotojen hermolihasliitosvaikutusten selvittämiseksi luotiin hiirilinja, jossa kollageeni XIII ilmenee geneettisen manipulaation seurauksena ainoastaan solukalvomuodossaan. Tutkimukset osoittivat solukalvomuotoisen kollageeni XIII:n tarvittavan hermon ja lihaksen kiinnittymiseen toisiinsa, hermovälittäjäainerakkuloiden ankkuroimiseen hermopäätteeseen, estämään Schwannin solujen tunkeutuminen synapsirakoon, asetyylikoliiniesteraasin sitomiseen ja asetyylikoliinireseptorien vakaantumiseen. Soluvälitilan kollageeni XIII:n puutos puolestaan johti lihaksen puolen liitoksen pirstaloitumiseen sekä hermopäätteiden liialliseen kasvuun ja aktiivisuuteen. Kollageeni XIII todettiin sitoutuvan asetyylikoliiniesteraasia hermolihasliitokseen ankkuroivan kollageeni Q:n kanssa. Lisäksi molempien kollageeni XIII:n muotojen suhteen poistogeenisten hiirten hermolihas- ja lihaslöydökset todettiin muistuttavan *COL13A1* geenin mutaatioista kärsivien ihmisten vastaavia löydöksiä todistaen nämä hiiret hyväksi tautimalliksi tulevaisuuden hoitomuotojen suunnitteluun.

Kollageeni XIII:n ylimäärän vaikutusta hermolihasliitokseen ja lihaskudokseen tutkittiin kollageeni XIII:a ylenmäärin ilmentävillä hiirillä. Kollageeni XIII todettiin ilmentyvän ylenmäärin lihaksessa fibroblastinkaltaisissa soluissa, lihasjänneliitoksessa ja hermolihasliitoksen lähettyvillä, mutta ei hermolihasliitoksessa. Osa hermolihasliitoksista näissä hiirissä ilmensi jopa vähemmän kollageeni XIII:a kuin normaalisti. Asetyylikoliinireseptorien ja hermojen valtaama alue todettiin leventyneeksi ja hermolihasliitoslöydökset muistuttivat molempien kollageeni XIII:n muotojen suhteen poistogeenisien hiirten löydöksiä.

Asiasanat: asetyylikoliiniesteraasi, asetyylikoliinireseptori, fibroblasti, hermolihasliitos, kollageeni Q, kollageeni XIII, lihasheikkous, lihasjänneliitos, synnynnäinen myasteeninen oireyhtymä

"Life requires movement"
-Aristotle, 4th century BC

Acknowledgements

This research was carried out in the Faculty of Biochemistry and Molecular Medicine, formerly the Institute of Biomedicine, Department of Medical Biochemistry and Molecular Biology, Faculty of Medicine, University of Oulu during the years 2009-2018.

I wish to express my sincere gratitude to my supervisor, Professor Taina Pihlajaniemi, for the privilege to work in her research group among interesting research projects and for having her as my principal supervisor. I admire her everlasting passion for science and expertise in the vast field of extracellular matrix research. I am also forever grateful to my other supervisor, Dr. Anne Heikkinen, for the excellent and continuous guidance and friendship throughout these years. Without her warm and patient way of introducing me to the world of science and our inspiring neuromuscular brainstorming, this thesis would have remained just a distant dream.

I wish to thank Professor Emeritus Ilmo Hassinen, Professor Emeritus Kari Kivirikko, Professor Kalervo Hiltunen, Professor Johanna Myllyharju, Professor Peppi Karppinen, Professor Seppo Vainio and all the other Professors and group leaders in the Faculty and Biocenter Oulu for providing an excellent research infrastructure and encouraging atmosphere.

I would also like to thank the official reviewers of this thesis, Associate Professor Hiroshi Nishimune and Assistant Professor Tadafumi Hashimoto, for their valuable feedback on this thesis. John Braidwood is acknowledged for his careful language revision of the thesis manuscript. My follow-up group members, Dr. Lauri Eklund, Professor Juha Tuukkanen and MD, PhD. Mika Kallio are warmly thanked for their comments and advice on my work during these years.

All the co-authors and collaborators are acknowledged for their valuable work and contribution. Especially, I want to thank Dr. Hongmin Tu for her *in vitro* ColQ-binding studies, Docent Raija Sormunen and Dr. Ilkka Miinalainen for ultrastructural images, MD. Rashid Giniatullin and his group members for the electrophysiological analyses and Associate Professor Michael A. Fox for his valuable comments on the first original publication included in this thesis.

I am also very grateful to Sirkka Vilmi for her valuable efforts with the everyday technical laboratory work and all the help that she has been giving me throughout these years. I also want to thank Aila White, Maija Seppänen, Päivi Tuomaala and Jaana Peters for their advice and help in the lab as well as all the personnel of the Biocenter Oulu Electron Microscopy Core Facility and the

Laboratory Animal Centre of the University of Oulu. In addition, Auli Kinnunen, Veli-Pekka Ronkainen, Sirpa Salo, Pertti Vuokila, Risto Helminen and Antti Viklund are acknowledged for all their help with various practical matters throughout these years.

Furthermore, I wish to thank all my current and former colleagues in the Faculty of Biochemistry and Molecular Medicine. I really have enjoyed working with you all. I owe special thanks to Dr. Jarkko Koivunen, Docent Ritva Heljasvaara and Dr. Joni Mäki for the great and joyful scientific and teaching related discussions. I also acknowledge my peer students who already have or are about to finish their enormous and fascinating task among collagen research, Ann-Marie Auvinen, Antti Kemppainen and Zarin Zainul for their friendship and support during these years.

I want to thank my family for their endless support, motivation and optimism throughout my life. It would be hard to imagine my world and achievements without their love and care. I also thank my dearest friend and colleague, Hanna-Riikka Teppo, for believing me and pushing me forward in studies, research and life. Finally, I wish to express my gratitude to my companion Jussi Airaksinen for his love, support and patience.

This work was supported by grants from the Sigrid Juselius Foundation, The Faculty of Biochemistry and Molecular Medicine and The Finnish-Norwegian Medical Foundation.

Oulu, December 2017 Heli Härönen

Abbreviations

ACh	acetylcholine
AChE	acetylcholine esterase
AChR	acetylcholine receptor
AChV	acetylcholine vesicle
AZ	active zone
BM	basement membrane
BDNF	brain-derived neurotrophic factor
BChE	butyryl cholinesterase
C. elegans	*Caenorhabditis elegans*
CaMKII	Ca^{2+}/Calmodulin-dependent protein kinase II
CAZ	cytoskeletal matrix of the active zone
ChAT	choline acetyltransferase
CLAC	collagen ‐ like Alzheimer amyloid plaque component/ectodomain of collagen XXV
CLAC-P	collagen ‐ like Alzheimer amyloid plaque component precursor/transmembrane collagen XXV
CMAP	compound muscle action potential
COL	collagenous domain
ColQ	collagen Q
Col13a1$^{+/+}$	wild-type mice expressing endogenous collagen XIII protein
Col13a1$^{tm/tm}$	mutated mice expressing transmembrane collagen XIII protein only
Col13a1$^{-/-}$	knock-out mice lacking collagen XIII protein
Col13a1^{oe}	transgenic mice overexpressing collagen XIII protein
CMS	congenital myasthenic syndrome
Cdk5	mouse cyclin-dependent kinase 5
DGC	dystrophin-associated glycoprotein complex
DHPR	dihydropyridine receptor
Dok7	downstream-of-tyrosine-kinase-7
E	embryonic day
ECM	extracellular matrix
EDL	extensor digitorum longus
EMG	electromyography
EPC	endplate current
EPP	evoked endplate potential
ER	endoplasmic reticulum

FACIT	fibril-associated collagen with interrupted triple helices
FGF	fibroblast growth factor
FGFR2	fibroblast growth factor receptor 2
FGFR2b	fibroblast growth factor receptor 2 splice variant b
GAG	glycosaminoglycan
GDNF	glial-cell derived neurotrophic factor
HA	hemagglutinin
H&E	hematoxylin and eosin
HSPG	heparan sulphate proteoglycan
IF	intermediate filament
LAIR-1	leukocyte-associated immunoglobulin-like receptor-1
LEMS	Lambert-Eaton myasthenic syndrome
LDLR	low density lipoprotein receptor
LRP4	low density lipoprotein receptor-related protein 4
MEF	mouse embryonal fibroblast
MEPP	miniature enplate potential
MACITs	membrane associated collagens with interrupted triple helices
MARCO	macrophage receptor with collagenous structure
MG	myasthenia gravis
multiplexin	Multiple Triple Helix domains with Interruptions
MyHC	Myosin heavy chain
MLC	Myosin light chain
MTJ	myotendinous junction
Myh3	gene for mouse Myosin heavy chain 3
Myh8	gene for mouse Myosin heavy chain 8
Na_v	sodium channel
NC	non-collagenous domain
NCBI	National Center for Biotechnology Information
NSCLC	non-small-cell lung cancer
P	postnatal day
PCR	polymerase chain reaction
PG	proteoglycan
RT-qPCR	real-time quantitative PCR
SR	sarcoplasmic reticulum
ShC	Schwann cell
SCLC	small cell lung carcinoma
SNAP25B	synaptosomal-associated protein 25-B

SNARE	soluble *N*-ethylmaleimide-sensitive factor attachment protein receptor
SIRP-α	signal regulatory protein α
SPF	specific pathogen free
SV	synaptic vesicle
Syt-2	synaptotagmin 2
TA	tibialis anterior
TAO	thyroid-associated ophthalmopathy
TEM	transmission electron microscopy
tShC	terminal Schwann cell
VAChT	vesicular acetylcholine transporter
VDCC	voltage-depended calcium channel
WES	whole-exome sequencing

Original publications

This thesis is based on the following publications, which are referred to throughout the text by their Roman numerals:

I Härönen H, Zainul Z, Tu H, Naumenko N, Sormunen R, Miinalainen I, Shakirzyanova A, Oikarainen T, Abdullin A, Martin P, Santoleri S, Koistinaho J, Silman I, Giniatullin R, Fox M. A, Heikkinen A, Pihlajaniemi T (2017) Collagen XIII secures pre- and postsynaptic integrity of the neuromuscular system. Hum. Mol. Gen. 1;26(11):2076-2090

II Härönen H, Zainul Z, Naumenko N, Sormunen R, Miinalainen I, Shakirzyanova A, Santoleri S, Giniatullin R, Pihlajaniemi T, Heikkinen A. Correct expression and localization of collagen XIII is crucial for the normal formation and function of the neuromuscular system. Manuscript.

Contents

1 Introduction

Synaptic connections between nerve cells and other cell types enable fast and reliable transmission and also respond well to internal and external stimuli. The neuromuscular junction (NMJ) is a synapse between the skeletal muscle fiber and a Schwann cell (ShC)-wrapped motoneuron passing the contraction signal from the central nervous system (CNS) to muscles. At the NMJ, a presynaptic electrical signal elicits exocytosis of the neurotransmitter acetylcholine (ACh) from the presynaptic ACh vesicles (AChVs) into the synaptic cleft thereafter rapidly diffusing through the basal lamina (BL) and the extracellular matrix (ECM) of the synaptic cleft, in order to bind its receptors, AChRs, and to trigger a cascade of molecular events to contract muscles. The signaling is terminated by ACh esterase (AChE) that hydrolyses ACh at the synaptic cleft. This peripheral synapse controls all voluntary muscle movements as well as, for example, breathing. Defective neurotransmission can vary from mild muscle weakness to lethality and many presynaptic, synaptic and postsynaptic molecules secure correct assembly, maturation and function of the NMJ.

Collagen XIII has recently been identified as one important component of the NMJ. It is a muscle-derived non-fibrillar type II transmembrane collagen harboring an N-terminal intracellular domain, a hydrophobic transmembrane domain and a large (150 nm long) extracellular C-terminal domain. The ectodomain of collagen XIII can be cleaved from the plasma membrane and in the trans-Golgi network by the proteinases of the furin family to become a soluble ECM protein. At the NMJ collagen XIII is synaptically-localized on the muscle fiber sarcolemma and in the adjacent BL. Work with collagen XIII-deficient mice and a recent discovery of human mutations in the *COL13A1* gene leading to congenital myasthenic syndrome type 19 (CMS19) have highlighted the role of collagen XIII at the NMJs of mice and humans. Mouse studies indicated delayed postsynaptic maturation, impaired acetylcholine vesicle (AChV) accumulation, compromised adhesion of nerve and muscle and, most importantly, decreased function of the NMJ due to the lack of collagen XIII. Furthermore, CMS19 patients suffered from muscle weakness starting soon after birth due to impaired function of the NMJ. However, the mechanism behind these alterations remained largely enigmatic and the intriguing question about possible distinct roles of the transmembrane and shed forms of collagen XIII in this process thus remains unanswered. Moreover, transgenic overexpression of collagen XIII in mice has been shown to result in excess bone

formation, while precise information on the collagen XIII expression and its effects on the NMJ and muscles of these mice has remained obscure.

Therefore, the first goal of this thesis project was to examine potential differential roles of the transmembrane and shed collagen XIII in the maturation, assembly and function of the NMJ by utilizing a novel genetically engineered mouse line exhibiting the transmembrane form of collagen XIII only and then to compare the findings with the total loss of collagen XIII. As a second objective, following the report of *COL13A1* mutations in CMS19, the murine neuromuscular phenotype of total loss of collagen XIII was set to compare with findings in the human disease and simultaneously to deepen knowledge about the effects of total collagen XIII loss in the knock-out mouse model. Furthermore, the expression profile and effects of the transgenic overexpression of collagen XIII at the neuromuscular system was elucidated. Altogether, these studies suggested important and diverse functions for the shed and transmembrane collagen XIII at the NMJ accentuating the importance of correct collagen XIII expression and localization at the neuromuscular tissues.

2 Review of literature

2.1 Synaptic connections in the nervous system

The nervous system is a complex system of cells, tissues and organs that sense and relay information about internal and external stimuli rapidly and regulates the body`s responses (Watanabe *et al.* 2009). The evolution of the complex nervous system in modern bilaterians began ~600 million years ago, from the gelatinous *Ctenophora* and *Cnidaria* that are widely regarded as the first class of organisms in the animal evolution harboring a nervous system (Emes & Grant 2012, Watanabe *et al.* 2009). In vertebrates, the nervous system is divided anatomically into two main parts; the CNS and the peripheral nervous system (PNS). The CNS is formed by the brain and the spinal cord which are connected to other parts of the body via nerves that belong to the PNS. The signal transduction in the nervous system is based on neurons and their connections, namely synapses, to other neurons and other cells, for example muscle fibers (Dale *et al.* 1936, Emes & Grant 2012, Haucke *et al.* 2011, Watanabe *et al.* 2009). Without synapses sensing and responding to the environment and innate signals, voluntary muscle movements, cognition and memory would be impossible. In the synapses signals can be transferred from a neuron to its target cell via two different mechanisms depending on the synapse type (Connors & Long 2004). Most commonly, neurons transmit their signals chemically to other neurons or to other cell types via neurotransmitters (Connors & Long 2004, Emes & Grant 2012). In addition, neuron-neuronsignalling can be mediated electrically through specialized junctions that allow ionic current to flow directly from one neuron to another (Connors & Long 2004).

Chemical synapses are highly specialized sites of cell-cell adhesion constituting of pre- and postsynaptic membrane specializations with synaptic clefts in- between (Lu & Lichtman 2007, Sanes & Lichtman 2001). Synapses have been of significant interest to many scientists for more than a century; important ideas about synaptic anatomy, development and physiology have been initially tested out at the NMJ - a chemical cholinergic synapse between a motor neuron and a muscle fiber. Compared to CNS synapses, the vertebrate neuromuscular synapses are about 1000 times larger, simpler in patterning (one muscle fiber is innervated by one motor neuron) and easier to access, thus they are often chosen for studies on synaptogenesis and physiology of synapses (Desaki & Uehara 1981, Sanes & Lichtman 2001, Singhal & Martin 2011). Moreover, studies of the synapse that

controls all voluntary muscle movements and breathing are important in their own right (Singhal & Martin 2011).

2.1.1 The neuromuscular junction

The mature, adult vertebrate NMJ is a tripartite system consisting of three different cell types; one motoneuron, one muscle fiber and ShCs that enclose preterminal structures (Sanes & Lichtman 1999). In addition, recent studies have also revealed novel, poorly characterized fibroblast-like cells, called kranocytes, forming a loose cover over the NMJ (Court *et al.* 2008, Tintignac *et al.* 2015). The vertebrate NMJ is a peripheral synapse belonging to the PNS and it passes the contraction signal from the CNS to the muscle. Its proper formation, maturation, stability and function are crucial for processes vital for life, such as breathing and muscle movements. A repertoire of presynaptic, synaptic and postsynaptic molecules controls this synaptic machinery and it is worth noting, that all synaptic parties contain high concentrations of organelles and molecules found at low concentrations extrasynaptically (Sanes & Lichtman 1999). This synaptic assembly enables the delicate and precise cross-talk between the CNS and muscles and when this cross talk is lost or compromised the outcome can vary from lethality to mild muscle weakness (Wu *et al.* 2010). A schematic structure of the musculoskeletal and neuromuscular system is presented in Fig. 1A-B.

Structure of the cholinergic motor synapse: presynaptic motor nerve

Skeletal muscles of mammals are innervated by axons originating from spinal motor neuron cell bodies that are themselves innervated by the primary motor cortex motoneurons, and lie in the ventral horn of the spinal cord (Singhal & Martin 2011). In the mammalian musculoskeletal system each muscle fiber is innervated by one motoneuron and the site of innervation most commonly lies in the middle of the muscle fiber length. In contrast, one motor neuron can innervate a group of muscle fibers by branching and this complex is called a motor unit. Axons of motor neurons are myelinated by ShCs although at the NMJ axon terminals are covered with a few un-myelinating ShCs called terminal (tShC) or perisynaptic ShCs (Fig. 1B) (Sanes & Lichtman 1999). The axon terminal forms multiple microbranches over the muscle fiber surface covering the postsynaptic structures. Almost all proteins and organelles important for the axon and the synaptic terminals are synthetized in the motor neuron soma in the spinal cord and thereafter transported

in an anterograde manner in the axon to the synaptic terminals via a variety of membranous vesicles and protein complexes (Hirokawa *et al.* 2010). These cargoes are transported along the axon cytoskeleton by cytoskeleton motors comprising Myosin, kinesin and cytoplasmic dynein (Xiao *et al.* 2016). The neuronal cytoskeleton is composed of actin microfilaments, intermediate filaments (IFs) and microtubules (Perrot & Eyer 2009). Neurofilaments are the most common IFs and cytoskeletal components of large myelinated axons, where they play a role, for example, in controlling the axonal caliber (Perrot & Eyer 2009).

The fundamental function of a nerve terminal is to release neurotransmitters that bind to the postsynaptic receptors (Sanes & Lichtman 1999). For that purpose, motoneuron terminals are filled with ~50 nm-diameter synaptic vesicles (SVs) containing the neurotransmitter, namely ACh in the vertebrate NMJs. Axon terminals also contain numerous mitochondria providing the energy for transmitter release and re-synthesis. Organization of organelles in the presynaptic terminal is polarized as most of the mitochondria are clustered in the half-terminal beneath the tShCs and most of the vesicles lie in the half-terminal facing the muscle fiber (Fig. 1B). Furthermore, SVs are organized into different vesicle pools including the readily-releasable pool (RRP), the recycling pool and the reserve pool (Haucke *et al.* 2011). Vesicles of RRP are available immediately upon stimulation and release their contents from the specialized preterminal membranes called active zones, or AZs, in response to action potentials that run down the axons (from the motoneuron cell bodies in the spinal cord). ACh is released to the synaptic cleft, thereafter diffusing rapidly towards the postsynaptic endplate to activate AChRs that in turn trigger a cascade leading to muscle fiber contraction (Sanes & Lichtman 1999).

Structure of the cholinergic motor synapse: postsynaptic muscle fiber

Skeletal, or striated, muscle is one of three muscle types in mammals along with smooth, or non-striated, muscle and cardiac muscle; the former is the only muscle type under voluntary control and harboring the NMJ. Skeletal muscles are composed of multinucleated cylinder-like elongated cells called muscle fibers that enclose striated appearance histologically (Clark *et al.* 2002, Schiaffino & Reggiani 2011).

Nuclei of the adult vertebrate skeletal muscle fibers are located on the periphery and near the plasma membrane of a muscle cell, the sarcolemma (Kierszenbaum & Tres 2015). The cytoplasm of the muscle cell, namely sarcoplasm, is filled with long striated rod-like myofibrils assembled side by side

as well as having cell organelles, for example mitochondria, between them. Myofibrils are surrounded by membranous sacs or channels of the endoplasmic reticulum (ER), which is also called the sarcoplasmic reticulum (SR). These contain high concentrations of Ca^{2+}, which is important for the contractile activity of muscle fibers. The SR is connected with the sarcolemma via finger-like invaginations called T-tubules that run down from the muscle plasma membrane. T-tubules spread the action potential triggered by the activation of the NMJ that in turn initiates the muscle contracting Ca^{2+} release from the SR to the sarcoplasm (Kierszenbaum & Tres 2015).

The striated structure of myofibrils and muscle fibers results from thecytoskeletal filament arrangement in the myofibrils, where four filament systems form sarcomeres, the basic contractile units of muscle fibers (Fig. 1B). Sarcomeres are composed of actin-containing thin filaments, Myosin-containing thick filaments, and titin and nebulin filaments. These filaments form alternating, microscopically seen light and dark bands called I- and A-bands, respectively. The Z-discs define the borders of the sarcomere and lie in the middle of I-bands anchoring actin, titin and nebulin filaments. The A-band is located between two Z-discs and I-bands, and contains Myosin filaments and superimposed actin, titin and nebulin heads. Myosin heads have ATPase activity and upon Ca^{2+} stimulation Myosin heads move actin filaments over the thick filaments and fundamentally produce muscle contraction (Clark *et al.* 2002).

Myosin molecules are composed of two Myosin heavy chains (MyHCs), two essential myosin light chains (MLCs), and two regulatory MLCs (Schiaffino *et al.* 2015). Different isoforms of MyHCs and MLCs exist encoded by distinct genes with varying expression depending on the muscle fiber type and developmental stage (Schiaffino *et al.* 2015). For example, embryonic and neonatal (or perinatal) MyHC isoforms coded by *MYH3* and *MYH8*, respectively, are abundant in the initial stages of muscle development and during muscle regeneration, but downregulated after birth (Schiaffino *et al.* 2015). Furthermore, major muscle fiber types classified by their metabolic (oxidative/glycolytic) and functional (slow/fast-twitch) properties can be further characterized by the MyHC composition (Pette & Staron 2000, Schiaffino & Reggiani 2011). Pure slow-twitch fatigue-resistant oxidative fibers (type 1) contain MyHC-β/slow isoform, fast-twitch fatigue-resistant oxidative/glycolytic fibers (type 2A) contain MyHC-2A isoform and fast-twitch fast-fatigable glycolytic fibers (type 2B) contain MyHC-2B (Schiaffino & Reggiani 2011). Moreover, type 2X fibers containing MyHC-2X exist with twitch properties similar to the fast fibers and resistance to fatigue intermediate to 2A and

2B fibers (Schiaffino & Reggiani 2011). In addition to these four major muscle fiber types, hybrid fibers of 1/2A, 2A/2X and 2X/2B exist (Schiaffino & Reggiani 2011). With this heterogeneity, muscles are capable of answering to their various different functional demands that can be categorized into three main types: postural joint stabilization, long-lasting and repetitive activities and fast powerful actions (Schiaffino & Reggiani 2011). Notably, in a motor unit one motor neuron innervates muscle fibers with similar structural and functional properties (Schiaffino & Reggiani 2011).

Postsynaptically at the NMJ, under the presynaptic nerve terminal, the sarcolemma sinks to form a gutter called the primary fold that is further ruffled into secondary junctional folds, and opens directly opposite to the AZs (Kummer *et al.* 2006, Sanes & Lichtman 1999, Wu *et al.* 2010). The molecular architecture of the synaptic sarcolemma varies between the crests and bottoms of the junctional folds and contains high concentrations of AChRs alongside other signaling molecules compared to extrasynaptic portions of the muscle plasma membrane (Kummer *et al.* 2006, Sanes & Lichtman 1999). AChRs are clustered at the crests of junctional folds in close proximity to the ACh-releasing sites, AZs. Other membrane and membrane-associated proteins such as muscle-specific kinase (MuSK), low density lipoprotein receptor-related protein 4 (LRP4), rapsyn, utrophin, and α-dystrobrevin-1 are colocalized with AChRs at the tops of folds, while the depths of the folds are concentrated with Na^{2+} channels, ankyrin, α-dystrobrevin-2, and dystrophin (Sanes & Lichtman 1999, Shi *et al.* 2012). Collagen XIII is one of the transmembrane proteins of postsynaptic sarcolemma that can also become a synaptic ECM component by its ectodomain shedding (Latvanlehto *et al.* 2010).

Structure of the cholinergic motor synapse: synaptic cleft and the basement membrane

Between the motoneuron terminal and the muscle lies a synaptic cleft that is approximately 50-80 nm wide and encloses many synaptic molecules and basement membrane (BM) components (Sanes & Lichtman 1999, Sanes 2003, Singhal & Martin 2011). The BM is a layer of specialized ECM material surrounding many cells including muscle fibers. The structure of the BM is assembled into internal and external layers including a felt-like BL linked directly to the plasma membrane of muscle fibers and a fibrillar reticular lamina (Sanes 2003). The fibrillar reticular lamina contains collagen fibrils embedded into a proteoglycan-rich ground substance and the BL consists of non-fibrillar collagens, non-collagenous

glycoproteins, and proteoglycans (Bonnans *et al.* 2014, Sanes 2003, Theocharis *et al.* 2016). When the BM meets the NMJ, only the BL passes between the nerve and muscle and further extends into junctional folds (Fig. 1B) (Sanes 2003).

The basic core of the muscle BL is formed by networks of collagen IV and laminins interconnected with entactin/nidogens (Sanes 2003). This scaffold binds other BL components and interacts with membrane-associated receptors, for example integrins and dystroglycans that further interact with the muscle fiber cytoskeleton. Ultrastructurally the synaptic and extrasynaptic BL appear uniform but still their molecular composition is quite distinct, since some BL components have different synaptic and extrasynaptic isoforms (laminins, collagen IV and nidogens) and some only exist at the synaptic BL (agrin, collagen XIII, ColQ, AChE, neuregulin) (Fox *et al.* 2007, Fox *et al.* 2008, Latvanlehto *et al.* 2010, Sanes 2003, Singhal & Martin 2011). The synaptic and extrasynaptic BL also share common components, for example heparan sulphate proteoglycan (HSPG), perlecan and fibronectin (Singhal & Martin 2011). This interconnected mesh of molecules gives mechanical support for muscles by stabilizing the muscle fiber sarcolemma (Sanes 2003). The BL components also serve to adhere nerve and muscle at the NMJ. The adhesive role of the BL is highlighted by the finding that nerve terminals start to detach from the synapse if the BL components are degraded by proteases. Furthermore, if muscle fibers are damaged without a nerve and BL degradation, nerve terminals remain at their original synaptic sites for months. Moreover, almost all synaptic BL components have been demonstrated to have roles in the NMJ biology and influence its development, maintenance, structure and/or function (Singhal & Martin 2011).

One synaptic molecule important for the function of the NMJ is AChE, an esterase hydrolyzing ACh and thereby terminating neurotransmission (Fig. 1B). AChE is localized within the synaptic BL by collagenous tail, Collagen Q (ColQ) (Karmouch *et al.* 2013, Plomp *et al.* 2015, Tintignac *et al.* 2015). ColQ is a muscle-driven ECM component expressed at the NMJs and interestingly also in lower amounts in extrasynaptic domains of slow muscle fibers (Sigoillot *et al.* 2010, Sigoillot *et al.* 2016). Major function of ColQ is to bind 1 to 3 AChE tetramers, and interaction with perlecan locates this complex to the NMJ and further binding of perlecan with dystroglycan assures this synaptic localization. Interestingly, ColQ has been shown to also bind to MuSK and via this interaction to further stabilizes AChE at the NMJ (Cartaud *et al.* 2004).

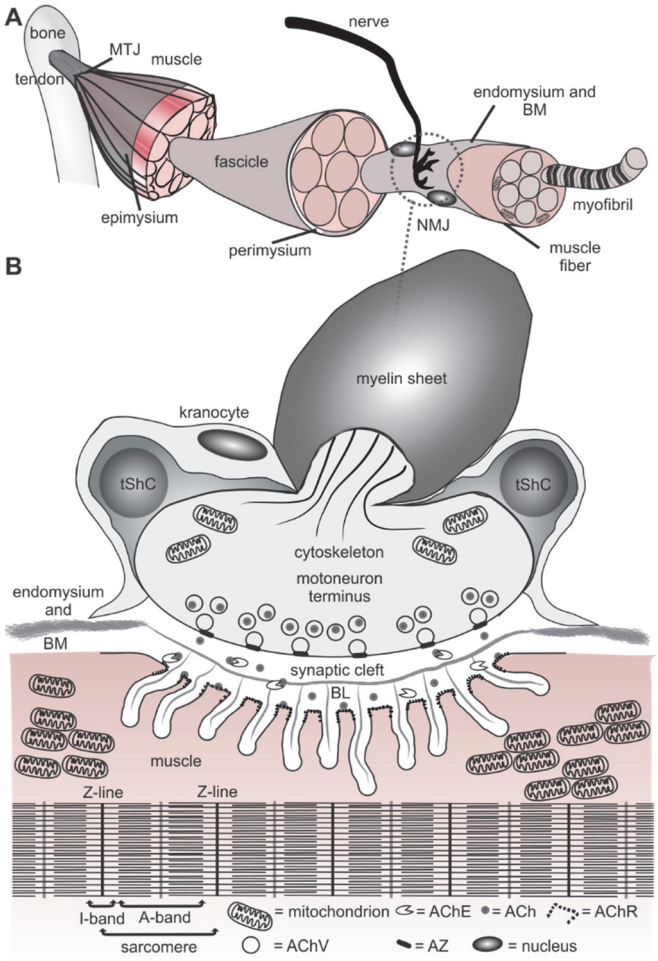

Fig. 1. The structure of the musculoskeletal and neuromuscular system. A) Muscles are attached to bones via tendons. The MTJ connects muscles to tendons. The epimysium surrounds the whole muscle, the perimysium the fascicles and the endomysium together with the BM the individual muscle fibers. The multinucleated myofibril-containing muscle fiber is innervated by one motoneuron. B) The NMJ with the tShC-wrapped motoneuron and muscle fiber. Preterminal structures are covered by a kranocyte and the axon is myelinated by ShCs. The motoneuron terminus encloses cytoskeletal structures, mitochondria, AChVs and AZs. The felt-like BL, released ACh molecules and AChE reside between the muscle and the motoneuron terminus. Postsynaptically the muscle sarcolemma forms primary and secondary junctional folds. AChRs are clustered on the top of secondary folds. Sarcomeres form the striated appearance of the muscle fiber.

2.2 The extracellular matrix and its components

The ECM is a non-cellular component present within all tissues and organs providing a three-dimensional scaffold and structural support for the cells (Bonnans *et al.* 2014, Daley *et al.* 2008, Frantz *et al.* 2010, Theocharis *et al.* 2016). In addition to the sheet-like, tightly compacted BMs in close contact with the cells, the ECM can be assembled into mesh-like scaffolds surrounding the cells called the interstitial connective tissue matrixes (Bonnans *et al.* 2014, Theocharis *et al.* 2016). These physical scaffolds between the cells generate the biochemical and mechanical properties of each organ, such as elasticity and compressive strength, that is extremely important in the contractile and force-transducing tissues such as muscles (Bonnans *et al.* 2014, Daley *et al.* 2008, Frantz *et al.* 2010, Singhal & Martin 2011, Theocharis *et al.* 2016). In addition to its structural roles, ECM also embeds and initiates cues that guide growth, survival, proliferation, migration, and differentiation. In other words, the ECM is not just a passive habitat for the cells, but rather an interactive platform essential for cell homeostasis, organ development and maintenance. Many diseases resulting from the defects in the ECM highlight the importance of the correct assembly and regulation of the ECM. For example, excessive ECM production due to chronic or severe injuries can lead to fibrosis, such as liver cirrhosis or myelofibrosis, and mutations in the genes coding for the ECM proteins can result in a wide range of tissue defects and even in embryonal lethality. Many matrix molecules participate in forming the ECM assembly and each organ has its unique ECM composition that can be secreted by the epithelial, immune and endothelial cells, and by fibroblasts. In addition, muscle fibers, ShCs and motor neurons can for example deposit ECM molecules (Bonnans *et al.* 2014, Daley *et al.* 2008, Frantz *et al.* 2010, Singhal & Martin 2011, Theocharis *et al.* 2016).

In mammals, the ECM of each organ is composed of about 300 proteins including 43 collagen subunits, 36 proteoglycans (PGs) and around 200 glycoproteins (Bonnans *et al.* 2014). Furthermore, composition of the ECM is under constant remodeling by many ECM-associated molecules including growth factors, cytokines and ECM-modifying enzymes (Bonnans *et al.* 2014, Daley *et al.* 2008, Frantz *et al.* 2010, Mouw *et al.* 2014, Theocharis *et al.* 2016). Collagens can be divided into fibril-forming and non-fibrillar forms and, for example, fibril-forming collagens provide tensile strength for the ECM. PGs with their glycosaminoglycan (GAG) side chains locate themselves among the collagen fibrils and bind water to provide hydration and resistance to the compression. Most

common GAGs are heparin, chondroitin, and dermatan and keratin sulphates. Glycoproteins include laminins, elastins, fibronectins, thrombospondins, tenascins and nidogens, and they harbor diverse roles in the ECM. Glycoproteins can for instance participate in the ECM assembly, mediate interaction between the ECM and the cells and sequester growth factors. The interstitial matrices surrounding the cells mainly consist of collagen I and fibronectin, whereas the BMs primarily comprise collagen type IV, laminins, nidogen 1 and 2, and perlecan as in the case of the muscle tissue already mentioned above (Sanes 2003, Theocharis *et al.* 2016). In addition to muscle fibers, the BM also surrounds fat and Schwann cells and coats the basal aspects of epithelial and endothelial cells (Theocharis *et al.* 2016, Yurchenco 2011).

The ECM of muscles can be anatomically subdivided into the BM surrounding the muscle fibers: endomysium, the fibrillar ECM surrounding the BM; perimysium: the ECM surrounding groups of muscle fibers, and epimysium: the ECM surrounding the whole muscle (Fig. 1A) (Gillies & Lieber 2011). Furthermore, muscles are connected to bones with ECM-rich structures, namely tendons (Gillies & Lieber 2011, Schweitzer *et al.* 2010, Subramanian & Schilling 2015). Tendons and muscle fibers are attached to each other through complex specialized regions of adhesion called myotendinous junctions (MTJs) (Charvet *et al.* 2012). At the MTJ muscle sarcolemma is ruffled into finger-like extensions and invaginations to increase the interface area and resistance to muscle contraction forces. At the muscle side of the junction, actin microfilaments extend from the last Z-discs of the sarcomere in to the finger-like protrusions of the sarcolemma and are bundled together by actin-binding proteins. Actin filaments are further linked via intracellular proteins to the sarcolemmal transmembrane proteins that are in turn connected to the ECM of the tendon. Main sarcolemmal transmembrane proteins include the dystrophin-associated glycoprotein complex (DGC) and α7β1 integrin complex, that both can bind to the BM component, laminin α2β1γ1. Furthermore, laminin α2β1γ1 connects with other ECM molecules of the tendon and forms a strong force-bearing junction (Charvet *et al.* 2012). Moreover, collagen XIII has been recognized as one MTJ component although its function at the MTJ remains unknown (Kvist *et al.* 2001, Latvanlehto *et al.* 2010).

2.2.1 Collagens

Collagens are the most abundant proteins in the ECM of mammals and comprise approximately 30% of their total protein mass (Ricard-Blum 2011). To date, 28

different collagens have been identified and collagens have been linked beyond their structural roles to be involved, for example, in cell adhesion, chemotaxis and migration (Gordon & Hahn 2010, Myllyharju & Kivirikko 2004). The roles of the collagens are further emphasized by the fact that many pathologic states exist due to mutations in the collagen genes affecting, for example, the integrity of cartilage and bone, muscle and skin (Myllyharju & Kivirikko 2004).

The aforesaid 28 distinct collagens can be divided into eight different subfamilies based on their supramolecular assemblies and other shared features highlighting the varying roles of collagens (Table 1.) (Myllyharju & Kivirikko 2004). There are seven fibril-forming collagens (types I, II, III, V, XI, XXIV and XXVII), nine fibril-associated collagens with interrupted triple helices (FACITs) (types IX, XII, XIV, XVI, XIX, XXII and XXVI), two collagens forming hexagonal networks (types VIII and X), the collagen type IV family, one collagen forming beaded filaments (type VI), one collagen forming anchoring fibrils (type VII), four membrane-associated collagens (types XIII, XVII, XXIII and XXV) and two multiplexins (Multiple Triple Helix domains with Interruptions), collagens that can be cleaved to generate antiangiogenic peptides (types XV and XVIII) (Gordon & Hahn 2010, Myllyharju & Kivirikko 2004). In addition, there are many other proteins that contain collagen-like structures, but are not, however, designated as collagens, for example Adiponectin, Ficolin 1, 2 and 3, and Macrophage receptor with collagenous sequences (MARCO) (Ricard-Blum 2011).

Albeit different supramolecular assemblies, all collagens bare a similar core structure that consists of three polypeptide chains, called α chains, and at least one stretch of repeating Gly-X-Y sequences (Myllyharju & Kivirikko 2004). These collagenous sequences (COL) are flanked by non-collagenous sequences (NCs) that often contain peptide modules found in other matrix molecules (Gordon & Hahn 2010). Within collagens, three identical (homotrimeric) or different (heterotrimeric) α chains are coiled into a triple helix to form a rope-like rod which thereafter form a quaternary structure typical for each subfamily (Myllyharju & Kivirikko 2004). Furthermore, the α chains undergo numerous posttranslational modifications intra- and extracellularly including hydroxylation, glycosylation and sulfatation of certain amino acid residues and the molecules are also subject to proteolytic cleavage (Myllyharju & Kivirikko 2004, Ricard-Blum 2011).

Table 1. Collagen superfamily.

Collagen subfamily	Collagen types
fibril-forming	I, II, III, V, XI, XXIV and XXVII
FACITs	IX, XII, XIV, XVI, XIX, XXII and XXVI
forming hexagonal networks	VIII and X
collagen type IV family	IV
forming beaded filaments	VI
forming anchoring fibrils	VII
membrane-associated	XIII, XVII, XXIII and XXV
multiplexin collagens	XV and XVIII

2.2.2 Membrane-associated collagens with interrupted triple-helices (MACITs)

In mammals there exist three distinct, albeit closely related, transmembrane collagens that form a subfamily of membrane-associated collagens with interrupted triple-helices (MACITs) (Tu *et al.* 2015). These non-fibrillar collagens, namely collagen XIII, collagen XXIII and collagen XXV, are type II transmembrane proteins that have an N-terminal intracellular domain, a hydrophobic transmembrane domain and a large extracellular C-terminal domain that can be cleaved by furin-type proprotein convertases (Fig. 2) (Banyard *et al.* 2003, Hägg *et al.* 1998, Hashimoto *et al.* 2002, Pihlajaniemi & Tamminen 1990, Väisänen *et al.* 2004, Veit *et al.* 2007). All MACITs have three collagenous (COL1-COL3) and four non-collagenous (NC1-NC4) domains. To highlight their structural similarity, the amino acid sequence of collagen XXIII, for example, shares a 54% and 56% identity to collagens XIII and XXV, respectively (Banyard *et al.* 2003). Although the previously mentioned homology exists primarily across the collagenous domains, interestingly, these three collagens have high identity across the 20-residue C-terminal domain, NC4 (Banyard *et al.* 2003). The structural similarities arise from the fact that distinct genes encoding MACIT collagens of jawed vertebrates are paralogues of a single MACIT gene in invertebrates (Tu *et al.* 2015). Based on their structure and ectodomain shedding, these collagens can have roles as cell surface receptors or as matrix components and soluble signaling molecules (Franzke *et al.* 2005). MACITs are widely distributed in tissues and all of them have been linked to various pathological conditions in humans and mice (Franzke *et al.* 2005, Logan *et al.* 2015).

MACIT collagens are homotrimeric proteins and the genes coding for α1(XIII), α1(XXIII), and α1(XXV) are located in *Homo sapiens* in the chromosome 10q22, 5q35 and 4q25, respectively and in *Mus musculus* in the chromosome 10B4, 11B1 + 2 and 3G3, respectively (Banyard *et al.* 2007, Hashimoto *et al.* 2002, Kvist *et al.* 1999, Shows *et al.* 1989). In the case of collagen XIII, the human gene (*COL13A1*) extends over 140 kb and the analogous mouse gene (*Col13a1*) covers 135 kb consisting of 42 exons in both species (Kvist *et al.* 1999). Furthermore, ten of the exons in the *COL13A1* and *Col13a1*, of which six are the same in humans and mice, undergo alternative splicing affecting the primary sequence of the COL1, NC2 and COL3 domains in both species and in addition the NC4 domain in humans (Hägg *et al.* 1998, Kvist *et al.* 1999, Peltonen *et al.* 1997, Pihlajaniemi & Tamminen 1990, Tikka *et al.* 1991). Limited published data exist about alternative splicing of collagen XXIII and XXV genes; however, in the NCBI (National Center for Biotechnology Information) non-redundant protein database (http://www.ncbi.nlm.nih.gov/protein/) many isoforms of these collagens can be found. Thus, alternative splicing has been suggested to be a common phenomenon in MACIT collagen genes due to alternative splicing detected in their common ancestor gene, *col-99*, in *Caenorhabditis elegans* (*C. elegans*). Due to alternative splicing, the longest human transcript of *COL13A1* would code for a 754-residue polypeptide and the shortest 596 residues (Heikkinen *et al.* 2012). Transcription of human genes for α1(XXIII) (*COL23A1*) and α1(XXV) (*COL25A1*) are predicted to code for 540- and 658-residue polypeptides, respectively (Banyard *et al.* 2003, Hashimoto *et al.* 2002).

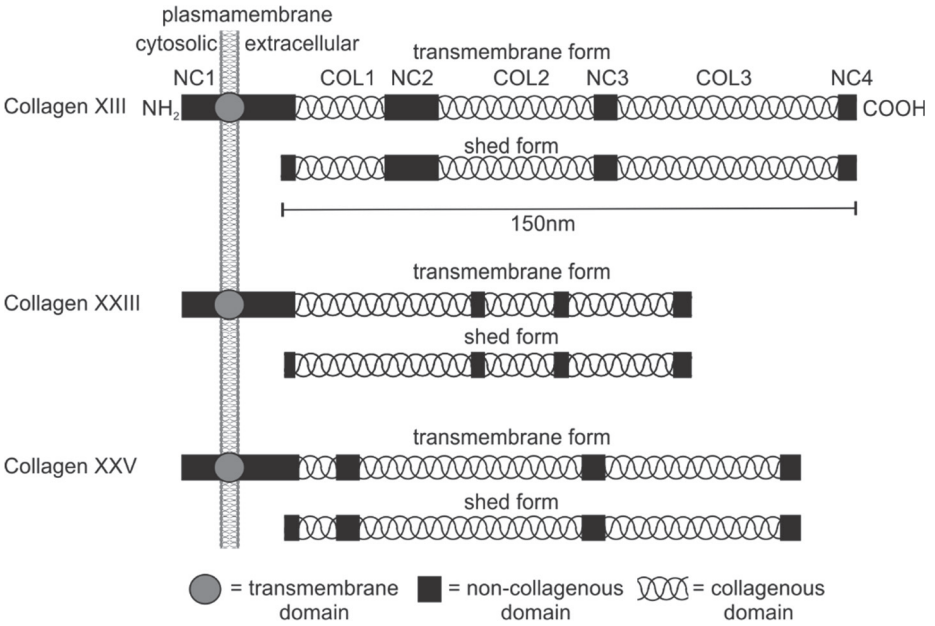

Fig. 2. Schematic presentation of collagen XIII-related transmembrane collagens. The extracellular domain of collagen XIII, XXIII and XXV vary in length on account of modifications based on alternative splicing of the representative collagen transcripts. COOH, C terminus; NH_2, N terminus.

Expression patterns and roles of collagens XXIII and XXV

Expression of collagen XXIII in the normal tissues of mice and humans is restricted, being most abundant in the lung followed in abundance by cornea, skin, tendon, and amnion (Koch *et al.* 2006). Furthermore, minor amounts of the mRNA were also found in the kidney and placenta. Immunofluorescence and *in situ* hybridizations of embryonal tissues have revealed collagen XXIII to be a component of many epithelia (epidermis, epithelia of the small intestine, oropharynx, and the dorsum of the tongue) as well as hair follicles (Koch *et al.* 2006). In contrast to normal tissues, expression of collagen XXIII is up-regulated in a highly metastatic rat prostate adenocarcinoma cell model albeit not found in non-metastatic models (Banyard *et al.* 2003). Moreover, collagen XXIII mRNAs were detected in immortalized human cell lines of a Barrett-associated adenocarcinoma, an esophageal epithelial adenocarcinoma and a non-small cell lung adenocarcinoma (Koch *et al.* 2006). Collagen XXIII serves also as a

biomarker for human non-small cell lung cancer (NSCLC) detection and recurrence and prostate cancer recurrence (Banyard *et al.* 2007, Spivey *et al.* 2010). The role of collagen XXIII in cancer metastasis and normal biology of the tissues is not clear, but the effects of collagen XXIII have been suggested as being mediated through cell adhesion (Spivey *et al.* 2012). Supportively, collagen XXIII knock-down in the human lung cancer cell line H460 revealed a decrease in the protein expression of OB-cadherin, β-catenin, α-catenin, and γ-catenin, vimentin, galectin-3 and potentially integrins containing α6 subunit — each of which can affect cell morphology and adhesion (Spivey *et al.* 2012). Collagen XXIII has also been shown to interact with α2β1 integrin and via this interaction to be sufficient to induce the attachment and subsequent spread of keratinocytes (Veit *et al.* 2011).

Collagen XXV is highly expressed in the CNS neurons of adult humans and mice. In addition, low expression of collagen XXV has been detected in other adult murine tissues including the heart, testis and eye. Originally, the cleaved ectodomain of collagen XXV (collagen-like Alzheimer amyloid plaque component: CLAC) was identified as a component of the senile plaques that are the pathological hallmarks in the brains of Alzheimer´s disease patients. Thus, collagen XXV is also known as a CLAC-precursor (CLAC-P). It has been suggested that CLAC acts to regulate amyloid formation during the development and progression of Alzheimer´s disease by binding amyloid-β fibrils, the primary constituent of senile plaques. The physiological function of collagen XXV remained unclear until the studies with collagen XXV knock-out mice revealed collagen XXV to be indispensable for embryonal intramuscular innervation of motoneurons (Tanaka *et al.* 2014). *In situ* hybridization of mouse embryonal tissues revealed strong collagen XXV expression in spinal cord neurons (including motoneurons) and developing muscles, in addition to weak signals in some other organs, including heart, lung and epidermis. Moreover, *in vitro* studies with a mouse muscle cell line (C2C12) specified the expression of collagen XXV to increase by 40-fold after myoblast fusion to myotubes. Collagen XXV deficiency was judged as neonatally lethal due to respiratory failure after birth. Studies of embryonal tissues revealed that axons of motoneurons projected properly towards the target muscles, but did not elongate and branch within the muscle. This led to degeneration of axons and apoptosis of motoneurons that had totally disappeared by embryonic day (E) 18.5. In addition, studies of neonatal skeletal muscles revealed generally thinner muscle tissue, smaller diameter of muscle fibers and increased number of central nuclei, indicating halted muscle development at an early stage of myotube formation due to failed innervation and NMJ formation. Furthermore, it was shown that

motoneuron cell death in collagen XXV knock-out mice resulted from the insufficient supply of target-derived survival factors for motoneurons (Hashimoto *et al.* 2002).

2.2.3 Expression of collagen XIII in human and mouse tissues

Collagen XIII is expressed in a wide range of developing and mature tissues both in humans and mice, but in relatively low amounts. In tissues collagen XIII has been located at cell-matrix and cell-cell adhesion sites, for example at the MTJs, intercalated discs of the heart and at the NMJ (Hägg *et al.* 2001, Latvanlehto *et al.* 2010, Sund *et al.* 2001a). In addition to junctional structures, collagen XIII is often associated with BMs, for example in the blood vessels (Heikkinen *et al.* 2012).

In situ hybridization of human fetal tissues at gestational weeks 15-19 have indicated the collagen XIII expression to be in the epidermis, hair follicles and nail root cells of the skin, the endomysium, the mucosal layer of the gut, chondrocytes and the mesenchymal cells forming the reticulin fibers of the bone marrow (Sandberg *et al.* 1989). In addition, *in situ* hybridization signals could be detected in many structures of the human fetal eye (Sandberg-Lall *et al.* 2000). Furthermore, *in situ* hybridization of the early human placenta has unveiled moderate signals in the endothelial cells of the developing capillaries, cytotrophoblastic columns and large decidual cells of the decidual membrane, and the stromal cells of the gestational endometrium (Juvonen *et al.* 1993). Expression analyses with northern blots of developing mouse fetuses indicated that overall expression of collagen XIII could already be detected in low amounts at E7, but stronger signals from E11 onwards, with the strongest signals at E17 (Sund *et al.* 2001a). *In situ* hybridization of developing mouse tissues suggested the strongest collagen XIII expression to be at E11.5 in the neuroectoderm of the developing brain and neural tube, as well as in the myocardium, and at E16.5 in the chondrocytes (developing cartilage and in the resting and the proliferative regions of developing bone). In addition, high amounts of collagen XIII expression were also found at E16.5 in the peripheral nerves, as well as in some cells of the brain, in the periosteum of ossified bone, myocardium, myotubes and epithelium of the intestine and lung. Furthermore, immunostainings with anti- collagen XIII antibody have revealed collagen XIII immunoreactivity at the junctions between the developing cardiomyocytes, becoming clearly visible at the intercalated discs of the adult mouse heart (Hägg *et al.* 2001, Sund *et al.* 2001a).

In mature tissues, collagen XIII immunoreactivity can be found at the NMJs and MTJs of humans and mice (Hägg *et al.* 2001, Latvanlehto *et al.* 2010, Logan *et al.* 2015). Moreover, collagen XIII is localized to the dermal-epidermal junction and to the periphery of keratinocytes in all epidermal layers of normal human skin and in the corneal epithelial cells and stromal keratocytes of the human eye (Määttä *et al.* 2006, Peltonen *et al.* 1999). Furthermore, increased expression of collagen XIII has been detected in the human scarred corneas, the reactive stromal cells of epithelial tumors, throughout mesenchymal tumors and in renal fibrosis (Dennis *et al.* 2010, Määttä *et al.* 2006, Väisänen *et al.* 2005).

2.2.4 In vitro studies of collagen XIII

In vitro studies of collagen XIII have provided further information concerning the structure and function of collagen XIII. Work with insect cells expressing recombinant human collagen XIII have pointed to two distinct conserved α-helical coiled-coil domains in the NC1 and NC3 domains of the collagen XIII α-chain (Latvanlehto *et al.* 2003, Snellman *et al.* 2000a). Interestingly, folding of the homotrimers occurs opposite to the folding of the classical fibrillar collagens in an N to C terminal direction. As already mentioned above, the ectodomain of collagen XIII can be cleaved by furin-type proprotein convertases and this can happen in the trans-Golgi network or at the plasma membrane (Snellman *et al.* 2000b, Väisänen *et al.* 2004). In more detail, the cleavage site of the collagen XIII ectodomain is preceded at the amino acid sequence of four arginines (RRRR) in the NC1 domain (Snellman *et al.* 2000b). The resulting ectodomain, a 150nm rod with two flexible hinges coinciding with the NC2 and NC3 domains, has been shown to interact with high affinity with fibronectin, nidogen-2, perlecan (Fig. 3) and heparin (Tu *et al.* 2002). Furthermore, moderate interactions were detected with vitronectin, perlecan, nidogen-1, fibulin-2, and type IV (Fig. 3) and VI collagens. In addition, the purified collagen XIII protein has been shown to interact with α1β1 (Nykvist *et al.* 2000) and α11β1 integrins (Fig. 3) (Tu 2004). In addition to other collagens (collagens I, II, III, V, VI, XVII and XXIII) collagen XIII has also been shown to act as a high affinity ligand for the inhibitory leukocyte-associated immunoglobulin-like receptor-1 (LAIR-1) (Fig. 3) (Lebbink *et al.* 2006, Lebbink *et al.* 2007). Interestingly, *in vitro* effects of collagen XIII ectodomain in the primary fibroblast cell cultures were anti-adhesive, anti-migratory and anti-proliferative (Väisänen *et al.* 2004). Furthermore, the ectodomain of collagen XIII was discovered to associate with its C-terminal end (the NC4 domain and part of the COL3 domain)

with the fibrillar fibronectin matrix and possibly interfering with the assembly of the fibronectin matrix *in vitro* (Väisänen *et al.* 2006). The effects of the recombinant collagen XIII ectodomain was also studied on primary neuronal cell cultures extracted from E18.5 rat fetal hippocampus where it was found to enhance neurite outgrowth *in vitro* (Sund *et al.* 2001a). *In vitro* immunoreactivity of collagen XIII has been detected in focal adhesions of human skin fibroblast and keratinocytes co-localizing with vinculin and talin at the end of actin filaments (Hägg *et al.* 2001, Peltonen *et al.* 1999).

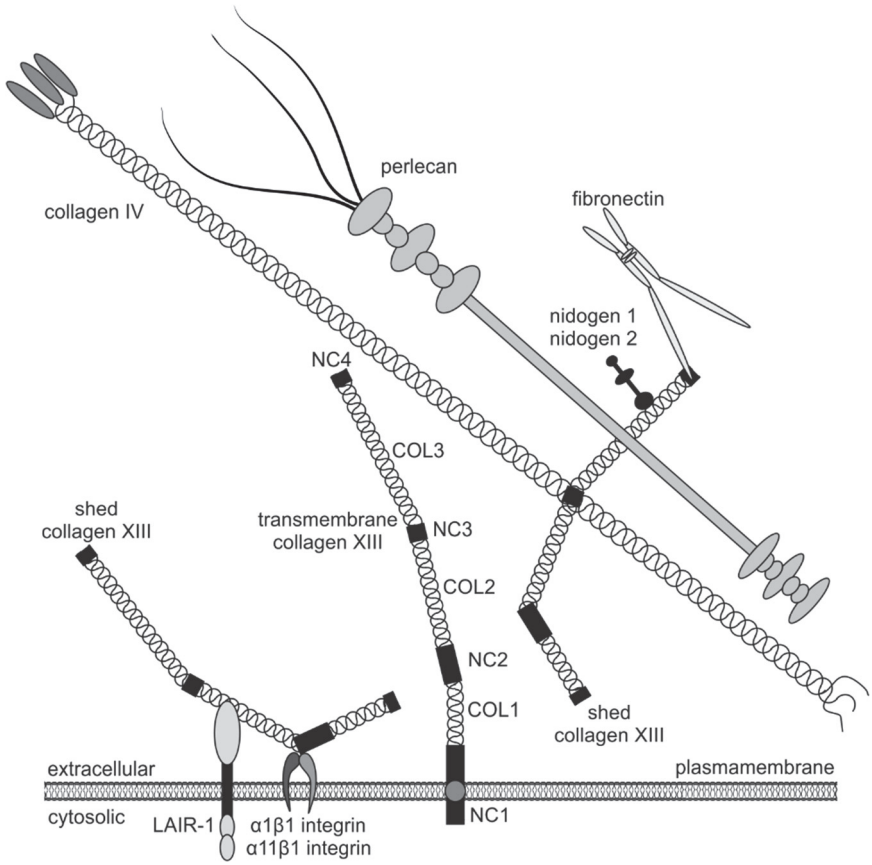

Fig. 3. Schematic representation of collagen XIII and *in vitro* interacting molecules. Binding sites are not precisely known and are therefore not necessarily accurately presented.

2.2.5 In vivo *studies of collagen XIII*

The *in vivo* effects of collagen XIII have been studied with different mouse lines and recently loss-of function mutations in the *COL13A1* have been proven to be a cause of the congenital myasthenic syndrome (CMS) type 19 in humans (Logan *et al.* 2015). Furthermore, autoantibodies for collagen XIII have been detected in thyroid-associated ophthalmopathy (TAO) in Graves' disease and in Hashimoto's thyroiditis (De Bellis *et al.* 2005, Gopinath *et al.* 2007). TAO is an autoimmune disorder affecting the extraocular muscles and surrounding orbital connective tissue with clinical signs including upper eyelid retraction, periorbital edema and impairment of eye motility (Sahli & Gunduz 2017). Interestingly, in Graves' disease higher levels of collagen XIII autoantibodies correlated with a more active type of ophthalmopathy and overexpression of collagen XIII in active TAO-affected fat was also found (De Bellis *et al.* 2005, Morris *et al.* 2016). Autoantibodies against collagen XIII have been suggested to serve as a good marker of active Graves' ophthalmopathy and play a role in the pathology of TAO (De Bellis *et al.* 2005). Moreover, whole-exome sequencing (WES) and genome-wide expression profiling have identified *COL13A1* as one of the novel candidate genes increasing the risk of diffuse cutaneous systemic sclerosis, osteoarthritis, non-alcoholic fatty liver disease, intracerebral hemorrhage and hypertension (Karlsson *et al.* 2010, Mak *et al.* 2016, Oguri *et al.* 2010, Shang *et al.* 2015, Yoshida *et al.* 2010). Furthermore, upregulation of the *COL13A1* gene expression has been associated alongside with other ECM genes in the pathogeny of Brittle cornea syndrome, a multisystemic rare connective tissue disorder with extreme corneal thinning (Porter *et al.* 2015). In mouse models, collagen XIII modifications have resulted in a variety of pathological conditions affecting the musculoskeletal tissues and microvessels and increasing inflammation (Heikkinen *et al.* 2012).

Transgenic overexpression of collagen XIII leads to overgrowth of bones

Transgenic overexpression of collagen XIII in the *Col13a1*^{oe} mice led to excess bone formation, most conspicuous in the long bones, but also evident in the calvarial bones and in the rib-vertebrae region (Ylönen *et al.* 2005). The increased bone mass was visible in long bones at 3-4-weeks of age and severe skeletal abnormalities could be detected by the age of 2 months. Despite the skeletal abnormalities, these mice were fertile and had a normal life span. The overexpression of collagen XIII was obtained by inserting a transgene construct

containing a predicted *Col13a1* promoter (nucleotides −984 to −231 of the 5′ -flanking sequences), the first exon and part of the intron 1 cloned in front of the rest of a collagen XIII cDNA containing exons 2-41 (length in amino acids: 689) and tailed by a hemagglutinin (HA) tag, sequences for transcription termination, and the SV40 Poly-A sequence (Peltonen *et al.* 1997, Ylönen *et al.* 2005). In these *Col13a1*^{oe} mice both endogenous and exogenous, transgenic collagen XIII are expressed, and both can be shed (Ylönen *et al.* 2005). The exogenous collagen XIII was proven to be capable of forming trimers. Excess collagen XIII expression was detected in the skin, cartilage and skeletal tissues, and immunohistochemistry highlighted overexpression of collagen XIII to localize in the proliferative zone of the growth plate and periosteum, as well as in the proliferating chondrocytes in the developing cartilage. Upregulated mRNA levels of Runx2 and IGF-II were detected and postulated as a reason for the high bone mass phenotype (Ylönen *et al.* 2005).

Transgenic overexpression of collagen XIII with a truncated COL2 domain results in embryonal lethality

Studies with the transgenic *Col13a1*^{COL2Del} mouse lines synthesizing α1(XIII) chains with a 90-amino acid in-frame deletion in the COL2 sequences resulted in embryonal lethality of the progeny inheriting transgenes from both of their parents (Sund *et al.* 2001b). The transgene construct was obtained in the same way as in the *Col13a1*^{oe} mice, by cloning the predicted *Col13a1* promoter before the mutated collagen XIII sequence. The large in-frame deletion was designed in such a manner that mutant α1(XIII) chains would associate with each other or endogenous ones and result in a synthesis of truncated and normal homotrimeric collagen XIII in transgenic mice and, in addition, the heterotrimeric form of these two different α-chains. The formation of abnormal collagen XIII molecules was proposed to lead to a dominant-negative phenotype. Interestingly, this large in-frame deletion resulted in embryonal lethality at two distinct time points, at E10.5 and E13.5. Abortions before E10.5 were discovered to result from a failure in the fusion of the chorionic and allantois membranes that lead to a defect in the formation of a functioning placenta, and abortions by E13.5 resulted from cardiac dysfunction (exemplified by detachment of myofilaments from adherence junctions and abnormal staining for the adherence junction component cadherin). Interestingly, these mice also harbored decreased microvessel formation in the CNS, the trigeminal ganglion and the placenta. Further characterization of the late phenotype

with Doppler ultrasonography at E12.5 suggested that 39.1% of the transgene-positive fetuses had atrioventricular valve regurgitation and a lower heart rate accompanied with decreased outflow compared to wild-type controls. Histological characterization of fetuses harboring atrioventricular valve regurgitation indicated reduced average trabeculation of the ventricles and thinner myocardium. Collagen XIII *in situ* hybridization of the wild-type and transgenic positive hearts at E12.5 located the signals at the trabeculated wall of the ventricle, the muscular part of the interventricular septum, the wall of the atria, atrio-ventricular valves and the epicardium confirming the important role of collagen XIII in the development of the heart (Tahkola *et al.* 2008). Interestingly, and unexpectedly, heterozygous *Col13a1*^{COL2Del} transgenic mice developed T-cell- and histiocyte-rich B-cell lymphomas appearing in mesenteric lymph nodes after one year of age with an incidence of 15.8% (wild-type incidence ~2%). The incidence of these lymphomas could be decreased to 7.4% when the transgenic mice were housed under specific pathogen-free (SPF) conditions. Furthermore, the structure of the epithelial BM of the intestine was found to be altered and expression levels of genes involved in immune responses to be increased suggesting a role for collagen XIII as a novel tumor suppressor gene for intestinal microbe-dependent lymphomas (Tuomisto *et al.* 2008).

Expression of the N-terminally altered collagen XIII leads to mild, but progressive myopathy and affects adhesion of fibroblasts

Function of collagen XIII has been studied with a genetically modified mouse line that expresses collagen XIII in an N-terminally altered form (*Col13a1*$^{N/N}$) through site-specific Cre-*loxP*-mediated deletion of most of the exon 1 sequences. The deletion led to the expression of collagen XIII protein lacking only the intracellular and transmembrane domains of collagen XIII. *Col13a1*$^{N/N}$ mice were born at a Mendelian ratio and showed no changes in their growth, behavior or reproductive capacity compared with wild-type controls. Systematic examination of gross anatomy of the 17-week-old *Col13a1*$^{N/N}$ mice revealed alterations only in the skeletal muscle histology. H&E staining revealed some muscle fibers to be uneven in size and have a smaller diameter. Furthermore, immunofluorescent staining of collagen IV, dystrophin-dystroglycan receptor complex and laminin $\alpha2\beta1\gamma1$ exhibited a fuzzy BM pattern in the muscle expressing altered collagen XIII, and muscle fibers seemed to be more loosely attached to each other. Ultrastructurally, 8-, 17-, and 43-week-old muscles of the *Col13a1*$^{N/N}$ mice showed vacuolization

and disorganization of myofilaments and z-bands. Moreover, a disorganized and fuzzy sarcolemma and the adjacent BM was discovered and was particularly evident at the MTJ. The ultrastructural defects were more pronounced in the older mice, suggesting a progressive condition. Furthermore, when mutant and wild-type mice were exposed to exercise, the *Col13a1*$^{N/N}$ mice were discovered to be more sensitive to exercise induced muscle damage (Kvist *et al.* 2001).

Interestingly, primary cutaneous fibroblast cultures extracted from homozygous and control mice showed similar staining patterns for collagen XIII immunoreactivity in sites of focal adhesions co-localizing with vinculin. This suggests cytosolic and transmembrane domains of collagen XIII are dispensable for the transport and localization of the collagen XIII protein at focal adhesions. However, primary E13.5 mouse embryonic fibroblasts (MEFs) harboring N-terminally altered collagen XIII showed lowered adherence to the cell culture plates; this was even more pronounced when plated on collagen IV coating, suggesting functional importance for the cytosolic residues of collagen XIII in the adhesion of MEFs (Kvist *et al.* 2001).

Collagen XIII is of muscle origin at the neuromuscular system

A novel reporter mouse line (*Col13a1*^{LacZ}) of collagen XIII was generated by inserting a cDNA encoding the *Escherichia coli* β-galactosidase (*LacZ*) into the *Col13a1* locus, thus replacing the extracellular sequences in order to determine the cellular origins of collagen XIII. This modification was designed to deteriorate the functional furin proprotease cleavage site leaving the collagen XIII/β-galactosidase fusion protein either inside or on the plasma membrane of its producing cells. Histochemical staining for β-galactosidase activity combined with fluorescently labeled α-BTX staining (neurotoxin binding to AChRs (Sanes & Lichtman 2001)) revealed collagen XIII expression enriched at synaptic sites exclusively at the outer edges of the muscle fibers and slightly broader than the labeled AChR clusters in the muscles of adult mice. In addition, collagen XIII immunostainings suggested a similar staining pattern at the NMJs, and further studies with immunoelectron microscopy confirmed collagen XIII to localize at synaptic sarcolemma and adjacent synaptic BL. Furthermore, β-galactosidase activity was also found at the MTJs in mice of the *Col13a1*^{LacZ} line (Latvanlehto *et al.* 2010). Interestingly and somewhat contrary to earlier findings of robust collagen XIII immunoreactivity signals at sarcolemmal membrane and intramuscular axon fascicles of adult mice, β-galactosidase activity was only found in association with capillaries of the nerve

fascicles (Hägg *et al.* 2001, Kvist *et al.* 2001, Latvanlehto *et al.* 2010). The β-galactosidase reporter expression was also studied at the NMJs of new-born mice and at the first few postnatal (P) weeks. The expression was detectable but weak at the former stage and dramatically increasing at the latter time points until the first month of age, where- after it remained stable. Collagen XIII mRNA expression confirmed the result and showed only little change at 1-month-old maturing mouse muscles compared to adult muscles (Latvanlehto *et al.* 2010). Furthermore, similar to its homologous protein, collagen XXV, collagen XIII was not detected by protein analyses at the myoblast phase of C2C12 immortalized mouse myoblast cell line, but clearly both its forms, the shed and transmembrane collagen XIII, were present after fusion to myotubes (Latvanlehto *et al.* 2010, Tanaka *et al.* 2014). Further protein studies indicated that the shed collagen XIII was found enriched at the membrane-associated fractions of C2C12 extracts and absent from the nuclear, cytoplasmic and membrane fractions (Latvanlehto *et al.* 2010).

Collagen XIII deficiency results in defects at the neuromuscular system

Studies with collagen XIII knock-out mice (*Col13a1*$^{-/-}$) have highlighted the important roles of collagen XIII at the NMJ. The *Col13a1*$^{-/-}$ mice were generated by deleting the predicted promoter, the 5´UTR, and the first protein-coding exon from the *Col13a1* gene. Successful deletion was confirmed by real-time quantitative PCR (RT-qPCR) and Western blotting, and no collagen XIII transcripts or protein were detected. The *Col13a1*$^{-/-}$ mice lived normally until adulthood and appeared outwardly normal despite the slower growth at puberty. Furthermore, these mice were fertile and born at a Mendelian ratio (Latvanlehto *et al.* 2010).

Evaluation of postsynaptic structures with α-BTX staining at P56 at four different muscles: the diaphragm, tibialis anterior (TA), soleus and extensor digitorum longus (EDL). This revealed small, simple, plaque-like and/or fragmented postsynaptic apparatuses in the *Col13a1*$^{-/-}$ mice compared to the complex, branched, pretzel-like morphology of the wild-type endplates. Interestingly, a large portion (over 80%) of the NMJs at the collagen XIII knock-out diaphragms and soleus muscles harbored the distorted postsynaptic morphology compared to TA and EDL muscles, where the abnormal assembly took place in ~50% and ~25% of the NMJs, respectively. Furthermore, when postsynaptic maturation was assessed by α-BTX staining at P0, P14, P28 and P56, halted development and immaturity became apparent at P14 and onwards leaving collagen XIII deficient endplates smaller and less complex compared to wild-type

controls. Postsynaptic maturation was also studied *in vitro* by adding soluble collagen XIII ectodomain to C2C12 muscle cell cultures and AChR clustering was found to be enhanced. In addition to postsynaptic defects, immunostainings of presynaptic components at P28 showed failed vesicle clustering in the nerve terminals (vesicles were also found in the preterminal axon), AChR clusters were not fully covered by presynaptic counterparts and some synaptic vesicle rich axonal sprouts extended beyond the endplate due to the lack of collagen XIII. Ultrastructural analysis at P28 and P56 revealed discontinuity in adhesion of the muscle and nerve terminal, seen as wider gaps in the synaptic cleft occasionally accompanied by erroneous tShC invagination between the two synaptic partners. Furthermore, presynaptic cells harbored changes indicating degeneration and fewer AZs (Latvanlehto *et al.* 2010).

Consistent with the morphological findings, *ex vivo* electrophysiological measurements at NMJs in the diaphragm indicated both post- and presynaptic defects in the *Col13a1*$^{-/-}$ mice, namely a decreased amplitude of postsynaptic potentials, diminished probabilities of spontaneous release and a reduced readily releasable neurotransmitter pool highlighting the importance of correct NMJ morphology to its function (Latvanlehto *et al.* 2010).

2.3 Formation of the NMJ and its molecular machinery

Taking into account the consequential role of the NMJ, its correct formation and function are supported by many molecules and further adjusted by others from developmental stage to adulthood. To accomplish this vital synapse, precise spatial and temporal interplay between presynaptic, synaptic and postsynaptic molecules is required. The formation of the NMJ starts from the embryonal establishment of its core molecules and is continued by postnatal maturation and lifelong administration to ensure the existence of voluntary movements (Sanes & Lichtman 1999, Tintignac *et al.* 2015, Wu *et al.* 2010).

2.3.1 Temporal aspects of the NMJ biology

The temporal aspects of the NMJ biology can be divided into the following: embryonal development, postnatal maturation and stabilization, maintenance and aging (Fig 4 A-C). In embryonal development precursor cells for skeletal muscles originate from the paraxial mesoderm segmented into somites and located on either side of the neural tube. In myogenesis, two waves of progenitor cell proliferation

take place temporally, situated at E9.5-E14.5 and E15-E17 in the mouse development. In the former, most of the myoblasts proliferate and fuse into primary myotubes in the somites and migrate to final locations. In the latter wave a fraction of undifferentiated myoblasts start to proliferate and fuse with pre-existing primary myotubes or fuse among each other and form secondary myotubes. Simultaneously, multipotential progenitors give rise to motoneurons in the ventral portion of the neural tube and to ShCs in the neural crest. Motoneurons emit their axons guided by extracellular cues towards developing muscle fibers, with ShCs migrating alongside. Axons of motoneurons meet their target muscles in the mouse between E12.5-14.5 depending on the muscle (Chal & Pourquie 2017, Sanes & Lichtman 1999, Tintignac *et al.* 2015).

At the beginning of the NMJ development and before innervation, muscle fibers already express diffuse clusters of AChRs on their sarcolemma. This phenomenon is called pre-patterning, and it takes place, for example in the mouse diaphragm, between E12.5 and E13.5. The role of pre-patterning still remains enigmatic, thus growing axons can innervate pre-patterned clusters or avert them and induce formation of new AChR clusters (Fig. 4B). However, pre-patterning has been suggested as acting as a primary determinant for the subsequent innervation pattern. Between E13.5 and E15.5 the proportion of innervated AChR clusters increases from <10% to ~50%. Furthermore, innervated clusters grow in size and by E18.5 aneural clusters have disappeared. Interestingly, at the beginning of the innervation process, one muscle fiber can be innervated by two or more motoneuron axons temporarily; however, within two weeks following birth during postnatal maturation muscle fibers become innervated only by one motoneuron and extra motoneurons perish (Fig. 4B) (Darabid *et al.* 2014, Liu *et al.* 2008, Tintignac *et al.* 2015, Wu *et al.* 2010).

After prepatterning and innervation, molecules secreted by the nerve, muscle and ShCs take part in the NMJ assembly and influence the further development, maturation and function of both pre- and postsynaptic sides of the junction. At the time of birth NMJs are functional, however they harbor highly distinct features compared to mature adult NMJs. Thus, the postnatal maturation needed to achieve stable and efficient synapses takes place after birth. In mice, postsynaptic maturation is complete within the first month of age. In this process, the shape and topography of the postsynaptic endplate changes from simple ovoid-like to complex pretzel-like morphology and junctional folds and gutters develop (Fig. 4C). Furthermore, the composition of the synaptic BL changes and the presynaptic motoneuron becomes functionally more efficient with axons becoming myelinated.

Moreover, some channel functions are altered in both the pre- and postsynaptic membrane and, for example, AChR clusters are further stabilized (Sanes & Lichtman 1999, Sanes & Lichtman 2001, Shi *et al.* 2012, Wu *et al.* 2010).

Interestingly, even after maturation adult NMJs are not rigid structures but harbor wide plasticity. For example, endurance training has been shown to increase the synapse size and nerve terminal branching length and complexity (Deschenes *et al.* 2006, Deschenes *et al.* 2016, Nishimune *et al.* 2014). In contrast, degenerative changes and nerve terminal sprouting have been seen after decreased physical activity. Furthermore, aging changes the morphology of the NMJ (Li *et al.* 2011, Punga & Ruegg 2012, Valdez *et al.* 2010). Aged NMJs can show partial denervation, AChR cluster fragmentation and decrease in AChR density. Moreover, preterminal and terminal axons of aged NMJs often harbor erratic patterns by being thinner or having swollen varicosities proximal to the nerve terminal (Fig. 4C) (Valdez *et al.* 2010). Swollen varicosities and accumulations of neurofilaments are also frequently observed in several neurogenerative disorders and as a hallmark of autophagosomes of dystrophic axons (Perrot & Eyer 2009, Yang *et al.* 2013). Interestingly, polyneuronal innervation is also seen in old NMJs. Some of these morphological changes can be detected already in 1-year-old mice, however to a much lesser extent, but not at the NMJs of 1- and 6-month-old mice (Valdez *et al.* 2010).

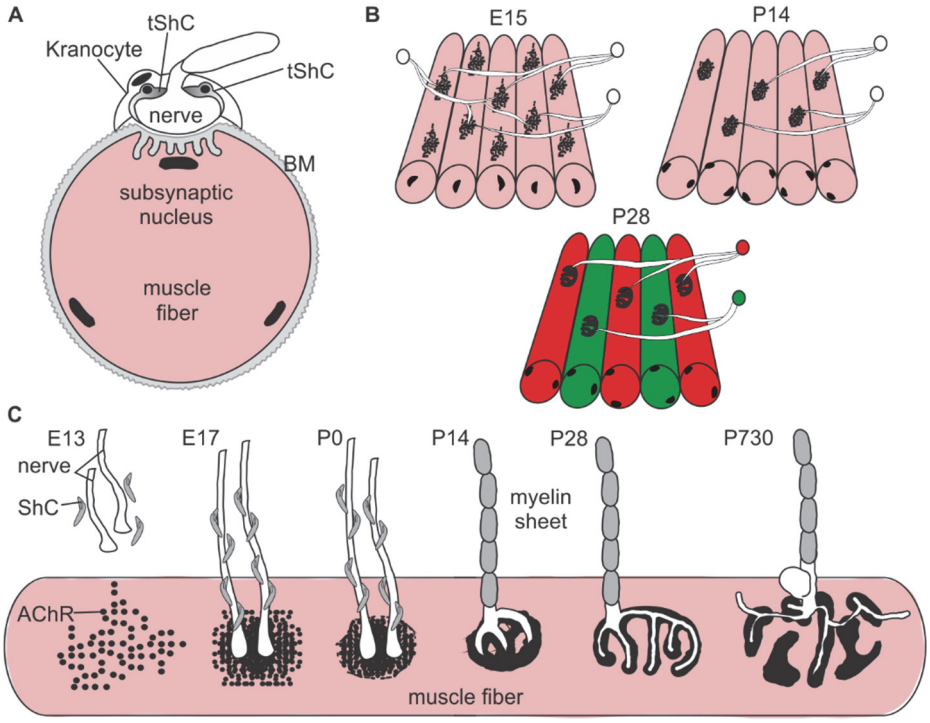

Fig. 4. Temporal aspects of NMJ biology. A) An overview of the cellular partners of the NMJ (modified from Court *et al.* 2008). B) Embryonally (E15) a developing muscle fiber harbors many AChR clusters and some of them are subject to multiple innervation by motoneurons (white circles represent cell bodies with white projections representing axons in both E15 and P14) while some lack a nerve contact. Clusters without innervation disappear before birth and innervated clusters become innervated only by one motoneuron postnatally (P14). At P28 NMJs exhibit pretzel-like shape and one motor nerve (red or green circle represent a cell body with white projections representing axons) innervates several muscle fibers with the same MyHC-properties forming together a motor unit (red; slow-twitch and green; fast-twitch). C) The NMJ morphology from E13 to P730. Note the myelin sheet at P14 and onwards and a preterminal swollen varicosity at P730.

2.3.2 Postsynaptic development and maturation of the neuromuscular junction

After AZs have been formed at the presynaptic membranes during the embryonal development AChVs start to fuse with the preterminal membrane and release their

contents, ACh, into the synaptic cleft. ACh has a dual role in the development of the NMJ; it binds to AChRs and elicits a muscle contraction while, on the other hand, it declusters aneural AChR clusters (Kummer *et al.* 2006, Samuel *et al.* 2012, Wu *et al.* 2010). Downstream mechanisms have been postulated to include activation of Ca^{2+}/Calmodulin-dependent protein kinase II (CaMKII) and serine/threonine kinase cyclin-dependent kinase 5 (Cdk5) (Wu *et al.* 2010). Another nerve-derived factor, the heparan sulphate proteoglycan agrin, counteracts the anticlustering effects of ACh (Kummer *et al.* 2006, Samuel *et al.* 2012, Wu *et al.* 2010). This counteraction rescues AChRs in the innervated sites and disperses prepatterned AChRs from the sites that lack nerve contact only. Muscle fibers and ShCs also synthetize agrin, but it is 1000-fold less effective than neural-derived agrin in terms of AChR clustering. This effect of agrin comes through the MuSK-LRP4-pathway and it clusters diffusely expressed local plaques of AChRs (Fig. 5) (Kummer *et al.* 2006, Samuel *et al.* 2012, Sanes & Lichtman 1999, Wu *et al.* 2010). Animal studies have shown that prepatterning of the AChRs requires MuSK, but not agrin, whereas development of the nerve-induced AChR clusters, and fundamentally, NMJs requires both. Hence, mice lacking agrin express AChRs uniformly on the muscle sarcolemma without proper clustering of the receptors while mice lacking MuSK show neither prepatterning nor clustering of the AChRs (Darabid *et al.* 2014, Wu *et al.* 2010). Furthermore, both of these animal models show presynaptic defects as aimless overgrowth of nerves (Darabid *et al.* 2014). MuSK is a muscle-derived single-pass transmembrane protein and once activated it stimulates pathways that cluster and anchor AChRs and additional proteins important for the synaptic transmission, enhances transcription of synaptic proteins and also promotes signals that stimulate presynaptic differentiation (Burden *et al.* 2013, Darabid *et al.* 2014, Wu *et al.* 2010). LRP4 belongs to a low-density lipoprotein receptor (LDLR) family and forms a complex with MuSK (Burden *et al.* 2013, Sanes & Lichtman 1999, Tintignac *et al.* 2015, Wu *et al.* 2010). NMJ aberrations in the mice lacking LRP4 resemble the defects seen in the lack of MuSK and both result in perinatal lethality (DeChiara *et al.* 1996, Wu *et al.* 2010). Direct binding of agrin to LRP4 leads to phosphorylation of the intracellular domain of LRP4 and it also activates MuSK phosphorylation (Burden *et al.* 2013, Tintignac *et al.* 2015, Wu *et al.* 2010). Furthermore, phosphorylated MuSK recruits the adapter protein downstream of tyrosine kinase 7 (Dok7), that further stimulates the phosphorylation and kinase activity of MuSK. Like LRP4, Dok7 is indispensable for the AChR prepatterning and clustering, since its absence in mice leads to similar NMJ defects seen in the MuSK deficiency. Dok7 has been postulated to work as an

inside-out ligand for MuSK and stimulate MuSK phosphorylation via dimer formation, where Dok7 proteins form a dimer that promotes MuSK activity. Rapsyn is another downstream molecule of MuSK signaling and a peripheral membrane protein, the gene disruption of which leads to a total absence of AChR clusters and abnormal nerve branching in mice (Legay & Mei 2017). Activation of MuSK leads through an unknown mechanism to the rapsyn-induced AChR clustering and scaffolding possibly via its binding capabilities with dystroglycan, actin and actinin (Legay & Mei 2017). Ultimately agrin-induced activation of LRP4, MuSK and its downstream proteins leads to the redistribution and anchoring of the postsynaptic proteins and development of the postsynaptic sites of the NMJ (Burden *et al.* 2013, Tintignac *et al.* 2015, Wu *et al.* 2010).

During the course of postnatal maturation the size and density of the AChR clusters increase and postsynaptic membranes invaginate to form junctional folds (Sanes & Lichtman 1999, Sanes & Lichtman 2001, Shi *et al.* 2012, Tintignac *et al.* 2015). AChRs are expressed only at the crests of the folds and the AChR clusters transform from plaque-like to characteristic pretzel-like morphology as described earlier (Fig. 4C). Moreover, AChRs become more stable and less susceptible to disassembly. Interestingly, during the postnatal maturation of the NMJ the AChR kinetics are also changed due to shifts in the AChR subunit composition (Sanes & Lichtman 2001, Shi *et al.* 2012, Tintignac *et al.* 2015). AChRs are pentameric ion channels composed of four different subunits. The fetal subtype consists of α2βγδ-subunits and the adult counterpart α2βεδ-subunits. Shift from the fetal γ-subunit to the adult ε-subunit shortens the open burst duration of the ion channels from ~4-5ms to ~1ms, while at the same time increasing conductance for Na^+, K^+, and Ca^{2+} ions. Replacement of fetal AChRs starts around the time of birth and is accomplished within 2 weeks following birth, however its physiological significance remains largely unknown. Furthermore, an analogous molecular switch occurs with voltage-gated Na^+ channels (Na_v) and, during the first two postnatal weeks, the $Na_v1.4$ isoform takes over the embryonal $Na_v1.5$ isoform (Tintignac *et al.* 2015). Maturation of the NMJ also changes structures inside the muscle cell by recruiting muscle nuclei to the cytoplasmic region below the synaptic membrane. Interestingly, these synaptic nuclei harbor different transcriptional patterns compared to non-synaptic nuclei and express genes encoding AChR subunits and some other postsynaptic components at higher rates (Sanes & Lichtman 2001, Shi *et al.* 2012, Tintignac *et al.* 2015). In addition to Agrin-MuSK-LRP4 interactions, many other molecules have been proven to influence the postsynaptic organization, including BL components collagen XIII,

laminins (with a dystroglycan-binding α4 or α5 subunit), nidogen 2, perlecan and ColQ (Arikawa-Hirasawa *et al.* 2002, Fox *et al.* 2008, Karmouch *et al.* 2013, Latvanlehto *et al.* 2010, Rogers & Nishimune 2017).

As already reviewed, compared with its extrasynaptic counterpart, the synaptic BL harbors many distinct molecular components playing a role in almost all aspects of NMJ formation including synaptic initiation, topography, ultrastructure, maturation, as well as stability and transmission (Singhal & Martin 2011). Loss of perlecan in mice leads to lethal respiratory failure soon after birth (Arikawa-Hirasawa *et al.* 2002). Studies on embryos indicated a loss of the collagen-like tail of AChE, ColQ, and AChE itself from the NMJs of perlecan- null embryos, guaranteeing the *in vivo* interaction of ColQ and perlecan (Fig. 5) (Peng *et al.* 1999). Otherwise and interestingly, the embryonal development of perlecan-null NMJs was normal. In addition to the structural roles of ColQ in localizing AChE at synapse by perlecan and MuSK binding, it participates in the postsynaptic differentiation via the latter interaction (Karmouch *et al.* 2013, Sigoillot *et al.* 2010, Sigoillot *et al.* 2016). ColQ deficiency in mice leads to an increase in the density and a decrease in the size of AChR clusters assessed at P7 and P20 (Feng *et al.* 1999, Sigoillot *et al.* 2010). Furthermore, some of the NMJs seemed to be fragmented and immature compared to controls at the latter time point. Ultrastructural analysis also showed holes at the cytoplasm beneath the postsynaptic membrane (similar local degeneration to that found after acute inhibition of AChE) and some ShC processes invaginating the synaptic cleft at P20 (Feng *et al.* 1999). These postsynaptic defects have been explained as being a consequence of the reduced level of membrane-bound MuSK and increased levels of all five AChR subunits, consequently leading to a mixture of mature and immature AChRs in the adult NMJs (Karmouch *et al.* 2013, Sigoillot *et al.* 2016). Interestingly and controversially, AChE deletion itself from the NMJ in mice did not lead to perinatal lethality, but premature death before P21. Such mice did not harbor a distinguishable phenotype at P0, but developed retarded weight gain and growth soon after. Furthermore, assessed at P12 these mice harbored ultrastructurally normal NMJs. However, these mice were extremely sensitive to butyrylcholinesterase (BChE)-specific inhibitors suggesting BChE, another enzyme capable of ACh hydrolysis, to compensate for the loss of AChE at the synaptic cleft (Xie *et al.* 2000). Nidogen-2 deficiency in mice leads to a postsynaptic maturation defect from P56 onwards seen as immature and fragmented AChR clusters that remain unchanged until adulthood (Fox *et al.* 2008).

2.3.3 Presynaptic development and maturation of the neuromuscular junction

To form a well-functioning synapse, the presynaptic counterparts of the NMJ also have to develop and maturate side by side with the postsynaptic endplate. Unfortunately, presynaptic development of the NMJ is less well characterized than development of the postsynaptic site. Nevertheless, it is known that the number of terminal branches, AZs and associated proteins increase in presynaptic development, and that there are changes in the distribution and types of calcium channels expressed. Furthermore, in the presynaptic development of the NMJ, synaptic vesicles are initially present throughout the motor axon and as the development continues vesicles progressively concentrate at the axon terminals. Moreover, excess nerve terminals innervating a single muscle fiber have to perish. Aggregation of mitochondria to the axon terminals also happens during presynaptic development. Interestingly, many ECM molecules have a role in presynaptic development (Darabid *et al.* 2014, Fox *et al.* 2007, Tintignac *et al.* 2015, Wu *et al.* 2010).

An important element of the presynaptic development is the formation of AZs, the electron-dense thickenings of the presynaptic membrane, where neurotransmitter vesicles fuse and release their contents. AZs are constituted from many membrane and intracellular proteins including Bassoon, CAST/ELKS/Erc family proteins, Munc13, Piccolo and RIM1/2 (Nishimune 2012). These proteins are also known as the cytoskeletal matrix of the active zone (CAZ) and have a role in vesicle accumulation and calcium-stimulated neurotransmitter release. AZ proteins are orchestrated to the presynaptic membrane via direct interaction with P/Q- and N-type voltage-dependent calcium channels (VDCCs) that enable calcium influx in response to presynaptic plasma membrane depolarization. Interestingly, both P/Q- and N-type VDCCs are expressed in the development of the NMJ, but in maturing NMJs P/Q-type VDCCs dominate by the second or third postnatal week (Nishimune 2012, Rogers & Nishimune 2017).

Laminins are heteromeric ECM molecules composed of α, β and γ subunits. There are three different muscle-derived laminin isoforms (α2β2γ1, α4β2γ1 and α5β2γ1) specifically expressed at the synaptic BL (Nishimune *et al.* 2008, Rogers & Nishimune 2017, Sanes 2003). However, the laminin α2 subunit can also be found extrasynaptically incorporated with the laminin β1 subunit. VDCCs constitute of two transmembrane and one cytosolic subunit and via its extracellular parts they interact with the laminin β2 subunit (Nishimune *et al.* 2004, Nishimune

et al. 2008, Rogers & Nishimune 2017). Studies with laminin β2 deficient mice have shown, that if the interaction between VDCCs and laminin β2 subunit is lost, the number of AZs and synaptic vesicles in close vicinity to the presynaptic membrane is decreased. Moreover, loss of laminin β2 prevents the maturational shift in the VDCCs towards P/Q-type VDCCs and reduces the protein levels of Bassoon and synaptic vesicle-related proteins. Interestingly, loss of laminin β2 also influences terminal ShCs and the postsynaptic endplate in the laminin β2 knock-out mice resulting in a ShC invasion into the synaptic cleft and reduced junctional folds. Studies with laminin α2 and α4 chain knock-out mice have shed light on subunit-specific functions and suggest that α4β2γ1 laminin has a role in aligning AZs with postsynaptic parts while α2 subunit-containing laminin acts more on the postsynaptic maturation. Laminins interact also with other proteins in addition to VDCCs including dystroglycan and integrins, and through these interactions further participate in organizing pre- and postsynaptic structures (Fig. 5). Thus, this interacting protein network between AZ proteins, VDCCs and laminins directs the AChV releasing sites directly opposite to the crests of the junctional folds and AChRs, and furthermore accumulates synaptic vesicles near the presynaptic membrane. Interestingly, pre- and postsynaptic changes were not detectable in the laminin β2 subunit deficient mice at the time of birth, but became apparent during the first few postnatal weeks, thereby suggesting additional presynaptic organizers either compensating or accounting for the embryonal presynaptic development (Fox *et al.* 2007, Rogers & Nishimune 2017).

Three muscle-derived members of the fibroblast growth factor (FGF) family (FGF7, -10, and -22) have been demonstrated to participate in embryonal synaptic vesicle clustering via signaling through an alternatively spliced form of FGF receptor 2 (FGFR2) called FGFR2b. When FGFR2b was selectively inactivated in mice, it led to less restricted vesicle accumulation and increased density of vesicles at the distal nerve branches near synaptic sites without effects on the vesicle formation or transport from the proximal parts of the axons. These presynaptic changes were apparent at E16, and, interestingly, studies with mice baring a conditional motoneuron-specific deletion of FGFR2 (FGFR2b knock-out mice die at birth due to lung defects) showed that the abnormality in the vesicle accumulation was transient since it was barely detectable during the third postnatal week. Furthermore, mutant mice lacking both FGFR2 and β2 subunit-containing laminins showed more severe neuromuscular phenotype than loss of each protein separately, but even so presynaptic differentiation proceeded to a considerable extent, again suggesting the existence of additional, but yet unidentified,

presynaptic organizers (Fox *et al.* 2007). In addition to laminins and FGFs, collagen IV has been associated with embryonal and postnatal presynaptic development.

Collagen IV is a heterotrimeric ECM and BM component consisting of three α chains encoded by six different genes (*COL4A1–COL4A6*). Interestingly, only three combinations of α-chains exist ($\alpha1_2\alpha2$, α3α4α5 and $\alpha5_2\alpha6$). Collagen IV α-1 and -2 chains are present at the muscle BMs from embryonal development throughout life and are not specific for the synapse. On the contrary, collagen α-3(IV) to α-6(IV) chains are synapse-specific in muscle, but not expressed at embryonal stages and are detectable only at the third postnatal week and thereafter. Studies with different α(-) chain-targeted mutant mice have shown that collagen IV α1 and α2 (-) chains are needed for the accumulation of vesicles at the embryonal stages and after birth, but no longer at the third postnatal week. In contrast, presynaptic sites of collagen IV α5 chain mutants, lacking both α3α4α5 and $\alpha5_2\alpha6$ heterotrimers, showed normal presynaptic assembly only during the first three postnatal weeks. These mutants developed many presynaptic defects thereafter, including axonal retraction from the AChR-rich postsynaptic membrane, neurofilament aberrations (ring-like structures in nerve terminals and segments of distension in the axons) and fragmentation of the postsynaptic specializations (Fox *et al.* 2007).

Altogether, many aspects of presynaptic development are affected by laminins, FGFs and collagen IV, yet many other molecules have proven to influence the presynaptic organization in embryonal stages as well as postnatally. For example, collagen XIII knock-out mice bare presynaptic defects, a decreased AZ number and AChV accumulation (Latvanlehto *et al.* 2010). In addition, the extracellular domain of the signal regulatory protein α (SIRP-α) has been proven to promote synaptic-vesicle clustering *in vitro*, and glial-cell and brain-derived neurotrophic factors (GDNFs and BDNFs, respectively) to regulate motor neuron survival (Darabid *et al.* 2014). Furthermore, the important postsynaptic organizer, LRP4, also acts retrogradely and independently of MuSK-signaling by binding to motoneurons and inducing the clustering of synaptic vesicles and AZ proteins (Yumoto *et al.* 2012). Interestingly, loss of presynaptic α3β1 integrin has been shown to result in decreased accumulation of AZ proteins (Bassoon, piccolo and P/Q-type VDCCs) at the embryonal stages and affect organization of the synaptic BL in mice (Ross *et al.* 2017). The α3β1 integrin deficient (α3 chain knock-out) mice die after birth, thus further analysis of postnatal NMJs was performed with mice lacking only one allele of the gene. A decreased level of α3β1 integrin was found to lead to detachment of the nerve and muscle, ShC invaginations, varicosities in the axons

and increased sprouting and branching of the nerve terminals at the NMJs, as assessed in 2-month-old mice. As well as the presynaptic defects seen in the reduced levels of α3β1 integrin, postsynaptic defects appeared, including fragmentation of the AChR clusters. Interestingly, the laminin β1 subunit has been proven to interact with the integrin α3 chain (-containing integrins) (Carlson *et al.* 2010). Moreover, mice lacking the integrin β1 chain conditionally only from the skeletal muscle tissue but not in motor nerves, exhibited a widened nerve pattern since axons failed to stop at the central endplate band of the muscles at E17.5 and P0. Pre-patterning of the AChRs was not affected in these mice, but already formed AChR clusters dispersed during embryonal development. At the time of birth these mice were devoid of synapses, thus highlighting the indispensable role of postsynaptic integrins in presynaptic development (Schwander *et al.* 2004).

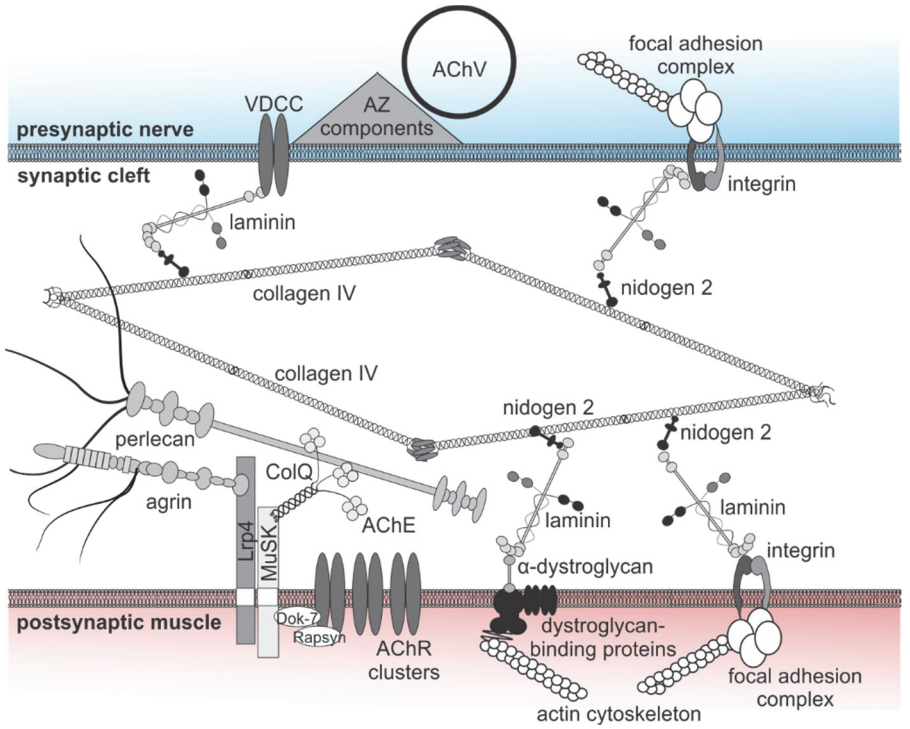

Fig. 5. Pre- and postsynaptic molecular assembly of the NMJ. The agrin-MuSK-LRP4 complex affects AChR clustering. Laminins are presented with their post- and presynaptic interaction partners. Synaptic collagen IV, nidogen-2, perlecan and ColQ interactions stabilize the synaptic cleft.

2.3.4 Role of Schwann cells and kranocytes in the development and maturation of the NMJ

Migrating neural crest cells give rise to immature ShCs at E13/15, whereafter they persist until the time of birth and start to proliferate and differentiate postnatally (Sugiura & Lin 2011, Tintignac *et al.* 2015). Depending on their locations, immature ShCs turn into myelinating ShCs in large axons and nonmyelinating ShCs or terminal ShCs in small axons and nerve terminals, respectively. ShCs promote the NMJ development and are indispensable for normal innervation of muscles; they also participate in postnatal synapse elimination and are required for maintenance of the NMJ (Darabid *et al.* 2014, Feng & Ko 2007, Sugiura & Lin 2011, Tintignac *et al.* 2015). Furthermore, ShCs have important roles in reinnervation after nerve injuries and they modulate synaptic activity of adult NMJs. In addition to terminal ShCs, the perisynaptic fibroblast-like cells, termed kranocytes, have been recognized as novel cellular components of the NMJ (Court *et al.* 2008). Their role at the NMJ still remains enigmatic. However, in new-born mouse muscles, kranocytes are evenly distributed, becoming restricted at the sites of the NMJ during postnatal maturation. Furthermore, they react upon denervation or paralysis by proliferating and spreading throughout the perijunctional regions of the NMJ (Court *et al.* 2008).

Kranocytes were discovered while testing the antibody 2166 originally raised against Tspan-2, an oligodendrocyte-specific tetraspanin protein. Interestingly, the 2166 antibody did not recognize Tspan-2 or oligodendrocytes, but revealed a subpopulation of the NMJ capping cells in several studied mouse skeletal muscles (for example soleus, EDL and diaphragm). Immunoreactivity of the 2166 antibody resembled cytoskeletal structures, frequently surrounding the cell nucleus and extending into numerous filopodial or lamellipodial cellular processes that from time to time extended over the NMJ boundaries. Furthermore, immunoreactivity of the 2166 antibody also showed some extra-synaptic cells with a bipolar form in the vicinity of intramuscular nerves, running along the longitudinal axis of the muscle fibers and also associated with intramuscular capillaries. Further immunocytochemical analysis distinguished these novel cells from ShCs, satellite cells and macrophages (Court *et al.* 2008).

2.4 Function of the neuromuscular junction

The fundamental purpose of the NMJ is to transmit nerve impulses from the CNS in a 1:1 ratio via motoneurons to muscle fibers and trigger a cascade that leads to muscle contraction. This is enabled via several ligand- and voltage-gated ion channels in pre- and postsynaptic membranes, including the already reviewed presynaptic VDCCs and postsynaptic AChRs, and, additionally, voltage-gated Na^+ channels (Plomp *et al.* 2015, Slater 2008, Slater 2015).

When the axonal action potential propagated by a motoneuron from the spinal cord reaches the motor nerve terminal, it elicits an influx of calcium via VDCCs (Plomp *et al.* 2015, Slater 2015). The ensuing calcium influx triggers the release of ACh from the AChVs, that have been docked at the AZ via interaction with AZ proteins and the soluble *N*-ethylmaleimide-sensitive factor attachment protein receptor (SNARE)-complex (Ackermann *et al.* 2015, Rogers & Nishimune 2017, Slater 2015). The released amount of ACh is referred to as a quantal content which varies between muscles and is roughly correlated with the NMJ size (Plomp *et al.* 2015). As described earlier, AChRs are pentameric structures (α2βγδ, α2βεδ) and after release ACh is bound by each of the α subunits. Binding of the ACh briefly opens the central pore of the AChR and induces endplate current (EPC) inward to the muscle fiber (Plomp *et al.* 2015, Slater 2015, Tintignac *et al.* 2015). EPC results in local depolarization of the muscle membrane, called the endplate potential (EPP). The resting membrane potential of the muscle fiber is around -80 mV and the EPP increases the membrane potential to ~15-30 mV depending on muscle type and species. EPPs have a rapid rise-time (<1 ms) and a near-exponential decay phase of a few ms. If the EPP is high enough, which in rats and mice is generally about 20–35 mV, and exceeds the endplate depolarization threshold, it opens sodium channels that lie at the bottom of the postsynaptic folds. Opening of the sodium channels produces an action potential that spreads away from the NMJ in both directions around the muscle fiber membrane and invades the T-tubule of the muscle fiber. At the T-tubule an excitation-contraction coupling molecular machinery is activated and a few ms later muscle fibers contract (Plomp *et al.* 2015, Slater 2015, Tintignac *et al.* 2015).

In general, EPPs are much larger than the endplate depolarization thresholds on the muscle membranes, therefore enclosing a ‘safety factor’ (Plomp *et al.* 2015, Slater 2015, Tintignac *et al.* 2015). In other words, preterminal axons release much more quanta than needed for triggering the muscle contraction in response to the axonal action potential. The safety factor is required to compensate for the

decreasing quantal content in sustained muscle contractions where frequencies of nerve impulses range from 20-100 Hz and within the first 10 impulses EPPs have decreased by about 20-30% before reaching a plateau. The diminishing quantal content presumably results from a limit in the size and replenishment rate of the releasable AChV pool and inactivation of VDCCs. NMJ disorders are characterized by a decreased safety factor leading to muscle weakness (Engel *et al.* 2015, Plomp *et al.* 2015, Tintignac *et al.* 2015). Presynaptic membranes also release quanta in small amounts without electrical stimulus, causing a postsynaptic miniature EPP (MEPP), the frequency of which for example in mice is ~1-4/s (Plomp *et al.* 2015, Slater 2015, Tintignac *et al.* 2015). The physiological purpose of the MEPP activity remains a puzzle. However, *in vitro* studies with CNS neurons have suggested a role for MEPPs in the postsynaptic protein synthesis, thereby providing support for subsistence (Plomp *et al.* 2015, Tintignac *et al.* 2015).

2.4.1 Electrophysiological methods to detect functional abnormalities at the NMJ

Electrophysiological methods are powerful diagnostic and scientific tools recognizing the electrical properties of tissues and cells. In the field of neuromuscular physiology, these techniques are used to measure the electrical activity of muscles or even a single muscle fiber to gain valuable knowledge about neurotransmission and the possible origin of any neuromuscular defect. Some of the methods can distinguish between the pre- and postsynaptic aberrations and give precise knowledge about the units of neurotransmission. Electromyography (EMG) is a widely used application in clinics to study patients with muscle weakness while *ex vivo* methods harbor a more important role in their scientific use (Howard 2013, Plomp *et al.* 2015, Raez *et al.* 2006, Stalberg 1980).

In vivo electrophysiological methods

EMG detects the electrical signal resulting from action potentials that propagate along the muscle fibers. Action potentials are typically recorded via extracellular needle electrodes inserted in the muscle. Muscle action potential can be achieved by electrode stimulation of the innervating nerve or voluntary contraction. EMG electrodes can be set to record the summed action potentials of the firing muscle fibers, called compound muscle action potential (CMAP), in the vicinity of the electrodes or the action potential of a single muscle fiber. To detect NMJ

dysfunction, the nerve is repetitively stimulated during a train of 5-10 nerve stimuli at 2-5 Hz whereafter CMAP is recorded. Repetitive stimulation causes a physiological decrement of EPPs. In healthy NMJs the safety factor reassures the initiation of muscle action potentials, but if the safety factor is compromised it leads to EPPs that are below the endplate depolarization thresholds, thus resulting in a decrease in the amount of activated muscle fibers and CMAP. If the CMAP is decreased by more than 10%, a pre- or postsynaptic NMJ defect is diagnosed. Furthermore, a presynaptic defect can be indicated if prolonged high-rate stimulation (5-10 s at 20-50 Hz) or voluntary muscle activation for 10 s increases CMAP more than 2-fold from an initial low value. In some cases, the EPP amplitude is decreased to just above the endplate depolarization threshold and repetitive nerve stimulation EMG appears normal. To detect NMJ defects in these cases, single-fiber EMG is used (Howard 2013, Plomp *et al.* 2015, Raez *et al.* 2006, Stalberg 1980).

Single-fiber EMG measures a variation in the delay between a nerve stimulus and the muscle fiber action potential, and this variation is called jitter. Jitter can be measured from a single muscle fiber or from two muscle fibers belonging to the same motor unit during subsequent nerve stimulation. Some jitter occurs naturally, but if EPPs are decreased pathologically (but not below the endplate depolarization threshold) jitter increases (Howard 2013, Plomp *et al.* 2015).

Ex vivo electrophysiological methods

The function of the NMJ can also be studied at a single synapse level from freshly dissected muscle biopsies of patients or animal models. In suitable conditions, muscle biopsies can be kept viable for many hours and electrophysiological parameters can be recorded. Unfixed muscle fibers are pinned in a mildly stretched position on a silicone-rubber base in a preparation dish and electrodes are set under the microscope. Synaptic potentials vary considerably between different NMJs within the same muscle and due to this inter-NMJ variation a sufficient number of NMJs can be studied and a grand mean value formed from the individual NMJ means (Plomp *et al.* 2015, Sugiura *et al.* 2011).

First, the resting membrane potential of the muscle fiber and MEPPs are recorded. To calculate a meaningful mean MEPP amplitude, several MEPPs should be recorded due to natural variability in the amplitude of MEPPs. Furthermore, muscle samples are incubated with an agent that disallows formation of the muscle action potentials and nerves are stimulated at desired frequencies to measure EPPs.

The inter-NMJ variation of synaptic potentials largely results from varying muscle fiber resting membrane potentials and can be minimized by normalizing recorded amplitudes (MEPPs and EPPs) with a standard resting membrane potential of -75mV. Quantal content of a single NMJ can be calculated from the division of normalized and corrected mean EPP amplitude by normalized mean MEPP amplitude. During the rising phase of the EPP amplitude, the effect of each additive ACh quantum gradually lessens because of the declining membrane potential. Thus, to calculate a correct quantal content EPP amplitude has to be corrected for non-linear summation with a specific formula. Furthermore, the rundown of EPP amplitude due to repetitive nerve stimulation can be recorded with this system (Plomp *et al.* 2015, Sugiura *et al.* 2011).

2.5 Neuromuscular junction disorders

A wide range of NMJ disorders exist with varying etiology, but they are all characterized by muscle weakness and fatigability resulting from dysfunction in the transmission from the motor nerve to the skeletal muscle. Muscle weakness usually predominates in certain muscle groups and this preferentially affects proximal, bulbar or extraocular muscles and characteristically fluctuates in response to effort and rest. NMJ disorders can be categorized into immune-mediated, toxic/metabolic or congenital based on the pathological processes and classified as pre-, synaptic and postsynaptic, depending on the site of the molecule or complex affected. The two most commonly encountered NMJ disorders are immune-mediated myasthenia gravis (MG) and Lambert-Eaton myasthenic syndrome (LEMS). In addition, there is a large family of congenital myasthenic syndromes (CMSs) that include many specific genetic conditions affecting the proteins of the NMJ. Furthermore, many species of snakes, spiders and other organisms produce neurotoxins that paralyze muscles via blocking ion channel functions or causing impairment or enhancement of ACh release (Liang & Han 2013, Souza *et al.* 2016, Spillane *et al.* 2010).

Neuromuscular junction disorders not only affect neurotransmission but can also influence the histological appearance of the muscle. Thus, alongside electrophysiological testing, muscle histology is often used as a diagnostic tool to distinguish NMJ disorders from other diseases causing muscle weakness (Joyce *et al.* 2012). Myopathologic patterns can be divided into neurogenic and myopathic changes, where the former result from innervation/transmission failure and the latter from muscle-intrinsic factors (Climie 1973, Joyce *et al.* 2012). However, and

unfortunately for the diagnostics, it is not uncommon to have pathohistologic findings of both entities (Joyce *et al.* 2012). The earliest structural changes in neurogenic findings include loss of the polygonal shape of the muscle fibers and appearance of angulated muscle fibers (Climie 1973, Joyce *et al.* 2012). Furthermore, atrophy of both fast- and slow-twitch fibers is seen. In the later stages and if re-innervation happens from stronger motor units, muscle fibers change their twitch properties to match the innervating motoneuron properties. In other words, for example, slow-twitch muscle fibers can turn into fast ones and *vice versa* depending on the innervating nerve. This phenomenon is called fiber-type grouping. Moreover, permanent loss of innervation results in muscle fiber atrophy and eventually cell death leading to replacement of muscle fibers by fat and fibrous tissue in a process/phenomenon referred to as group atrophy. Another interesting neurogenic change is the presence of nuclear bags that appear as clumps of nuclei encircled by the remaining sarcolemmal membrane. If muscle fibers attempt regeneration, internal nuclei start to appear (Climie 1973). Myopathic changes include fiber size variation with both atrophied and hypertrophied muscle fibers that still keep their round appearance combined with early ingrowth of interstitial connective tissue and fat (Climie 1973, Joyce *et al.* 2012). Furthermore, these hypertrophied muscle fibers may be divided into two and referred to as split fibers (Joyce *et al.* 2012). In addition, focal fiber necrosis surrounded by focal inflammatory infiltrates is often seen in myopathies (Climie 1973). Other myopathic changes with specialized staining techniques can include red cytoplasmic inclusions (nemaline rods) with the modified G□m□ri trichrome and central cores with cytochrome c oxidase staining indicating loss of mitochondria (Sewry & Wallgren-Pettersson 2017). Major myopathologic patterns of neurogenic origin are represented in Fig. 6.

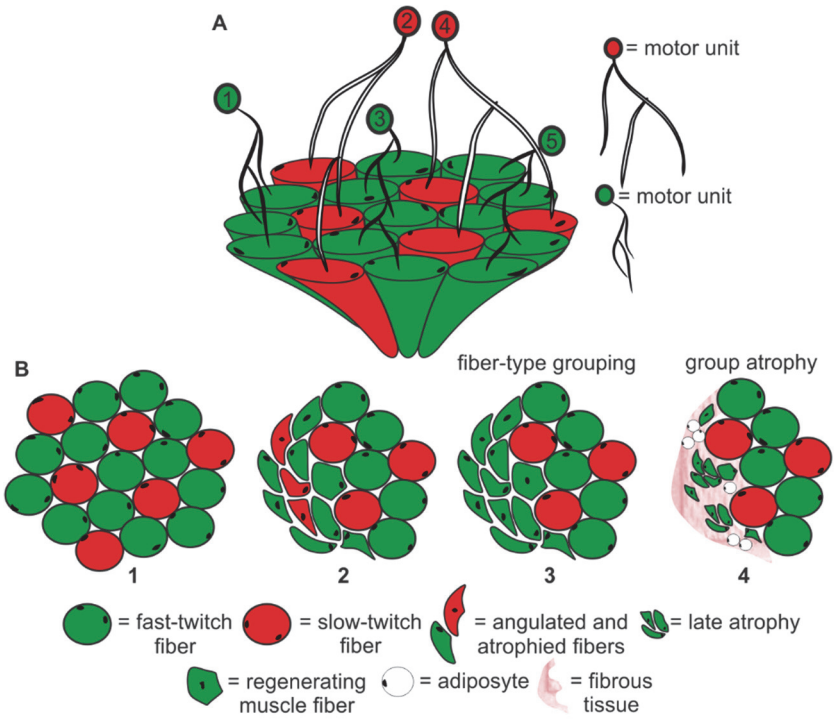

Fig. 6. Neurogenic muscle pathology. A) Overview of a fascicle containing fast (green)- and slow (red)-twitch motor units. B) 1; Normal appearance of muscle fibers. 2; If motor units 1-3 are denervated, muscle fibers become angulated and atrophied at early stage of denervation 3; At later stage and if re-innervation happens, "stronger" motor units innervate uninnervated muscle fibers and change their twitch properties to match their own. Here, the motor nerve 5 re-innervates muscle fibers (fiber-type grouping). Note the regenerating muscle fibers with central nuclei 4; Late atrophic state, where some muscle fibers are replaced by fat and fibrous tissue (group atrophy).

2.5.1 Immune-mediated neuromuscular junction disorders

Myasthenia gravis

MG is an autoimmune disease and the most common NMJ disorder. MG results from pathological autoantibodies against AChRs, MuSK and LRP4 on the postsynaptic endplates and synaptic agrin at the NMJ. It can be classified into subgroups based on the autoantibody profile, onset of the disease (early <50 and

late >50 years) and clinical presentation. In some cases of MG (less than 5%), patients lack circulating autoantibodies against the aforesaid molecules and this is referred to as seronegative MG. Interestingly, approximately 10-15% of the MG patients have thymoma and another 60% have thymic hyperplasia. The thymoma has been postulated to influence the initiation of the disease via multiple mechanisms including the expression of self-antigens by thymoma cells and impaired negative selection of autoreactive T lymphocytes (Gilhus & Verschuuren 2015, Gilhus *et al.* 2016, Ha & Richman 2015).

The incidence and prevalence rate of MG assessed from worldwide peer reviewed literature published from January 1990 up until July 2014 is 1/100000 and 10/100000 (Deenen *et al.* 2015). In other references, the worldwide prevalence is estimated at 40-180 and an annual incidence to be 4-12 per million people (Gilhus & Verschuuren 2015). Overall, MG is still considered a rare disease. Muscle weakness, the major symptom of MG, can be focal or generalized and often arises in the extraocular, bulbar, limb and axial muscles and is nearly always asymmetrical in extraocular muscles and symmetrical in limb muscles (Gilhus & Verschuuren 2015, Spillane *et al.* 2010). Furthermore, the limb weakness is more often proximal than distal. A high proportion of the MG patients have ocular manifestations as an initial symptom and the maximum progression to other muscle groups is reached within 3 years after onset in 85% of cases (Berrih-Aknin *et al.* 2014). 20-30% of the patients suffer from severe forms of MG that are characterized by an involvement of the respiratory muscles and severe swallowing disorders. Interestingly, patients with severe MG have been associated with additional autoantibodies, including antibodies against titin and voltage-gated K^+ and Ca^{2+} channels (Ha & Richman 2015). 60% of the MG patients suffer from diplopia, commonly known as double vision, or ptosis, a drooping of the upper eyelid, or both (Gilhus & Verschuuren 2015). In 20% of the MG cases the disease is restricted to ocular MG and considered mild. Onset of the symptoms vary, however. AChR-associated MG has an increasing peak of incidence within young adults aged 30 with a steadily increasing incidence rate after 50 years of age (Gilhus & Verschuuren 2015).

About 85-90% of the generalized MG cases result from complement binding IgG_1 and IgG_3 AChR autoantibodies (Berrih-Aknin *et al.* 2014, Ha & Richman 2015). These AChR autoantibodies block ACh binding sites and inhibit the opening of the ion channels, accelerate endocytosis and degradation of AChRs by cross-linking AChRs, and cause complement-mediated damage to the entire muscle endplate (Ha & Richman 2015).

Approximately 1-10% and 1-5% of the MG patients have autoantibodies against MuSK and LRP4, respectively (Gilhus *et al.* 2016). Most autoantibodies against MuSK belong to the IgG_4 subclass without the capability to bind complement and interfere MuSK functions via inhibition of the MuSK-ColQ and MuSK-LRP4 complexes. Autoantibodies against MuSK reduce AChR density and impair the pre- and postsynaptic alignment. Based on mouse studies, LRP4 autoantibodies are mainly of the complement-binding IgG_1 subclass and pathophysiology results from disruption of the interaction between LRP4 and agrin, and inhibition of AChR-mediated neurotransmission. Coexistence of AChR and MuSK autoantibodies in the same patient is rare and LRP4 autoantibodies are primarily found without AChR or MuSK antibodies (Gilhus & Verschuuren 2015, Gilhus *et al.* 2016).

Lambert-Eaton myasthenic syndrome

LEMS is a rare autoimmune disease affecting the presynaptic sites of the NMJ with pathological autoantibodies against VDCCs. LEMS can be idiopathic but in 50-60 percent of the cases LEMS occurs as a paraneoplastic syndrome with a small cell lung carcinoma (SCLC) as the most common tumor. The mean onset age of the disease is around 60 years in tumor-related cases and bimodal with two peaks of onset at around 35 and 60 years of age in non-tumor-related cases. Muscle weakness in LEMS predominantly affects proximal muscle groups and initial symptoms include proximal leg muscle and arm weakness. As the disease progresses, weakness generally spreads from the proximal to distal and from caudal to cranial muscle groups of the body. In addition to the muscle weakness, autonomic dysfunction (xerostomia=dryness in the mouth, erectile dysfunction, constipation, and hypohidrosis=diminished sweating in response to appropriate stimuli) and areflexia are characterizing symptoms of LEMS (Hulsbrink & Hashemolhosseini 2014).

About 85-90% of the LEMS patients harbor autoantibodies against P/Q-type VDCCs and some patients have autoantibodies against N- and L-type VDCCs as well. These autoantibodies decrease ACh release from the presynaptic membrane via blocking calcium influx during depolarization and/or down-regulating VDCCs. Furthermore, patients with LEMS and mouse models lacking P/Q-type and N-type VDCCs show reduced numbers of AZs and docked vesicles further explaining the reduction of the neurotransmitter release in LEMS. Down-regulation of VDCCs also impairs transmitter release from parasympathetic and sympathetic neurons and

explains the autonomic dysfunction in LEMS (Hulsbrink & Hashemolhosseini 2014).

2.5.2 Congenital myasthenic syndromes

CMSs are a diverse and wide group of rare genetic disorders, where impaired neuromuscular transmission results from mutations in the genes encoding NMJ molecules and can be classified into presynaptic, synaptic and postsynaptic based on the site of the affected NMJ component (Engel *et al.* 2015). To date, more than 20 different genes have been linked to the development of different CMS forms and these mutations can be inherited in an autosomal recessive or an autosomal dominant manner. Some patients suffering from the autosomal dominant CMS carry a *de novo* pathogenic variant. Accurate prevalence rates of the CMSs are hard to determine because of the wide group of distinct neuromuscular disorders with clinical variability and diagnostic challenges. However, genetically confirmed cases in the UK reach at least 3.8 per million (Hantai *et al.* 2013) and 9.2 cases per million children under 18 years old in the population (Souza *et al.* 2016).

Postsynaptic forms of CMS constitute about 75-80 percent of the CMS cases, 14-15% are of synaptic origin and 7-8% are presynaptic (Lorenzoni *et al.* 2012). The most common clinical manifestation of CMS is early-onset fatigable muscle weakness and it mainly involves ocular, bulbar and proximal limb musculature (Souza *et al.* 2016). However, in some cases muscle weakness can appear in adolescence or adulthood. Usually CMS patients harbor a positive family history of a specific disorder or a history of hypotonic infant and decremental responses in EMG studies or a single-fiber EMG showing NMJ dysfunction (Souza *et al.* 2016).

Postsynaptic syndromes

Most common causes of postsynaptic CMSs (34-50%) are mutations in genes encoding AChR subunits which can reduce the amount of AChRs or influence the channel kinetics by prolonging or shortening the opening time (slow-channel and fast-channel syndrome, respectively) (Engel *et al.* 2015, Rodriguez Cruz *et al.* 2014, Souza *et al.* 2016). As already reviewed, mature AChR consist of four different subunits: α2βεδ encoded by *CHRNA1*, *CHRNB1*, *CHRND* and *CHRNE*, respectively (Rodriguez Cruz *et al.* 2014). Most commonly, mutations lead to AChR deficiency and clinical symptoms include severe muscle weakness of the limbs, ptosis and ophthalmoparesis (Rodriguez Cruz *et al.* 2014, Souza *et al.* 2016).

Slow-channel syndromes resemble in many aspects the AChE deficiency and fast-channel syndromes mimic MG, with both starting in the first decade of life (Souza *et al.* 2016). Other postsynaptic CMSs arise from mutations in genes encoding proteins important for NMJ development and maintenance, including *RAPSN* (~14% of the postsynaptic CMS cases), DOK7 (~10% of the postsynaptic CMS cases), *LRP4* (~0.6% of the postsynaptic CMS cases), *MUSK* (~0.3% of the postsynaptic CMS cases) and *COL13A1* (Logan *et al.* 2015, Rodriguez Cruz *et al.* 2014, Souza *et al.* 2016).

Synaptic syndromes

Mutations in the *COLQ* and *LAMB2* genes are known to cause synaptic CMSs. Mutations in *COLQ* cause endplate AChE deficiency leading to prolonged synaptic currents and action potentials, which in turn desensitize AChRs and produce a secondary myasthenic syndrome and it is the cause of ~12.6% of the CMS cases. Mutations in the *LAMB2* gene are extremely rare and to date have been found in only one patient suffering from CMS (Engel *et al.* 2015, Souza *et al.* 2016).

Presynatic syndromes

Mutations in *CHAT* coding for choline acetyltransferase (ChAT) are the most common causes of presynaptic CMS (Engel *et al.* 2015). ChAT is an enzyme in cholinergic neurons catalyzing ACh (re)synthesis from coenzyme A and choline, and its deficiency results in incomplete filling of the AChVs. ChAT deficiency leads to sudden episodes of breathing suspension (apnea) and can occur at birth or be developed during infancy or childhood. These children can also be hypotonic at birth, but apnea can appear without clear signs of myasthenia. Apneic episodes can be provoked by stress and, in some children, lead to ventilatory failure for weeks. Other known causes of the presynaptic CMS are mutations in SNAP25B (encoding synaptosomal-associated protein of 25kD, splice variant B) and in the calcium-binding domain of synaptotagmin 2 (Engel *et al.* 2015, Shen *et al.* 2014). SNAP25 is a component of the SNARE-complex and with syntaxin it forms a t-SNARE-complex that participates in vesicle anchorage and the exocytosis process (Shen *et al.* 2014).

Table 2. CMS subtypes and corresponding affected genes. Modified from Engel *et al.* 2015 and Rodriguez Cruz *et al.* 2014.

CMS subtypes	Gene affected/mutated
Postsynaptic syndromes	
Primary AChR deficiency	CHRNA1, CHRNB1, CHRND and CHRNE
Slow-channel syndrome	CHRNA1, CHRNB1, CHRND and CHRNE
Fast-channel syndrome	CHRNA1, CHRNB1, CHRND and CHRNE
Agrin	AGRN
MuSK	MUSK,
LRP4	LRP4
Rapsyn	RAPSN
DOK7	DOK7
Collagen XIII	*COL13A1*
Synaptic syndromes	
AChE deficiency	COLQ
Laminin β2 deficiency	LAMB2
Presynaptic syndromes	
ChAT deficiency	CHAT
SNAP25B	SNAP25
Synaptotagmin-2	SYT2

Congenital myasthenic syndrome type 19

Mutations in *COL13A1* have been recently linked to causing a novel CMS referred to as congenital myasthenic syndrome type 19 (CMS19, OMIM:616720). When WES was performed on 15 CMS patients without known etiology, 3 patients were discovered to harbor two different mutations in the *COL13A1* gene. One female individual with a homozygous frameshift variant and one female and one male with a homozygous splice-site mutation, were expected to allow splicing but instead it was reported that this led to premature termination due to a single-base deletion in the coding sequence. At the time of study, the female individual with the homozygous frameshift variant was 2-years-old, the male individual with the homozygous splice-site mutation was 27-years-old and the female individual with the latter mutation had already died at the age of 8 years. Both mutations led to increased jitter in stimulated single-fiber EMG and decrement of the CMAP in repetitive nerve stimulation as a sign of impaired neurotransmission (Logan *et al.* 2015).

Clinically these mutations affected bulbar, axial and limb muscles and led to weakness exemplified by feeding and breathing problems starting soon after birth.

Despite the presence of severe defects in the muscle function, muscle morphology analyzed at the age of 6-12 months from two individuals remained relatively normal except for a mild variation in the fiber size, a few central nuclei and the presence of fetal Myosin. Whole-muscle MRI assessed from the female individual carrying the homozygous frameshift variant mutation did not show muscle atrophy at the age of 2 years, but the homozygous splice-site mutation in the other female patient led to reduced muscle bulk assessed clinically at the age of five. Other clinical and common features of both mutations included low-set ears, micrognathia, high-arched palate and pectus carinatum (barrel chest). Furthermore, both individuals with the homozygous splice-site mutation suffered from recurrent chest infections and the female individual developed a chronic lung disease. It was suggested that the death of the female individual with the homozygous splice-site mutation resulted from severe respiratory problems related to muscle weakness and chronic lung disease (Logan *et al.* 2015).

To further understand the role of collagen XIII at the NMJ, Logan *et al.* conducted antibody staining of the NMJs and introduced the homologous *COL13A1* frameshift mutation into the immortalized mouse myoblast C2C12 cell line. Antibodies against the collagen XIII C-terminal region showed loss of the collagen at the NMJ in 8-10 μm thick quadriceps muscle frozen in sections from one individual that harbored the homozygous frameshift variant; however, other key NMJ proteins (synaptophysin to show preterminal endplate, S100 calcium-binding protein B to show terminal ShCs, α-bungarotoxin to show AChR clusters, fasciculin to show AChE and antibodies against DOK7 and MuSK) had normal localization at the age of 6 months. The homozygous frameshift mutation *in vitro* did not affect the average size of AChR clusters but decreased the number of AChR clusters longer than 3 μm by approximately 50%. Furthermore, protein and RNA studies conducted with human laryngeal muscle extracts from unaffected individuals indicated that the endogenous muscle protein was produced from the *COL13A1* transcript variant 21 (exons 3, 5, 6 and 30 spliced out). Still, the exact mechanism by which collagen XIII conducts its NMJ-related effects remained enigmatic and the integrin α1 subunit was postulated as one potential interacting partner (Logan *et al.* 2015).

2.5.3 Treatment of the neuromuscular junction disorders

Many different drugs are used alone or in combination to manage and ease the symptoms of patients suffering from an NMJ disorder. The selection of drugs

depends on the pathophysiology of the NMJ disorder highlighting the importance of correct diagnosis and studies in the field of NMJ disorders. Many symptomatic drugs enhance the activation of AChRs by increasing the availability of ACh at the synaptic cleft with different mechanisms. For example, the AChE inhibitors inhibit degradation of ACh at the synaptic cleft and 3,4-diaminopyridine (3,4-DAP) blocks neuronal efflux through K^+ channels, prolongs the duration of action potential and the opening of VDCCs, and leads to increased release of ACh (Gilhus *et al.* 2016, Hulsbrink & Hashemolhosseini 2014). The AChE inhibitors include pyridostigmine, neostigmine and ambenonium chloride (Gilhus *et al.* 2016). The AChE inhibitors are the first-choice drugs for all MG subtypes and used alone or in combination with 3,4-DAP in LEMS (Gilhus *et al.* 2016, Hulsbrink & Hashemolhosseini 2014). AChE inhibitors are also used to help symptoms of different CMS patients including ChAT deficiency and in combination with 3,4-DAP in primary AChR deficiency, fast-channel syndrome and rapsyn deficiency (Engel *et al.* 2015). However, 3,4-DAP is the first choice for symptomatic treatment in LEMS and in CMS due to SNAP25B deficiency (Engel *et al.* 2015, Hulsbrink & Hashemolhosseini 2014). Furthermore, it is worth noting that the AChE inhibitors and 3,4-DAP can be ineffective or even harmful for some type of CMS including slow-channel syndromes, Dok7 deficiency and AChE deficiency (Engel *et al.* 2015). In addition to the AChE inhibitors and 3,4-DAP, adrenergic agonists, such as salbutamol and ephedrine, and open-channel blockers of AChRs are used in the symptomatic treatment of certain CMS subtypes (Engel *et al.* 2015). For example, 3,4-DAP and salbutamol produced a remarkable improvement in the motor and respiratory functions of one patient suffering from CMS19, while pyridostigmine had no effect on any of the patients (Logan *et al.* 2015).

Immune-mediated or cancer-related NMJ disorders can be further treated with immunosuppressive agents or cancer-therapies, respectively (Gilhus *et al.* 2016, Hulsbrink & Hashemolhosseini 2014). Immunosuppressive drug therapy suppresses the autoantibody production and is used in almost all MG subtypes and in LEMS if symptoms are not controlled by symptomatic treatment. Thymectomy has been proven to benefit only thymoma-associated MG and early-onset MG patients (Gilhus *et al.* 2016). Furthermore, surgical removal of SCLC in paraneoplastic LEMS usually significantly improves NMJ-related symptoms and the tumor treatment is considered to be of the highest priority (Hulsbrink & Hashemolhosseini 2014).

2.6 Mouse as a model organism to study the NMJ

The house mouse, *Mus musculus*, has a long history in the understanding of biological phenomena and is widely in use as a disease model because of its phylogenetic relatedness and physiological similarities to humans (Perlman 2016). Furthermore, mice are relatively easy and inexpensive to maintain and breed. However, many aspects of the mouse differ from humans; for example mice are roughly 2500 times smaller than humans, have a much shorter life expectancy (the mouse has a life span of about 3–4 years), reach sexual maturity at the age of 6-8 weeks, have a shorter gestation period of 19-20 days and about a 7-fold higher metabolic rate. From the point of view of NMJs, mice and humans both share common features yet also present some differences (Slater 2008).

The morphology of mouse NMJs is characterized by a pretzel-shape where as human NMJs consist of small boutons of postsynaptic specializations interconnected with terminal axon branches forming a spot-like appearance (Plomp *et al.* 2015). Human NMJs are also relatively small compared to NMJs in mice but harbor increased postsynaptic surface area through denser muscle membrane folding compared to mouse NMJs (Slater 2008). Furthermore, the quantal content of the human NMJ is about 50-73% smaller than in the mouse NMJs, resulting in a low safety factor (Plomp *et al.* 2015, Slater 2008). The low safety factor in humans has been postulated to be compensated by the relatively deep postsynaptic folding that increases the depolarizing effect of ACh quanta (Plomp *et al.* 2015). Despite their differences, these species share 99% of their genes (Rosenthal & Brown 2007). Moreover, proteomic studies have revealed a more than 70% overlap in the human and mouse postsynaptic proteins in the CNS and the same important molecules for the NMJ development and maintenance have been found in both species (Bayes *et al.* 2012). Furthermore, several mouse models harboring neuromuscular phenotypes similar to human diseases have been identified in nature or generated in a laboratory and used to increase knowledge of human diseases (Vainzof *et al.* 2008).

All in all, considering the accessibility (short generation time, large litters), availability of transgenic technologies (monogenetic disease models either overexpressing/lacking specific proteins), inbred backgrounds (providing uniform experimental conditions), relatively easy maintenance and phylogenetic relatedness to humans, the mouse is a good model for studying human diseases and the NMJ (Vaquer *et al.* 2013).

3 Outlines of the present study

When this study was started, mouse and *in vitro* studies had indicated collagen XIII to be a muscle-derived component of the NMJ. Loss of collagen XIII delayed postsynaptic maturation, impaired AChV accumulation, compromised adhesion of the nerve and muscle, and, importantly, disturbed the function of the NMJ in *Col13a1*$^{-/-}$ mice. Subsequent studies have revealed human mutations in *COL13A1* affecting neuromuscular transmission and leading to the development of early-onset CMS19. Indeed, such mutations are the only ones so far recognized in *COL13A1*. Thus, deficiency of collagen XIII leads to abnormalities at the NMJ, yet the mechanism behind these alterations has remained unknown and a further intriguing question is posed by the possibility of distinct roles of the transmembrane and shed forms of collagen XIII in this process.

At the commencement of this thesis study a novel *Col13a1*$^{tm/tm}$ mouse line harboring a mutation in the furin-type proprotein convertase recognition sequence in exon two of the *Col13a1* gene had already been generated. This line was designed in order to examine potential differential roles of the transmembrane and shed collagen XIII, but the *Col13a1*$^{tm/tm}$ mice had not yet been analyzed before the present work. Furthermore, transgenic overexpression of collagen XIII in the *Col13a1*^{oe} mouse line was known to result in excess bone formation clearly seen at the age of 3-4 weeks and onwards. However, precise information on collagen XIII overexpression and its effect on the NMJ and muscles of these mice was lacking.

The following goals were set for this doctoral project;

1. To confirm that the targeted mutation of the furin-type proprotein convertase recognition sequence in exon two of the *Col13a1* gene enables expression but prevents collagen XIII ectodomain shedding, leading to the expression of only transmembrane collagen XIII in *Col13a1*$^{tm/tm}$ mice.
2. To analyze the maturation and function of the NMJ in the *Col13a1*$^{tm/tm}$ mice and compare the findings with the *Col13a1*$^{-/-}$ mice.
3. To further deepen knowledge about the effects of total loss of collagen XIII on the NMJ in the *Col13a1*$^{-/-}$ mice, and, following the report of *COL13A1* mutations in CMS19, to compare the results of mouse models with findings in the human disease.
4. To elucidate the expression profile and effects of the transgenic overexpression of collagen XIII at the NMJs and muscles of *Col13a1*^{oe} mice.

4 Materials and methods

4.1 Generation and maintenance of mice

The *Col13a1*$^{tm/tm}$ mouse line was generated by targeting with a vector containing a selection cassette flanked by LoxP sites in the first intron and an –RRRR– to –ATAA– mutation in the exon two to delete a furin type proprotein convertase recognition sequence. Mice were backcrossed to C57BL/6 background and the selection cassette was removed by breeding with Tg(CAG-cre)13Miya mice (Sakai & Miyazaki 1997). Generation of the two other C57BL/6 backcrossed mouse lines, collagen XIII knock-out and transgenic overexpression mice, have been described earlier (Latvanlehto *et al.* 2010)(Ylönen *et al.* 2005). Permission to maintain mice was granted by the Finnish Animal Care and Use Committee. All the mouse experiments followed the European Community Council Directive (September 22, 2010; 2010/63/EEC), national legislation and the regulations for the care and use of laboratory animals. Mice were maintained in a conventional or SPF facility in the University of Oulu. Mice of both sexes were used in the experiments and wild-type littermates were used as controls. Schematic presentation of the collagen XIII proteins in the mouse lines used in this thesis work are represented in Fig. 7.

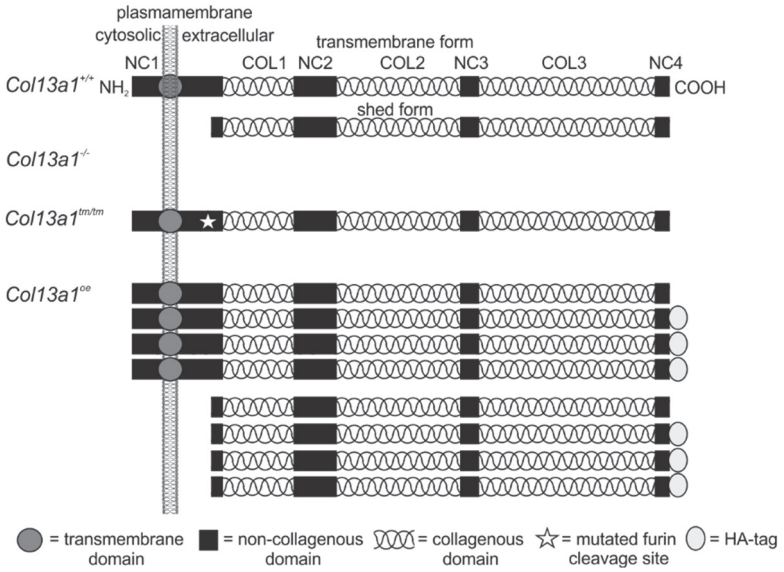

Fig. 7. Schematic presentation of the collagen XIII proteins in the mouse lines used.

4.2 Tissue transcript and protein level analyses

Total RNA and whole tissue proteins as well as proteins from E13.5 mouse embryonal fibroblast cultures were extracted using the Tri Reagent system (Sigma-Aldrich). Extracted proteins and precipitated culture media were run in 8 % reduced SDS-PAGE gels and blotted with primary and secondary antibodies. Total RNA was used for reverse transcription with iScript^{tm} cDNA Synthesis Kit (Bio-Rad) and quantitative real-time PCR using iTaq^{tm} Universal SYBR® Green Supermix kit (Bio-Rad) according to the manufacturers' protocols.

4.3 Cell Culture

To establish mouse embryonic fibroblasts E13.5 embryos from heterozygous matings were dissected out, and the head and hematopoietic organs were removed. The trunk was cut into small pieces and incubated in 0.25 % trypsin/PBS containing 100 µg/ml DNase for 15 min at +37 °C in a 1 ml volume. The cells were plated on 10 cm dishes with 10 % FBS, 1 % non-essential amino acids, 1 % penicillin and 1 % streptomycin/DMEM, and the medium and cells were collected at passage two. The cells were lysed with PBS-0.1 % Triton X-100 and proteins in the medium were precipitated with an equal volume of methanol at -20 °C. Proteins were run in 8 % reduced SDS-PAGE gels and blotted with a rabbit anti-mouse collagen XIII antibody (ColXIII/NC3) (Kvist *et al.* 2001).

4.4 Histochemistry and morphometric analyses

Muscle cryosections were stained with hematoxylin & eosin (H&E) and imaged using a Leica Histology Microscope. Sections were stained with anti-fast and -slow Myosin heavy chain antibodies (fMHC/sMHC; Sigma-Aldrich) and tiled images were captured with a Zeiss Cell Observer spinning disc confocal microscope. Muscle fiber area and fiber type distribution was determined using ImageJ 1.48V software.

4.5 Histochemical detection of AChE and nerve pattern analysis

For overall nerve pattern analysis diaphragm muscles were collected at P84 and freshly imaged with a Leica Microsystems microscope and analyzed with ImageJ 1.48V software. For histochemical detection of AChE diaphragm muscles were

collected at P84 and freshly incubated with the staining solution containing (in mM): 5 acetylthiocholine iodide, 40 glycine and 8 $CuSO_4$ (added lastly and slowly to prevent precipitation)/120 phosphate buffer, pH 6.4 (Karnowsky & Roots 1964). After a 1 hour-incubation at RT samples were mounted on microscopic glass slides with Thermo Scientific™ Shandon™ Immu-Mount™ (Fisher Scientific) anti-bleaching reagent and imaged with a Leica Microsystems microscope and analyzed with ImageJ 1.48V software.

4.6 Whole mount immunofluorescent staining

To study the postsynaptic development in the *Col13a1*$^{tm/tm}$ and *Col13a1*^{oe} mice, diaphragm muscles at P0, P14, P28, P56, P84, P182 and P525 (the latter time point only in I) were dissected, fixed with 4 % PFA/PBS o/n at +4 °C and immunostained as a whole mount with α-BTX to show AChR clusters, and muscles/NMJs in the wild-type; collagen XIII knock-out mice were used as a reference. For further immunofluorescent staining and co-location analyses fresh muscle samples were fixed with 2 % PFA/PBS 10 min at RT and immediately stained as whole mount with primary antibodies followed by Alexa Fluor-conjugated (Molecular Probes, Invitrogen) secondary antibodies in combination with Alexa Fluor-conjugated α-Bungarotoxin (α-BTX; Biotium and Molecular Probes, Invitrogen) or Fasciculin II (Fasc II; Latoxan). All immunostainings were imaged using an Olympus FV1000 scanning confocal microscope, a Zeiss Cell Observer spinning disc confocal microscope or a Zeiss LSM 780 laser scanning confocal microscope, and the NMJ size and fragmentation was analyzed by ImageJ 1.48V software.

4.7 Ultrastructural analyses

1 x 1 mm pieces of the diaphragm muscle at NMJ-rich areas were fixed with 1 % glutaraldehyde, 4 % PFA/100 mM phosphate buffer, pH 7.3 o/n at +4 °C after which they were postfixed with 1 % osmium tetroxide, dehydrated in acetone, and embedded in Epon LX112. Samples were cut in semi-thin sections and after further selecting NMJ-rich areas thin sections were prepared and analyzed with a Tecnai G2 Spirit 120 kV transmission electron microscope (TEM) with Veleta and Quemesa CCD cameras and a Philips CM100 equipped with a CCD camera.

4.8 *Ex vivo* endocytosis

Immediately after euthanasia the diaphragm muscle from P84 mice was gently pinched on a Sylgard dish in ice-cold Ca-free Ringer solution containing (in mM): 138 NaCl, 5 KCl, 1 $MgCl_2$, 1 EGTA, 11 glucose, 5 HEPES, pH 7.2. Vesicle cycling was induced with High KCl/Ringer solution containing (in mM): 93 NaCl, 50 KCl, 2 $CaCl_2$, 1 $MgCl_2$, 11 glucose, 5 HEPES, pH 7,2 in the presence of 5 µg/ml FM 1-43X lipophilic dye (Molecular Probes, Invitrogen) and Alexa Fluor 594-conjugated α-BTX for 15 min at RT (Denker *et al.* 2011). Samples were briefly rinsed with Ca-free Ringer solution and post-fixed with 4% PFA/Ringer solution containing (in mM): 138 NaCl, 5 KCl, 2 $CaCl_2$, 1 $MgCl_2$, 11 glucose, 5 HEPES, pH 7.2 for 20 min at RT. After two short rinses with Ringer solution, samples were mounted on microscopic glass slides with Thermo Scientific™ Shandon™ Immu-Mount™ (Fisher Scientific) anti-bleaching reagent and imaged with an Olympus FV1000 scanning confocal microscope on the same day or on the following day at the latest.

4.9 Electrophysiological measurements *ex vivo*

Electrophysiological recordings were made from diaphragm muscles *ex vivo* at RT. Mice were euthanized and diaphragms were immediately dissected into 2-4 muscle strips with 4–12 synapses. Release of the readily releasable pool of transmitters was induced by 500 mM sucrose. EPPs were induced by the suprathreshold stimulation of the phrenic nerve. EPPs (recorded at the membrane potential ~40-45 mV) and MEPPs (recorded at the membrane potential ~70-72 mV) digitized at 50 kHz were recorded using a low-noise custom-made amplifier and acquired for the PC using the data acquisition board NI PCI6221 (National Instruments) and visualized with the WinEDR V3.0.4 software (Strathclyde University, Glasgow, Scotland, UK). Amplitudes of EPPs and MEPPs, and interevent intervals of MEPPs were analyzed off-line with the WinEDR V3.0.4 and ClampFit V10.2.0.14 (Molecular Devices) software.

4.10 Grid hanging

Mice were placed on a wire-rack with 1 x 1 cm grids, inverted slowly, placed at a height of 30 cm where- after latency to fall was measured. 5 minutes was set as a maximum hanging time. 3,4-DAP in saline (1 mg/kg) was injected intra

peritoneally and the hanging time was evaluated 10 to 20 minutes later (Shi *et al.* 2014). The same was repeated the following day with a saline injection.

4.11 Binding assays

Globular AChE dimer, tetramer, and asymmetric collagen-tailed forms were extracted and purified from *Torpedo californica* or *Electrophorus electricus* (Dudai *et al.* 1972, Dudai *et al.* 1973, Lwebuga-Mukasa *et al.* 1976, Sussman *et al.* 1988). All the samples were extracted by sedimentation in 5-20 % sucrose gradients. Recombinant human collagen XIII or its pepsin-resistant collagenous domains (Tu *et al.* 2002) was coated onto the surface of a 96-well plate (MaxiSorb, NUNC). Diluted AChE samples were incubated on wells coated with either collagen XIII or control proteins and after washing bound AChE was evaluated by the Ellman's AChE activity assay using acetylthiocholine as a substrate (Ellman *et al.* 1961) by measuring products at 405 nm using a Victor Multilabel Plate Reader® (PerkinElmer).

4.12 Statistical analyses

The data is presented as mean ± SEM mouse-wise calculated, if not otherwise stated. Normality of the data was evaluated using the Kolmogorov–Smirnov test. Statistical significance of normally distributed data was calculated by the unpaired, two-tailed t-test, and for non-parametric data, or if the sample number was too small for evaluating normality, the Mann-Whitney test was used. Statistical analyses were performed using the Prism (GraphPad Software, Inc.) and Origin graphic software (v.8.0, OriginLab Corp.). Statistically significant differences are indicated as *$p<0.05$, **$p<0.01$ and ***$p<0.001$.

5 Results

5.1 Collagen XIII is not shed in a novel *Col13a1*$^{tm/tm}$ mouse model and transmembrane form alone is present (I)

To further elucidate the roles of both transmembrane and shed collagen XIII, a novel mouse model was generated in which the furin-type pro-protease convertase recognition sequence required for shedding (Snellman *et al.* 2000b) was mutated (Original publication I (I), Fig. 2A and B). Protein analysis of wild-type and *Col13a1*$^{tm/tm}$ tissues (kidney and lung) showed one or two high-mobility band(s) representing the transmembrane form(s) of collagen XIII (I, Fig. 2C). In contrast to wild-type tissues, where the shed form detected as a lower molecular weight band(s) was present, the band was absent in all *Col13a1*$^{tm/tm}$ tissues studied. To further analyze shedding in *Col13a1*$^{tm/tm}$ mice, embryonic day 13.5 mouse fibroblast (MEF) cultures were established. Shed collagen XIII could be only found in the wild-type conditioned medium while it was lacking in the *Col13a1*$^{tm/tm}$ medium (I, Fig. 2D). The cell lysates of both genotypes contained the transmembrane form of collagen XIII. Furthermore, collagen XIII mRNA expression was slightly, but not significantly decreased in P84 muscles of the *Col13a1*$^{tm/tm}$ mice varying from 73 % to 93%, when compared to controls (I, Fig. 2E and F). Western blots revealed relative amounts of total collagen XIII protein in comparison to the wild-type controls to be 133% and 16% in the *Col13a1*$^{tm/tm}$ diaphragm and soleus muscles, respectively (I, Fig. 2G-J). In the wild-type muscles the proportion of the transmembrane form was about 20% of the total collagen XIII amount and in the *Col13a1*$^{tm/tm}$ soleus the transmembrane form occurred at roughly normal levels, although the overall total collagen XIII protein level was reduced. In the diaphragm, with a slightly increased total collagen XIII level, there was a 5.6-fold increase in the amount of the transmembrane form compared with wild-type. The *Col13a1*$^{tm/tm}$ mice were macroscopically normal and fertile, and had a normal life-span accompanied by a significant decrease in body weight at aging (I, Fig. S2A).

5.2 Collagen XIII overexpression in the muscles of *Col13a1*^{oe} mice (II)

The muscles of the *Col13a1*^{oe} mice have been shown to overexpress collagen XIII (Ylönen *et al.* 2005) and to reveal possible muscle and NMJ phenotypes; three

different muscles, the respiratory muscle diaphragm, the mainly slow-twitch muscle soleus and the mainly fast-twitch muscle extensor digitorum longus (EDL) were studied at P84. Compared to the wild-type controls transcript levels of *Col13a1* in all muscles studied revealed in the *Col13a1*^{oe} mice a significant 28-fold increase in the diaphragm, 2-fold in the soleus muscle and 6-fold in the EDL (Original publication II (II), Fig. 1B). The total collagen XIII protein levels were in line with the transcript levels by being clearly elevated by 20- and 6-fold in the diaphragm and EDL muscles, respectively, but comparable to the wild-type in the soleus, possibly reflecting the lowest difference at RNA level (II, Fig. 1F). Protein analyses of wild-type mice revealed that about 20% of the total collagen XIII exists as transmembrane form and about 80% is shed in the diaphragm and soleus while both forms represented about 50% in the EDL (II, Fig. 1G-I). In the *Col13a1*^{oe} mice shedding of exogenous collagen occurred with similar efficacy in the soleus and EDL muscles, while shedding of total collagen XIII in the diaphragm was decreased from 80% to 54% suggesting insufficient shedding in such a dramatic overexpression (II, Fig. 1G-I).

5.3 Collagen XIII location at the NMJ (I, II)

To analyze the location of collagen XIII at the NMJ, the diaphragm, soleus and EDL (the latter studied only in II) muscles of 12-week-old wild-type, *Col13a1*$^{tm/tm}$ (studied only in I), *Col13a1*$^{-/-}$ and *Col13a1*^{oe} (studied only in II) mice were dissected, fixed and immunostained as whole mounts with an anti-collagen XIII antibody and α-BTX to show the AChR clusters. In all muscles studied collagen XIII was located at the NMJs, indicated by α-BTX, in the wild-type, *Col13a1*$^{tm/tm}$ and *Col13a1*^{oe} mice in a spot-like manner but not in the *Col13a1*$^{-/-}$ mice as expected (I, Fig. 2K-L and Fig. S3A-C and II, Fig. 1J-L). In the *Col13a1*$^{tm/tm}$ mice the collagen XIII staining was strongest at the borders of the NMJs in the diaphragm and soleus muscles. Unexpectedly, the immunoreactivity of collagen XIII was for the most part comparable with the wild-type controls in the *Col13a1*^{oe} mice at the AChR positive postsynaptic areas in all muscles studied (II, Fig. 1J-L). However, the collagen XIII immunoreactivity was clearly detected to be increased at some NMJs adjacent to the AChR-positive areas in the diaphragm and EDL muscles of the *Col13a1*^{oe} mice compared to controls but not exactly co-localizing with the AChR positive areas (referred to as perijunctional collagen XIII immunoreactivity at the NMJs) (II, Fig. 1J-L). The perijunctional collagen XIII immunoreactivity showed a diffuse staining pattern and in some cases extended to the postsynaptic

apparatus with similar morphology as the presynaptic structures. Interestingly, in the diaphragm of the *Col13a1*^{oe} mice we also found NMJs without postsynaptic or perijunctional collagen XIII immunoreactivity (II, Fig. 1J), and by rough estimation this was the case in one third of the NMJs. This may signify the association of transgene polypeptides with endogenous ones, and such heterotrimers possibly being unstable in the cells and hence not detectable. Further immunostainings with an anti-HA-tag antibody, detecting specifically the transgene collagen XIII products, revealed no immunoreactivity co-localizing with AChR positive areas of the *Col13a1*^{oe} mice in the studied muscles and the tag signal was found mainly perijunctional in the diaphragm and EDL muscles (II, Fig. 2A-C).

5.4 Exogenous collagen XIII expression in the *Col13a1*^{oe} mice is mainly extrasynaptic (II)

Unexpectedly and despite highly increased transcript and protein levels of collagen XIII in the selected muscles of the *Col13a1*^{oe} mice, the excess collagen XIII did not accumulate at the AChR positive areas at the NMJs. Instead and in addition to perijunctional collagen XIII immunostaining in the diaphragm and EDL muscles, the collagen XIII immunoreactivity was found extrasynaptically to be clearly elevated at the myotendinous junction (MTJ) of the diaphragm, soleus and EDL muscles in the *Col13a1*^{oe} mice compared to controls (II, Fig. 3A-B). Furthermore, in the *Col13a1*^{oe} mice the collagen XIII immunoreactivity extended over the muscle fibers and formed fibrillar-like structures at the tendon area of the diaphragm and the soleus muscles, whereas in the wild-type controls collagen XIII localized at the end of the muscle fibers with a diffuse staining pattern and not clearly extending to the tendon area. Moreover, the collagen XIII immunoreactivity coincided with fibroblast-like cells at the tendons of the *Col13a1*^{oe} mice, possibly representing tenocytes. Immunostainings with the anti-HA-tag antibody revealed the collagen XIII expression at the MTJs and tendons of the *Col13a1*^{oe} mice to be mainly of transgene origin (II, Fig. 3D-F).

Furthermore, examination of the collagen XIII immunoreactivity of the *Col13a1*^{oe} diaphragms at low magnification revealed collagen XIII to locate to other extrasynaptic structures that resembled fibroblast-like cell morphology on the infra- and supradiaphragmatic surfaces (II, Fig. 3G). Such staining could also be found in the wild-type diaphragms, but to a much lesser extent. Further staining with an anti-HA-tag antibody again revealed most of the collagen XIII expression to be of exogenous origin (II, Fig. 3H). High-magnification of co-staining with the

anti-HA-tag antibody and DAPI indicated these collagen XIII accumulations to localize around the nucleus and unipolarly in the cytoplasm and possibly at the plasma membrane of cells that lie on the surface of the diaphragm (II, Fig. 3I-J). These staining did not co-localize with endothelial marker PECAM-1 and instead some co-localization was found with an anti-alpha smooth muscle actin (α-SMA) antibody, which stains activated fibroblasts (Serini & Gabbiani 1999).

5.5 Postsynaptic maturation of the NMJ in the *Col13a1*$^{tm/tm}$ and *Col13a1*^{oe} mice (I, II)

The AChR cluster size and fragmentation was analyzed at P28 and P84 in the wild-type mice as well as *Col13a1*$^{-/-}$ and *Col13a1*$^{tm/tm}$ mice (only in I). Compared to the wild-type AChR clusters, the cluster size was decreased in the *Col13a1*$^{-/-}$ mice by 33% but unchanged in the *Col13a1*$^{tm/tm}$ mice at P28 and decreased in the *Col13a1*$^{-/-}$ mice by 41% and increased in the *Col13a1*$^{tm/tm}$ mice by 37% at P84 (I, Fig. 3C). Furthermore, there were no significant differences in the fragmentation of the AChR clusters in both mouse lines at P28, but at P84 AChR clusters in the *Col13a1*$^{tm/tm}$ mice were significantly more fragmented than those in the wild-type controls (I, Fig. 3D). Morphological analyses of the maturing and adult AChR clusters in the *Col13a1*$^{tm/tm}$ mice revealed that fragmentation and increase in the AChR cluster size was apparent from P56 onwards until P525, the last time point studied (I, Fig. 3A). In addition to already established defects in AChR clustering in the *Col13a1*$^{-/-}$ mice (Latvanlehto *et al.* 2010), we found dispersion of the AChR pattern at some NMJs in the diaphragm at P56 and onwards, and in the soleus at P84 (I, Fig. 3A-B and Fig. 2K-L, Fig. 4A-B, F-G and Fig. 6B, G-H).

When maturation of the AChR clusters was studied in the diaphragm of the *Col13a1*^{oe} mice and compared to wild-type controls (only in II), it revealed simple and small AChR clusters from P28 onwards to the last time-point studied, P182 (II, Fig. 4A). The AChR cluster size and fragmentation was analyzed using α-BTX-immunostained diaphragm, soleus and EDL muscle whole mounts at P84 in the wild-type and *Col13a1*^{oe} mice (II, Fig. A-C). The size of the AChR clusters was decreased in the diaphragm, soleus and EDL muscles at P84 by 24%, 38% and 42%, respectively, in the *Col13a1*^{oe} mice compared to wild-type controls (II, Fig. 4D). Division of the AChR clusters into fragments at P84 was decreased only in the diaphragm of the *Col13a1*^{oe} mice while it was comparable with controls in the soleus and EDL muscles (II, Fig. 4E).

5.6 Collagen XIII localization in relation to other NMJ components (I)

To study collagen XIII localization with respect to other NMJ components, the diaphragm and soleus muscles of the 12-week-old wild-type, *Col13a1*$^{tm/tm}$ and *Col13a1*$^{-/-}$ mice were immunostained as whole mounts with different antibodies combined with α-BTX (I, Fig. 2K-L and Fig. S3A-C). NMJs of both fast and slow muscle fibers in the wild-type and *Col13a1*$^{tm/tm}$ mice contained collagen XIII (data not shown) and the strongest collagen XIII signal was detected at NMJs of soleus muscles. As expected collagen XIII knock-out NMJs were devoid of staining. In the *Col13a1*$^{tm/tm}$ mice the collagen XIII pattern was not as evenly distributed as the synaptic AChE pattern that extended slightly beyond the borders of the collagen XIII staining (I, Fig. S3A). In contrast, the collagen XIII pattern appeared slightly broader than that for the synaptic vesicle protein synaptotagmin 2 (Syt-2) and it was adjacent rather than overlapping with localization of the AZ protein Bassoon (I, Fig. S3B-C).

5.7 Effects of collagen XIII misexpression on other NMJ components (I, II)

To study the effects of misexpression of collagen XIII with respect to other NMJ components, the diaphragm, soleus and EDL (the latter studied only in II) muscles of the 12-week-old wild-type, *Col13a1*$^{tm/tm}$ (only in I), *Col13a1*$^{-/-}$ and *Col13a1*^{oe} (only in II) mice were immunostained as whole mounts with different antibodies combined with α-BTX. Immunoreactivity of an anti-neurofilament antibody in the diaphragm muscle revealed decreased terminal complexity measured as the number of terminal divisions, branches and tips in the *Col13a1*$^{-/-}$ mice compared to controls (I, Fig. 6A and C-F). In contrast, the terminal complexity was increased in the *Col13a1*$^{tm/tm}$ mice (I, Fig. 6A and C-F) and normal in the *Col13a1*^{oe} mice compared with controls (II, Fig. 5A and D-G). Furthermore, in the absence of total collagen XIII, neurofilament-containing elements were thin and the nerve termini failed to fully cover AChR-rich clusters, and in some NMJs they appeared to retract from the synapse (I, Fig. 6A-B). All collagen XIII modified mice had neurofilament containing structures that occupied a larger area and formed nodules in the preterminal axons (I, Fig. 6A-B and II, Fig. 5A-B). The proportion of NMJs with axons containing neurofilament nodules was calculated in the wild-type and *Col13a1*^{oe} mice where it was significantly increased as 64 % of the NMJs were

aberrant while only 24 % NMJs in the wild-type controls exhibited the same characteristic (II, Fig. 5H). There was no difference in the tShC coverage, labeled with an anti-S100 antibody, in any muscle studied in the *Col13a1*$^{tm/tm}$, *Col13a1*^{oe} and wild-type mice at P84 (I, Fig. 6G-H and II, Fig. 5I-K). In contrast, retraction of tShCs was observed in the mice lacking collagen XIII (I, Fig. 6G-H). To analyze presynaptic vesicle structures muscles were co-stained with an anti-Syt-2 antibody and α-BTX. In the controls, *Col13a1*$^{tm/tm}$ and *Col13a1*^{oe} mice vesicle structures could not be detected outside of the synaptic end-plate (I, Fig. S5A and II, Fig. 5L-N). In contrast, immunoreactivity of Syt-2 and the vesicular acetylcholine transporter (VAChT) could also be found distally in the preterminal axon in the *Col13a1*$^{-/-}$ mice (I, Fig. S5A-B). Moreover, staining for Syt-2 appeared enriched at NMJs of the *Col13a1*$^{tm/tm}$ mice compared to controls, whereas Syt-2 levels appeared reduced and patchy at the *Col13a1*$^{-/-}$ and *Col13a1*^{oe} synapses. Immunoreactivity of an anti-Bassoon antibody was also reduced in the *Col13a1*$^{-/-}$ synapses and comparable to controls in the *Col13a1*$^{tm/tm}$ synapses (I, Fig. S3C). Immunoreactivity of an antibody against the α-1A subunit of P/Q-type-VDCCs was only tested for the wild-type and *Col13a1*^{oe} mice and did not show any marked differences (II, Fig. 5O-Q). Furthermore, immunoreactivity of an anti-dystrophin antibody was tested in the diaphragm of the wild-type, *Col13a1*$^{tm/tm}$ and *Col13a1*$^{-/-}$ mice and no differences were detected (I, Fig. S4A). To analyze synaptic structures, muscles of the wild-type, *Col13a1*$^{tm/tm}$, *Col13a1*$^{-/-}$ and *Col13a1*^{oe} mice were stained with an anti-AChE antibody or Fasciculin II combined with α-BTX (I, Fig. 4A-B, Fig. S3A and II, Fig. 5R-T). An aberrant AChE staining was found only in the *Col13a1*$^{-/-}$ mice where the AChE pattern was diffused and clearly extended beyond the postsynaptic structures (I, Fig. 4A-B). Muscles in the wild-type, *Col13a1*$^{tm/tm}$ and *Col13a1*$^{-/-}$ mice were also stained for ColQ expression, found to resemble the AChE pattern in the *Col13a1*$^{-/-}$ mice and appear normally distributed in the *Col13a1*$^{tm/tm}$ mice compared to controls (I, Fig. 4F-G).

5.8 Collagen XIII ectodomain binds with ColQ-tailed AChE *in vitro* and the binding is mapped to the COL3-domain (I)

To test whether collagen XIII directly interacts with AChE, the amount of AChE bound on a solid collagen XIII surface was measured (Ellman *et al.* 1961) (I, Fig. 4C). AChE dimers extracted from *Torpedo Californica* or AChE tetramers extracted from *Electrophorus electricus* were allowed to bind on collagen XIII and after washing no significant AChE activity was detected. In contrast, AChE activity

was significant when ColQ-tailed AChE extracted from *Torpedo Californica* or *Electrophorus electricus* was applied on collagen XIII. Furthermore, the ColQ-tailed AChE did not bind to BSA or collagen I (I, Fig. 4D). To map the binding site on collagen XIII, ColQ-tailed AChE was seeded on pepsin-digested and purified collagen XIII fragments, and the binding was found to be mediated through the COL3 domain (I, Fig. 4E).

5.9 Ultrastructural analysis of the *Col13a1*$^{tm/tm}$ and *Col13a1*^{oe} motor synapses (I, II)

The diaphragm muscle of the wild-type, *Col13a1*$^{tm/tm}$ (only in I) and *Col13a1*^{oe} (only in II) mice was analyzed ultrastructurally at P84 with TEM (I, Fig. 5A-B and II, Fig. 6A-C). Adhesion between pre- and postsynaptic structures in the *Col13a1*$^{tm/tm}$ NMJs was comparable to wild-type and no tShC invagination could be seen (I, Fig. 5A-B), whereas disrupted adhesions of the nerve terminus and muscle as well as tShC invaginations were detected in the *Col13a1*^{oe} mice (II, Fig. 6A-C). In the *Col13a1*$^{tm/tm}$ presynaptic termini AChVs were densely packed and 2.7-fold more numerous than in controls and the AZ numbers were significantly elevated by 1.6-fold (I, Fig. 5C-D). The AChV and AZ numbers were normal in the *Col13a1*^{oe} mice compared to controls (II, Fig. 6D-E). Additionally, we detected increased endocytosis in the *Col13a1*$^{tm/tm}$ termini in the diaphragm (I, Fig. 5B) and multilamellar inclusions in the nerve termini of *Col13a1*^{oe} mice as a mark of neurodegeneration (II, Fig. 6A-C).

5.10 Neurotransmission in the *Col13a1*$^{tm/tm}$ and *Col13a1*^{oe} neuromuscular synapses (I, II)

To analyze whether misexpression of collagen XIII have any effect on neurotransmission in the *Col13a1*$^{tm/tm}$ (only in I) and *Col13a1*^{oe} (only in II) mice, electrophysiological measurements were performed. In both mouse lines the resting membrane potential of muscle fibers was unaltered (data not shown). The amplitude of MEPPs was also unchanged compared to controls in both lines (data not shown and II, Fig. 6F). The spontaneous release of MEPPs was significantly increased in the *Col13a1*$^{tm/tm}$ NMJs (I, Fig. 5F-G) but comparable to controls in the *Col13a1*^{oe} mice (II, Fig. 6G). The frequency of sucrose-induced evoked MEPPs was significantly increased in both the *Col13a1*$^{tm/tm}$ and the *Col13a1*^{oe} mice (I, Fig. 5H-I and II, Fig. 6H-I). Furthermore, the amplitude of evoked EPPs was

significantly increased in the *Col13a1*$^{tm/tm}$ mice (I, Fig. 5J) and slightly but not significantly reduced in the *Col13a1*^{oe} mice (II, Fig. 6J and L). The quantal content of the *Col13a1*$^{tm/tm}$ mice was also significantly increased (I, Fig. 5K) but unaltered in the *Col13a1*^{oe} mice (data not shown). Repetitive nerve stimulation at 30 Hz evoked a significantly elevated amplitude in the *Col13a1*$^{tm/tm}$ mice at all phases of the stimulation when compared to wild-type mice (I, Fig. 5L) and it was significantly decreased in the *Col13a1*^{oe} mice (II, Fig. 6J and L). The EPP decay time was unchanged in the *Col13a1*^{oe} mice.

5.11 *Ex vivo* endocytosis (I)

Ex vivo analysis of endocytosis after induction of exocytosis in the presence of lipophilic dye FM 1-43FX confirmed that endocytosis was efficient at NMJs of the *Col13a1*$^{tm/tm}$ diaphragm, while it was patchy and not fully covering the receptor cluster area in the *Col13a1*$^{-/-}$ mice (I, Fig. S5C).

5.12 Muscle pathology of the collagen XIII modified mouse lines (I, II)

To evaluate muscle pathology, the diaphragm, soleus and EDL (the latter studied only in II) muscles of the 4- and 12-week-old wild-type, *Col13a1*$^{tm/tm}$ (only in I), *Col13a1*$^{-/-}$ and *Col13a1*^{oe} (only in II) mice were weighted and stained with H&E. The muscle weight was normalized by body weight. Muscle weight of the diaphragm at P28 and P84 was normal compared to controls in both *Col13a1*$^{tm/tm}$ and *Col13a1*$^{-/-}$ mice (I, Fig. S2B and Fig. IB) and in contrast, it was significantly decreased by approximately 20% at both time points in the *Col13a1*^{oe} mice (II, Fig. 7B). The weight of the soleus muscle was unchanged in the *Col13a1*$^{tm/tm}$ mice compared to controls at both time points and at P28 in both *Col13a1*$^{-/-}$ and *Col13a1*^{oe} mice (I, Fig. S2C, Fig. IC and II, Fig. 7C). However, the weight of the soleus was decreased at P84 in *Col13a1*$^{-/-}$ and *Col13a1*^{oe} mice compared to controls by 40% and 15%, respectively (I, Fig. 1C and II, Fig. 7C). There was no change in the weight of the EDL in the *Col13a1*^{oe} mice compared to controls at P28 and P84 (II, Fig. 7D). For muscle fiber morphological analysis, the muscle fiber size and proportion of fibers with central nuclei were calculated and compared to controls. There were no significant changes in the fiber size or proportion of central nuclei in the soleus or EDL (the latter assessed only in the *Col13a1*^{oe} mice) muscles of the *Col13a1*$^{tm/tm}$ and *Col13a1*^{oe} mice (I, Fig. S2G-I and II, Fig. 7F-G and J-M). Instead,

in the *Col13a1*$^{-/-}$ mice, the proportion of small muscle fibers (<1.0mm^2) was increased at the expense of middle-sized fibers (1-1.5mm^2) and the proportion of central nuclei was elevated in the soleus muscles (I, Fig. 1I and J-K). The fiber size composition of the diaphragm was significantly shifted towards small muscle fibers (<0.5mm^2) in all studied collagen XIII mutant mouse lines while the proportion of central nuclei was increased only in the *Col13a1*$^{tm/tm}$ mice (I, Fig. 1D and E-F, S2D-F and II, Fig. 7E and H-I). The proportion of fast and slow muscle fibers was assessed in the diaphragm and soleus muscles of the wild-type, *Col13a1*$^{tm/tm}$ and *Col13a1*$^{-/-}$ mice by immunostainings and only the soleus muscle of the *Col13a1*$^{-/-}$ mice harbored a decreased and an increased amount of slow and fast muscle fibers, respectively (I, Fig. 1G-H, L-M and S2J-M). To test if fetal Myosins were expressed in the soleus muscle of the *Col13a1*$^{-/-}$ mice at P84, RT-qPCR was performed to test transcription of Myosin heavy chain 3 (*Myh3*) and *Myh8* genes, and indeed a significant increase was found in the transcript levels of both genes in the *Col13a1*$^{-/-}$ mice compared to the wild-type (I, Fig. 1N-O).

5.13 Effects of intra-abdominal injection of 3,4-DAP on muscle strength in the *Col13a1*$^{-/-}$ mice (I)

To test the effects of intra-abdominal injection of 3,4-DAP on muscle strength in the *Col13a1*$^{-/-}$ mice, the baseline of the grid hanging time of the wild-type and *Col13a1*$^{-/-}$ mice was first measured without any injected substances (I, Fig. 1P-Q). The wild-type controls could hang for at least 5 minutes, set as a maximum while in contrast, the latency to fall for *Col13a1*$^{-/-}$ mice was around one minute. 10 to 20 minutes after intra-abdominal injection of 3,4-DAP, the grid hanging time was significantly extended in the *Col13a1*$^{-/-}$ mice, while saline injection used as a control had no effect on the grid hanging time.

5.14 Dysmorphic nerve and AChR cluster pattern in the *Col13a1*^{oe} mice (II)

To study the patterns of motor nerves and AChR clusters at tissue level, freshly dissected whole diaphragms of the P84 wild-type and *Col13a1*^{oe} mice were imaged and half of the diaphragm (hemidiaphragms) were either stained with α-BTX to show AChR clusters or AChE activity was utilized to show the AChE pattern. Misexpression of collagen XIII led to the secondary nerve branches being significantly longer and fewer in number compared to controls (II, Fig. 8A-D) and

the pattern of AChE and AChR clusters was significantly wider in the *Col13a1*^{oe} mice compared to controls (II, Fig. 8E-F and H). In addition, the hemidiaphragm length was increased (II, Fig. 8G) and the width decreased in the *Col13a1*^{oe} mice. Furthermore, the nerve and AChR cluster pattern was also studied at E17.5 to reveal a possible congenital origin of such a phenotype. Indeed, the AChR cluster and nerve pattern was discovered already widened at E17.5 in the *Col13a1*^{oe} mice compared to controls (II, Fig. 8I).

5.15 Embryonal collagen XIII immunoreactivity pattern in the *Col13a1*^{oe} mice (II)

Immunoreactivity of the collagen XIII antibody at the E17.5 diaphragms revealed three distinct localizations in the *Col13a1*^{oe} fetuses, but only two in the wild-type (II, Fig. 8J). Firstly, collagen XIII immunoreactivity was found at the synaptic sites indicated by α-BTX staining in both genotypes. Furthermore, the collagen XIII staining pattern at the synapses was diffuse and appeared evenly occupying the postsynaptic sites, while in the adult NMJs it had a more spot-like appearance and from time to time it strongly stained the edges of the α-BTX-positive clusters. Secondly, the collagen XIII staining was discovered at the sarcolemma or at the BMs of the muscle fibers in both genotypes, but it was clearly elevated in the *Col13a1*^{oe} fetuses compared to controls. Thirdly, the anti-collagen XIII antibody also revealed accumulation to cell-like processes at E17.5 fetuses like those seen in the adults, but only in the *Col13a1*^{oe} mice. Furthermore, an anti-HA-tag antibody staining revealed the collagen XIII immunoreactivity to be of exogenous origin in the cell-like processes (II, Fig. 8K)

6 Discussion

6.1 Phenotypes in the collagen XIII knock-out mice resemble human muscle pathologies in CMS19

If we sum up the neuromuscular junction and muscle phenotypes in the collagen XIII knock-out mice and compare them to the findings of the 3 individuals harboring mutations in the *COL13A1* gene, remarkable similarities can be detected, even though mice appeared to better endure the loss of collagen XIII. Firstly, both addressed human mutations are expected to disrupt the collagen XIII gene in such a way that it leads to a loss of the collagen XIII protein, or at least its function. In agreement, the human NMJs were shown by immunoreactivity to lack collagen XIII as is also the case in the knock-out mice. Secondly, the collagen XIII deficiency led to compromised neuromuscular transmission and muscle weakness both in humans and mice. Thirdly, defective AChR clustering in both human and mouse was detected due to collagen XIII loss-of-function mutations. Fourthly, the histology of the muscles revealed fiber size variability and a modestly increased number of central nuclei both in man and mouse. Muscle atrophy was detected in the soleus muscle of the collagen XIII knock-out mice at P84 and clinically assessed atrophy was also present in one of the patients at the age of 5 years. Fifthly, the collagen XIII deficiency led to an increased expression of fetal muscle proteins in both patients and in mice. Sixthly, the 3,4-DAP treatment improved the muscle strength in the collagen XIII deficient mice and in combination with salbutamol it also benefited one of the patients. However, normal localization of the NMJ components were shown at infancy in one patient and in contrast we demonstrated misplacement of presynaptic, synaptic and postsynaptic components in the adult mice lacking collagen XIII. This could be due to the different time point of the assessment, the small number of human samples analyzed resulting from low availability, difference in the sample type and its potency to expose such changes, or it may simply reflect compensating mechanisms in humans compared to mice. However, in the light of all these findings, we can conclude that collagen XIII deficient mice serve as a good animal model for studying the NMJ and muscle phenotype in human CMS19 to further reveal the molecular pathology behind the disease.

6.2 Collagen XIII in the presynaptic assembly of the NMJ

In all studied collagen XIII modified mouse lines presynaptic assembly was affected, suggesting a strong role for collagen XIII as a retrograde organizer of the presynaptic endplate. When both forms of collagen XIII were lacking from the synapse the presynaptic skeleton revealed by immunoreactivity for neurofilament was fragile and sometimes implicated that the nerve was retracting to the synapse. Furthermore, the complexity of the presynaptic apparatus was decreased when measured by the number of terminal branching points, branches and tips. In contrast, when only the shed collagen XIII was missing while the transmembrane collagen XIII was present at the synapse, the terminal cytoskeleton showed increased complexity. Furthermore, by ultrastructural analysis we did not detect any interruptions in adhesion of the nerve and muscle in the mice that harbored only transmembrane collagen XIII, whereas this was evident and combined with tShC invaginations in the loss of both collagen XIII forms. From these studies at P84 it can be concluded that collagen XIII is needed for transsynaptic adhesion of the nerve and muscle, and this is a significant role especially of the transmembrane collagen XIII. The presynaptic organization was not studied at earlier time points and therefore it cannot be confirmed if the decline in the presynaptic cytoskeleton is a developmental or progressive event during the maturation of the synapse in the lack of collagen XIII. The results raise the question as to whether the loss of adhesion is causing the degradation in the presynaptic cytoskeleton or *vice versa*? The fact that presynaptic complexity was increased when only the transmembrane form of collagen XIII was present (and no shed form occurred) suggests that direct or indirect interaction(s) between collagen XIII and presynaptic/synaptic molecule(s) stabilize the presynaptic cytoskeleton (Fig. 8A; 1-2 and C; X_1), and without such consistence axons start to retract and adhesion gets interrupted. Another explanation could arise from the synapse activity, as it was decreased and increased depending on the collagen XIII modifications.

In the development of the NMJ and in the reinnervation after peripheral nerve injury, elimination of excess nerve innervation of the same postsynaptic area is shaped by activity-dependent competition between innervating nerves. Unfortunately, little is known about the molecular mechanisms behind this elimination, but the basic idea is that the terminal with the strongest activity and the highest release of neurotransmitters wins the competition and persists in association with the ShCs and the postsynaptic endplate (Darabid *et al.* 2014). Furthermore, increased activity in the form of exercise training have been shown

to result in greater complexity of terminal branching patterns and higher total length of branching, as well as increased staining of AChVs compared to decreased or sustained activity in rats. On the other hand, decreased activity by unloading the muscle for ten weeks did not have any effect on the presynaptic organization (Deschenes *et al.* 2006). In the loss of shed collagen XIII and presence of only the transmembrane form, electrophysiological measurements indicated increased frequency of spontaneous presynaptic activity (frequency of spontaneous MEPPs), an enlarged pool of docked vesicles (frequency of evoked MEPPs released independently of Ca^{2-} with a hypertonic induction), increased quantal content (elevated amplitudes of EPP in maximal nerve stimulation) and enlarged vesicle number in all vesicle pools (amplitudes of EPPs in repetitive nerve stimulation). In other words, spontaneous spill of ACh from the presynaptic terminal was increased and the induced activity releases more quantal content in the *Col13a1*$^{tm/tm}$ compared to controls. Could the more complex assembly of the presynaptic structures result from increased activity in the *Col13a1*$^{tm/tm}$ mice? Studies with glutamatergic larval NMJs of *Drosophila melanogaster* have shown that the specific blocking of evoked neurotransmission by genetically encoded peptide toxins did not have any effects on the synaptic terminal area, the number of synaptic boutons (varicosities in the synaptic terminals typical for the *Drosophila* NMJs), or the bouton size (Choi *et al.* 2014). In contrast, decreased spontaneous activity in *Drosophila* diminished the synaptic terminal area and the bouton size while increased spontaneous activity in the *complexin* null *Drosophila* resulted in opposing effects; a larger terminal area, a higher AZ number and an increased terminal bouton number (Choi *et al.* 2014, Huntwork & Littleton 2007). However, in mammals the physiological purpose of the MEPP activity is enigmatic and *in vitro* studies with CNS neurons have suggested a role for MEPPs in the postsynaptic protein synthesis (Plomp *et al.* 2015). It remains unclear if the increased MEPP activity is responsible for the increased complexity of the preterminus in the loss of collagen XIII shed form combined with the presence of the transmembrane form alone.

On the other hand, the observed age-related morphological changes of the NMJ resemble the presynaptic and postsynaptic findings in the presence of the transmembrane collagen XIII only, suggesting earlier senescence of these NMJs. Aged NMJs often exhibit increased branching complexity of presynaptic nerve terminals and preterminal thinning, distensions and disorganization (KrauseNeto & and Gama 2013). Postsynaptically, aged AChR clusters often tend to be fragmented and harbor a wider diameter, as seen in the *Col13a1*$^{tm/tm}$ mice. However, one explanation for the increased complexity of the preterminal structures of aged

NMJs has been suggested to involve partial and complete denervation following the sprouting of the nerve terminal (Valdez *et al.* 2010). This differs from the *Col13a1*$^{tm/tm}$ mice, where we could not detect any visible denervation. Nonetheless, even harboring the adhesive transmembrane collagen XIII, the *Col13a1*$^{tm/tm}$ mice lack the soluble shed collagen XIII that is suggested to assemble into the BL at the synaptic cleft. When the collagen IV α-5 chain was mutated it led to loss of both α3α4α5 and $\alpha5_2\alpha6$ collagen IV heterotrimers and many presynaptic defects appeared after the first three postnatal weeks (Fox *et al.* 2007). These included neurofilament aberrations (ring-like structures in nerve terminals and segments of distension in the axons) and fragmentation of the pre- and postsynaptic specializations, similarly to what have been detected in *Col13a1*$^{tm/tm}$ mice. In addition, the collagen IV mutants also harbored some axonal retraction from the AChR-rich postsynaptic membrane. Interestingly, collagen XIII has been proven to interact with collagen IV with moderate affinity (Tu *et al.* 2002). One explanation for the apparent presynaptic changes at the NMJs of the *Col13a1*$^{tm/tm}$ mice could be postulated to result through this interaction. We thus consider it possible that shed collagen XIII is needed to stabilize the synaptic BL (Fig. 8A; 3 and C; 2, X_2) and when this stabilization is lost preterminal structures respond by increasing the terminal complexity.

In addition to collagen XIII, other synaptic and postsynaptic proteins have been linked to postnatal presynaptic maturation of the NMJs. These include the already reviewed BL components, laminins (α2β2γ1, α4β2γ1 and α5β2γ1) and presynaptic molecules including α3β1 integrin (Rogers & Nishimune 2017, Ross *et al.* 2017). Interaction of the laminin β2 subunit and VDCCs is well established in addition to the laminin α4 subunit's role in fine tuning the location of the AZs to match postsynaptic junctional openings and restricting the ShC invaginations into the synaptic cleft (Rogers & Nishimune 2017). Similarly to the laminin β2 and α4 subunit deficient mice, the collagen XIII deficient mice harbored a decreased number of AZs and synaptic vesicles as well as the presence of ShC invaginations (Latvanlehto *et al.* 2010) and, as shown in this thesis study, lowered Bassoon protein levels. Another similar mouse phenotype was recently detected in the mice heterozygote for the integrin α3 deletion with postnatal ShC invaginations and reduced levels of Bassoon, synaptic vesicles and AZs (Ross *et al.* 2017). The integrin α3β1 dimers have been reported to interact with laminin α4β2γ1 and some AZ proteins in *Torpedo californica* electric organ synapses and suggested to have a role in the laminin α4-mediated AZ organization (Rogers & Nishimune 2017). Based on our findings, we also hypothesize that collagen XIII influences this

interconnected mesh of laminin α4β2γ1, AZ proteins and integrin α3β1, resulting in the detected presynaptic defects (Fig. 8A; 1-2).

6.3 Collagen XIII in the synaptic and postsynaptic assembly of the NMJ

As already shown previously, lack of both collagen XIII forms resulted in a halted postsynaptic AChR cluster maturation seen at P14 and onwards leaving the AChR clusters small and immature (Latvanlehto *et al.* 2010). In the present study AChR cluster dispersion was detected in addition to those AChR cluster defects in the lack of both collagen XIII forms (Latvanlehto *et al.* 2010). Interestingly, the lack of shed collagen XIII and the presence of only transmembrane collagen exhibited a distinct AChR cluster maturation pattern, the clusters becoming large and fragmented by P56 and onwards. From these findings, we can conclude that transmembrane collagen XIII harbors a role in the AChR cluster maturation and stabilization. A similarly fragmented postsynaptic apparatus appearing postnatally, as found in the lack of the shed and presence of the transmembrane collagen XIII, has been seen in the aging NMJs and in the deficiency of some other synaptic BL components, including collagen IV α3α4α and $\alpha5_2\alpha6$ heterotrimers, nidogen 2 and laminin α4 subunit (Fox *et al.* 2007, Fox *et al.* 2008, Patton *et al.* 2001). In addition to interaction with collagen IV, collagen XIII has been proven to interact with high affinity with nidogen-2 and other BL components that are not only restricted to the synapse, namely perlecan and fibronectin (Tu *et al.* 2002). Taking this into consideration, one could postulate that the postsynaptic defect in the lack of shed collagen XIII from the synaptic BL could result in an unstabilized synaptic BL composition (Fig. 8C; 2 and X_4). Additionally, shed collagen XIII has been proven to enhance AChR clustering *in vitro* (Latvanlehto *et al.* 2010) suggesting a direct interaction with AChRs or other postsynaptic receptors affecting AChR accumulation (Fig. 8B; 3-4). On the other hand, exercise and increased activity of the presynaptic terminal have also been shown to increase the fragmentation and size of the postsynaptic apparatus (Deschenes *et al.* 2006, Deschenes *et al.* 2016, Nishimune *et al.* 2014). This could provide another explanation, since the *Col13a1*$^{tm/tm}$ mice harbor increased synaptic activity. Furthermore, considering the fact that the *Col13a1*$^{tm/tm}$ mice produce transmembrane collagen that cannot be shed, the lack of such a modification found to be present in wild-type mice could lead to unmodifiable interactions with presynaptic components and result in detected increased activity and presynaptic complexity in the *Col13a1*$^{tm/tm}$ mice.

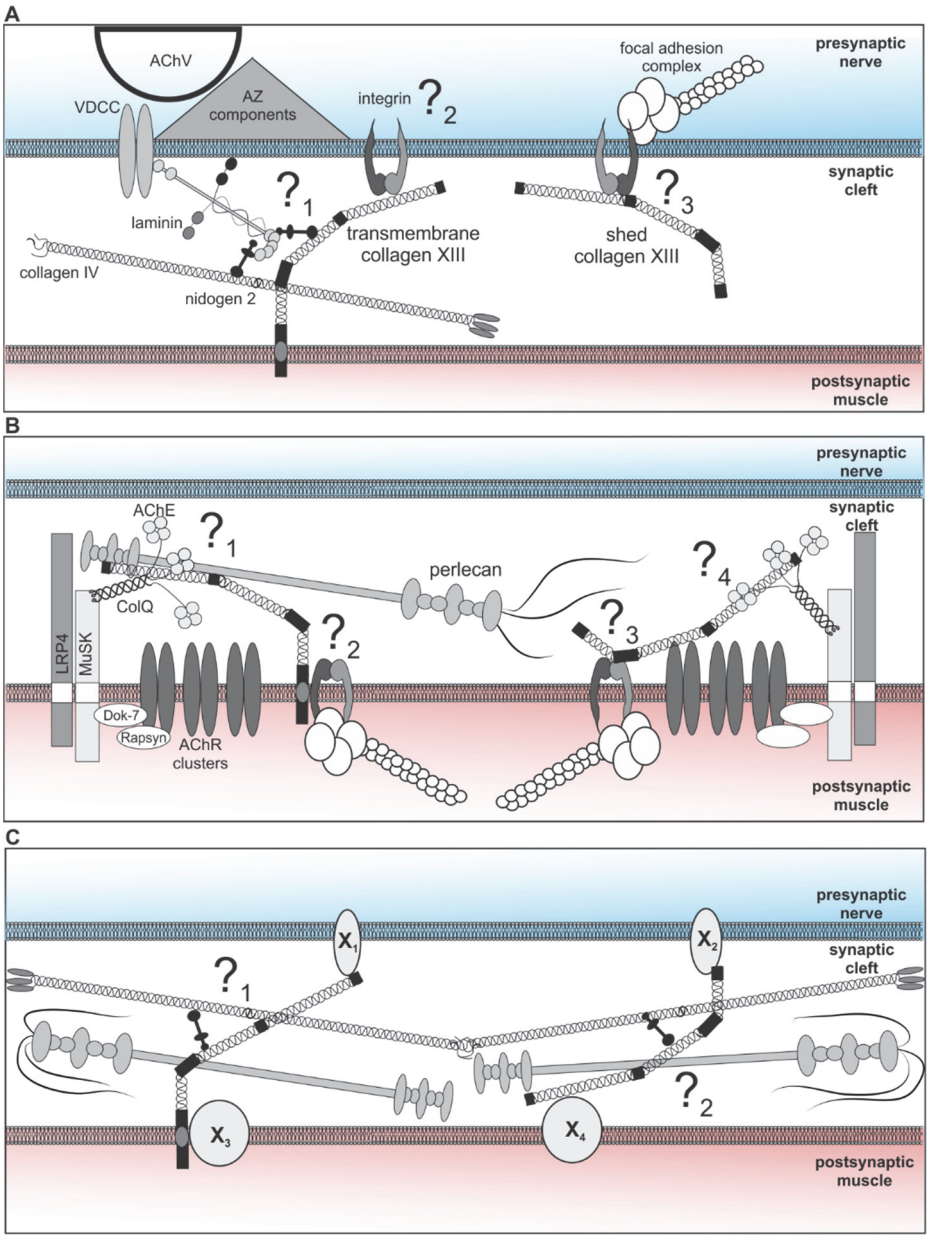

Fig. 8. Possible roles and interactions of the transmembrane and shed collagen XIII at the NMJ. A) Collagen XIII as a presynaptic organizer. Transmembrane collagen XIII interacting indirectly with laminin/VDCC-complex via nidogen-2 and collagen IV binding

(1) in addition to possible direct interaction with presynaptic receptors (2). Shed collagen XIII with presynaptic receptor binding (3). B) Collagen XIII as a postsynaptic organizer. Transmembrane collagen XIII and ColQ interaction (1) is proven *in vitro* and *in vivo*, in addition to *in vitro* binding with perlecan and possible cytoskeletal link via integrins and the focal adhesion complex (2). Shed collagen XIII interacting with postsynaptic integrin (3) and affecting AChR clustering (4). C) Collagen XIII as a synaptic stabilizer. Transmembrane (1) and shed (2) collagen XIII as a BL stabilizer via perlecan, nidogen-2 and collagen IV interactions. Postulated binding of shed and transmembrane collagen XIII to unknown pre- and postsynaptic receptors (X1-4).

Interestingly, in this present study we established a novel binding partner for collagen XIII, namely the AChE-binding ColQ. In the collagen XIII deficiency both AChE and ColQ immunoreactivity extended over the synaptic sites, and *in vitro* binding was discovered between the COL3 domain of collagen XIII and ColQ. Interestingly, the existence of the transmembrane collagen XIII was enough to rescue the AChE and ColQ dispersion, suggesting this binding to happen via the transmembrane collagen XIII. Furthermore, postsynaptic defects of the *Col13a1*$^{-/-}$ mice closely resemble those seen in the ColQ deficiency: both harboring small, immature and fragmented AChR clusters postnatally and ShC invaginations (Feng *et al.* 1999, Latvanlehto *et al.* 2010, Sigoillot *et al.* 2010). In addition, lack of ColQ decreased the muscle fiber diameter in both fast and slow-twitch muscles and lack of collagen XIII decreased the weight of the slow-dominant muscle soleus. A similar switch of slow to fast fibers in the soleus muscles happened in both mouse models. Postsynaptic defects of the ColQ knock-out mice have been explained to be a consequence of its interaction with MuSK, since reduced levels of membrane-bound MuSK have been detected in these mice (Karmouch *et al.* 2013, Sigoillot *et al.* 2016). We also propose that the effects of collagen XIII on postsynaptic stabilization could result from the ColQ-MuSK interaction (Fig. 8B; 1). Furthermore, collagen XIII binds to perlecan, which is known to further stabilize and localize ColQ and AChE to the synaptic cleft. Collagen XIII has been localized to cell adhesion structures co-localizing with vinculin, talin and at the end of the actin filaments in the cultured fibroblasts and keratinocytes (Hägg *et al.* 2001, Peltonen *et al.* 1999). Altogether, we suggest that transmembrane collagen XIII has distinct roles in the stabilization of the postsynaptic and synaptic structures by binding to ColQ, perlecan and nidogen-2 and connecting them to the underlying cytoskeleton of muscle fibers (Fig. 8B; 2 and C; 1, X_3).

6.4 Transgenic overexpression of collagen XIII at the neuromuscular tissues

Many aspects of the neuromuscular and musculoskeletal findings of the transgenic overexpression of collagen XIII in *Col13a1*^{oe} mice were intriguing and somewhat unexpected. Firstly, all studied muscles, the diaphragm, EDL and SOL, harbored significantly increased transcription of the *Col13a1* gene and, excluding the latter one, protein levels of collagen XIII. However, immunostainings of collagen XIII in the adult mouse muscles did not indicate high collagen XIII accumulations at the NMJ as the increased collagen XIII immunoreactivity was discovered to be mainly extrasynaptic or perijunctional. Extrasynaptic immunoreactivity of collagen XIII located at the MTJs of the studied muscles and into enigmatic cell-like processes found in some cases to associate closely with the NMJs but more often found at the muscle tissue surrounding the NMJs. Especially in the diaphragm, these cells associated with the supra- and infra diaphragmatic surfaces and collagen XIII immunoreactivity appeared to surround the cell nucleus and also locate unipolarly at the cell cytoplasm and possibly to the plasma membrane, displaying an elongated morphology of the cells. Co-staining revealed some localization of α-SMA in these cells. The perijunctional collagen XIII immunoreactivity did not clearly form a cell-like appearance as in the extrasynaptic staining but it instead formed a more diffuse arrangement, possibly localizing at the presynaptic structures, it did not howeverclearly resemble, for example, ShCs or motor neurons. Moreover, highly collagen XIII-positive cells were found at the tendon area, the cells morphologically resembling fibroblasts of the tendon and tenocytes. Furthermore, in the adult diaphragms, by rough estimate, one third of the NMJs were devoid of collagen XIII staining in the *Col13a1*^{oe} mice, possibly resulting from a dominant negative effect of the transgene. Concomitantly, postsynaptic AChR cluster maturation was discovered halted at P28 and onwards in the diaphragm of the *Col13a1*^{oe} mice leaving AChR clusters small and immature looking, similar to what has been seen in the *Col13a1*$^{-/-}$ mice. In addition, the size of the adult NMJs in the soleus and EDL muscles of the *Col13a1*^{oe} mice was also decreased compared to controls. Secondly, co-immunostainings revealed a normal complexity of presynaptic terminals, but an increased number of swollen varicosities in the preterminal axons and occasionally patchy AChV staining. ShCs, VDCCs and AChE appeared immunohistochemically normal. Thirdly, ultrastructural analyses revealed no change in the number of synaptic vesicles or AZs, but evident detraction of the nerve and muscles occasionally accompanied by ShC

invaginations into the synaptic cleft. Furthermore, presynaptic nerves harbored signs of neurodegeneration. Fourthly, electrophysiological parameters indicated slower replenishing of the readily releasable vesicle pool. Fifthly, the AChR and AChE cluster pattern alongside a widened nerve pattern was discovered in the adult diaphragm of the *Col13a1*^{oe} mice. Similarly, a widened AChR cluster and nerve pattern was also discovered at embryonal stages (E17.5). Sixthly, collagen XIII immunoreactivity in the diaphragm of the wild-type and *Col13a1*^{oe} mice indicated both synaptic and extrasynaptic localization at E17.5, the latter one possibly at the BM or the muscle sarcolemma. In addition, the *Col13a1*^{oe} embryos exhibited similar kinds of cell-like accumulation of collagen XIII in the surrounding muscle tissue than adult *Col13a1*^{oe} diaphragms. Wild-type controls harbored collagen XIII immunoreactivity at the NMJs and also at the muscle sarcolemma or at the muscle BM at E17.5 in the diaphragm. However, the sarcolemmal/BM staining in the wild-type mice was fainter compared to that in the *Col13a1*^{oe} diaphragms. Seventhly, muscle parameters were altered in the *Col13a1*^{oe} diaphragm and soleus muscles showing decreased muscle weight at P84 and in the case of the diaphragm also already at P28. Moreover, the muscle fiber size was shown to be decreased in the diaphragm muscles and the hemidiaphragm length widened while the width was reduced.

The aforesaid *Col13a1*^{oe} neuromuscular phenotypes were complicated and therefore not straightforward to interpret. Firstly, overexpression of collagen XIII did not accumulate precisely at the NMJs and only perijunctionally in some portion of the NMJs in the diaphragm and EDL but not in the soleus. Furthermore, the diaphragm was the only muscle harboring a portion of the NMJs without collagen XIII, but still in all studied muscles the size of AChR clusters was decreased accompanied by immature morphology in the diaphragm. Moreover, swollen varicosities in the preterminal axons and occasionally patchy AChV staining were found in the diaphragm and also in the soleus muscle. The NMJ phenotype in the diaphragm could be explained by the lack of collagen XIII in a portion of the NMJs and by perijunctional collagen XIII accumulation, but the former do not apply in other studied muscles and the latter not in the soleus. In other words, decrease in the AChR cluster size, patchy AChV staining and swollen preterminal structures might be secondary phenotypes resulting from extrasynaptic causes. It is known that AChR cluster size follows the muscle fiber size and we could detect significant reduction in muscle fiber sizes in the diaphragm and a shift towards the smaller fibers in the soleus and EDL muscles, possibly explaining the phenotype. Furthermore, both diaphragm and soleus muscles were found to be atrophied,

which could further suggest some of the post- and presynaptic changes to be of secondary origin resulting from the muscle tissue. The fact that the soleus muscle also harbored changes in NMJ morphology and muscle atrophy without clear elevation in the collagen XIII protein levels analyzed by Western blots is conspicuous. However, the MTJs of soleus muscles were detected and clearly overexpress collagen XIII by immunostainings with an anti-collagen XIII antibody and further confirmed by an anti-HA-tag antibody, thereby possibly indicating a reduction in the endogenous collagen XIII production. These facts raised the following questions: 1) what is the role of the collagen XIII overexpression at the MTJs and can it cause muscle atrophy, 2) what are the fibroblast-like cells overexpressing collagen XIII in the diaphragm and what is their role at the NMJ and muscle, 3) how can collagen XIII overexpression extrasynaptically cause a widening of the central AChR cluster and nerve patterning in the diaphragm?

6.5 Possible reasons behind the widened AChR cluster and nerve pattern in the extrasynaptic overexpression of collagen XIII

Embryonal overgrowth and defective nerve patterns in the diaphragm muscles in addition to collagen XIII overexpressing mice have been seen for example in the lack of agrin, MuSK, Dok7, LRP4, integrin β1 subunit (conditionally lacking from the skeletal muscle only) and β-subunit of dihydropyridine receptor (DHPR, the L-type Ca^{2+}channel in the muscle) (Chen *et al.* 2011, Choi *et al.* 2013, DeChiara *et al.* 1996, Gautam *et al.* 1996, Okada *et al.* 2006, Schwander *et al.* 2004). Furthermore, mice lacking ChAT, the biosynthetic enzyme for ACh, exhibit no ACh-mediated neurotransmission and develop abnormally with increased nerve branching occurring at the time of initial nerve-muscle contact until the birth, resulting in enhanced motor neuron survival and widened AChR cluster pattern (Brandon *et al.* 2003). However, all these genetic modifications led to embryonal or perinatal lethality, which was not the case in the collagen XIII overexpressing mice that had a normal life span. For example, agrin deficient mice developed normally until E18, but thereafter died *in utero* or were stillborn (Gautam *et al.* 1996).

Lack of agrin assessed at E18 resulted in a decrease in the AChR cluster size and staining intensity in addition to defective AChR cluster localization, although agrin deficient mice were shown to have normal synthesis of AChRs. In the wild-type embryos at E18 one muscle fiber had one AChR cluster located at the central endplate band, while agrin deficient mice harbored muscle fibers without clusters

and, in contrast, fibers with several clusters scattered along the length of the muscle fiber. Furthermore, many of the clusters in the agrin null mice were uninnervated and axons terminated blindly without a postsynaptic endplate. The overall nerve pattern was also defective in such mice as the secondary branches from the main nerve trunk did not form branches and arbors such as in the wild-type controls but, instead, ran long distances parallel to myotubes ending without apparent specializations. Furthermore, *in situ* hybridization revealed AChR α- and δ-subunit RNAs diffusely distributed along the muscle fibers in the agrin deficiency, while in the wild-type controls these mRNAs were concentrated near the prospective endplate band. As in the case of agrin deficiency lack of MuSK produced aimless overgrowth of nerves without proper terminal specializations and MuSK was found to be required for synapse-specific transcription in muscle nuclei and perinatal survival (DeChiara *et al.* 1996). However, unlike with agrin deficiency, MuSK deficient mice did not harbor any AChR clusters, neither pre-patterned nor after axons had reached muscles. Furthermore, lack of Dok7, a muscle-intrinsic activator of MuSK described earlier, and LRP4 resulted in pre- and postsynaptic phenotypes which were highly similar to the MuSK deficiency in mice (Okada *et al.* 2006, Weatherbee *et al.* 2006). These studies regarding the agrin-MuSK signaling axis highlight the importance of the synapse formation for the development of correct nerve and AChR cluster patterning and could not explain the phenotype in the collagen XIII overexpression, because synapses do form in *Col13a1*^{oe} mice. Furthermore, we do not consider the ultrastructural adhesion phenotype to be sufficient to explain the phenotype. We base this on the facts that the collagen XIII deficient mice also harbor a similar detraction in the muscle and nerve, but do not have a widened AChR and nerve pattern (Latvanlehto *et al.* 2010). A more appealing explanation could rise from the aberrant downregulation of the synaptic gene transcription outside the prospective endplate band in the overexpression of collagen XIII at extrasynaptic sites, as seen for example in the lack of agrin and MuSK (Gautam *et al.* 1996, Okada *et al.* 2006).

Conditional lack of the integrin β1 subunit in the skeletal muscle resulted in perinatal lethality, overgrowth of axons from the central band combined with excess nerve branching and arborizations after crossing the prospective central sites of the muscle (Schwander *et al.* 2004). Presynaptic defects were apparent at E15.5 in the integrin β1 subunit deficient mice. Pre-patterning of AChR clusters was not affected by the loss of the integrin β1 subunit, but at E15.5 AChR clusters were small, faint in their staining intensity, uninnervated and scattered along the length of the muscle fiber similarly to the agrin deficiency (Gautam *et al.* 1996, Schwander

et al. 2004). By that time, preformed AChR clusters dispersed and at the time of birth those mice lacking the integrin β1 subunit conditionally from muscle tissue were devoid of synapses (Schwander *et al.* 2004). Furthermore, agrin was capable of inducing AChR clustering of integrin β1 subunit deficient muscle fibers *in vitro,* suggesting additional models for the perturbated synapse formation and widened central endplate band, for example retrograde signals regulating presynaptic differentiation. Indeed, for example, collagen XXV, a highly homologous molecule to collagen XIII, has been proven to be indispensable for developmental intramuscular innervation (Tanaka *et al.* 2014). The loss of collagen XIII results in a much less drastic phenotype (Latvanlehto *et al.* 2010), but here we observed a clearly aberrant nerve pattern in the overexpression of collagen XIII. In a way, postsynaptic integrins containing the β1 subunit and collagen XXV can be seen as signals that prevent nerve growth over the endplate band and which attracts nerves at the right side of innervation. We consider it possible that collagen XIII also acts as an attractant for the nerves and when expressed extrasynaptically leads to widened nerve pattern. Interestingly and supporting this idea, the recombinant collagen XIII ectodomain has been found to enhance neurite outgrowth *in vitro* in primary neuronal cell cultures extracted from E18.5 rat fetal hippocampus (Sund *et al.* 2001a)

Another perinatally lethal genetic modification affecting the AChR and nerve patterning resulted from a deletion of the β1 subunit of DHPR (the L-type Ca^{2+}channel in the muscle) (Chen *et al.* 2011, Gregg *et al.* 1996). At E14.5 pre-patterned AChR clusters were broadly distributed across the muscle in addition to a highly branched and hyper-innervated nerve pattern over a broad region of the muscle of such mice (Chen *et al.* 2011). Furthermore, similar defected nerve and AChR cluster patterning was also found at E18.5 and several clusters were found scattered along the length of the muscle fibers such as occurs in agrin deficiency (Chen *et al.* 2011, Gautam *et al.* 1996). In contrast to the agrin null mice, every endplate was fully innervated and AChR clusters were larger and exhibited more mature morphology compared to controls in the lack of the β1 subunit of DHPR (Chen *et al.* 2011). Furthermore, *in situ* hybridization of such mice revealed mRNA for MuSK and AChR α-subunit to be distributed abnormally on the entire muscle surface. Furthermore, Ca^{2+} influx was detected as decreasing the expression of MuSK and AChR *in vitro*. Results suggested that without the Ca^{2+} influx and the normally appearing muscle fiber depolarization during development, negative regulation of the MuSK and AChR expression is lost, resulting in defective pre-patterning following aberrant and excess survival of synapses outside of the

prospective endplate band. In the case of the *Col13a1*^{oe} mice, we did not study AChR cluster patterning at earlier embryonal days representing pre-patterning. Hence, we cannot rule out the possibility that the widened nerve and AChR pattern observed in the *Col13a1*^{oe} mice could already result from a pre-patterning defect as in the lack of β1 subunit of DHPR (Chen *et al.* 2011). Furthermore, changes in the neurotransmission that could possibly also change the muscle depolarization in the *Col13a1*^{oe} mice are excluded as the cause of the widened endplate band because increased sucrose-induced MEPP activity, which resembled the findings in the *Col13a1*$^{tm/tm}$ mice as well as the slightly decreased EPP activity which was the finding in the *Col13a1*$^{-/-}$ mice, did not cause widening of the enplate bands in these mice (Latvanlehto *et al.* 2010). In contrast to the aforesaid molecules affecting either the pre-patterning or synapse formation after innervation, lack of nestin and MyoD in addition to transgenic expression of altered AChR γ-subunit resulted in similar disturbed nerve and AChR patterning while genetic modification was not lethal (Koenen *et al.* 2005, Mohseni *et al.* 2011, Wang *et al.* 2003).

Nestin is an intermediate filament expressed by neural progenitors and muscle precursors developmentally and in mature tissues at the CNS, NMJ, MTJ and renal podocytes (Mohseni *et al.* 2011, Vaittinen *et al.* 1999). Adult nestin deficient mice harbored widened AChR cluster and nerve pattern with a larger number of clusters and it was already evident at P0 suggesting a congenital condition (Mohseni *et al.* 2011). Muscle histology was not altered in these mice and postsynaptic sites were innervated. Further studies with agrin and nestin double knock-out mice suggested enhanced AChR cluster survival and the synaptic gene transcription outside the prospective endplate band similar to double knock-out mice of agrin and Cdk5, a decomposer of aneural AChR clusters in the NMJ development. Nestin is known to serve as a scaffold for Cdk5 and regulate its kinase activity *in vitro* and this interaction was proposed to be responsible for *in vivo* results of nestin deficiency. Nestin/Cdk5-pathaway could also serve as a mediator of collagen XIII overexpression, since in cultured fibroblast collagen XIII is known to co-localize with vinculin, talin and the membrane end of the actin filaments (Hägg *et al.* 2001). It is possible that this cytoskeletal association also links collagen XIII into the intermediate filaments of the muscle fiber and interferes with nestin and Cdk5 assembly. Future experiments should be performed to test nestin immunostainings in collagen XIII overexpression mice at the NMJ and also at the MTJ.

Interestingly, a similar phenotype was obtained by recreating a chimeric AChR subunit replacing some amino acids of the fetal AChR γ-subunit with adult ε-subunit referred as γ^{ε} (Koenen *et al.* 2005). AChR γ^{ε}-subunits harbored ε-subunit-

like functional properties, a temporal expression pattern and the ability to form pentamers with other AChR subunits as the fetal γ-subunits. In these AChR$\gamma^{(\varepsilon/\varepsilon)}$ mice myoblast fusion, muscle and preterminal end-plate differentiation was normal, while synapses were scattered over a wider muscle territory and overall nerve pattern was widened and highly branched, as assessed at P6 and P70. These studies indicate that by changing the AChR kinetics embryonally towards the properties of mature AChR the stability of the pre-patterned clusters increases and leads to aberrant dispersion of AChR clusters and widened endplate band. In our study the AChR kinetics were discovered to be normal in mature NMJs, but we did not study embryonal neurotransmission. Thus, we cannot rule out the possibility that the phenotype seen in the collagen XIII overexpression could result from embryonal shift in the AChR kinetics.

Furthermore, a lack of MyoD, one of the myogenic regulatory factors, did not interfere with pre-patterning of the AChR clusters, but led to extensive secondary branching of the nerves and widely distributed AChR clusters (Wang *et al.* 2003). The phenotype was present after the pre-patterning and until P42, the last time point studied. In addition, MyoD deficient mice harbored reduced density and depth of junctional folds and markedly delayed transition of fetal AChR subunit to adult subunit. However, the agrin–MuSK–rapsyn signaling cascade was shown to be unimpaired in MyoD null mice. Effects of MyoD were discussed as resulting from aberrant retrograde signaling to the nerve terminals or lack of downregulation in the expression of growth-promoting signaling factors present in the extrasynaptic regions of developing muscle before innervation. In a similar way, overexpression of collagen XIII in the muscle tissue could interfere with muscle intrinsic factors and lead to detected defects.

All in all, these studies show that initial pre-patterning and later synapse formation and adhesion is needed for the correct AChR cluster and nerve patterning. After innervation has occurred retrograde signals start the presynaptic differentiation and stop axons to wander over the central endplate band. Muscle intrinsic depolarization is demanded for the proper pre-patterning and later correct localization of muscle and nerve contact. Furthermore, the above- represented mouse studies highly emphasize the role of correct transcriptional spectrum of synaptic nuclei versus non-synaptic nuclei in this process. We consider it possible that the widened endplate band seen in the collagen XIII overexpression can result from defects in the transcriptional differentiation of subsynaptic and extrasynaptic nuclei of muscle fibers and this could, for example, result from nestin/Cdk5-pathaway or MyoD-like muscle intrinsic factors that might be interfered with by

the drastic collagen XIII overexpression. On the other hand, there is evidence supporting collagen XIII as a survival signal for the nerves, but further studies are needed to shed light on this matter.

6.6 Collagen XIII overexpression in fibroblast-like cells

Perijunctional collagen XIII immunoreactivity at the adult *Col13a1*^{oe} NMJs did not clearly resemble any cell-like morphology and was possibly located at the presynaptic structures but did not clearly co-localize with the postsynaptic apparatus. We consider it possible that this diffuse accumulation of the transgene protein in the vicinity of the NMJs may represent the novel and poorly characterized kranocytes, fibroblast-like cells capping the NMJ and co-localizing with the Schwann cells (Court *et al.* 2008). Interestingly, and as already reviewed, kranocytes were discovered to be homogenously located within the muscles postnatally and thereafter to be restricted to the endplate region at P28 (Court *et al.* 2008). Furthermore, denervation and atrophy was identified to activate kranocytes to proliferate and spread from the synaptic sites and invade a larger muscle territory (Court *et al.* 2008). The antibody that was serendipitously found to identify cells capping the NMJs was also found to stain a morphologically distinct population of cells in the vicinity of intramuscular nerves and capillaries (Court *et al.* 2008). Morphologically these cells closely resemble transgene collagen XIII-positive cells seen in the embryonal and adult diaphragm of the *Col13a1*^{oe} mice. On the other hand, immunoreactivity of collagen XIII has been found *in vitro* at focal adhesions of cultured human cutaneous fibroblasts (Hägg *et al.*, 2001). Furthermore, we found some immunoreactivity of α-SMA suggesting a myofibroblast-like phenotype (Serini & Gabbiani 1999) within these collagen XIII overexpressing cells (Hägg *et al.* 2001). Moreover, taking into consideration the localization of these cells at the infra- and supra diaphragmatic fasciae, one could postulate these cells to be fascial fibroblasts overexpressing collagen XIII. This claim is also supported by the fact that immunostainings of the collagen XIII overexpression mice heart fibroblasts and dermal fibroblasts extracted from such mice showed increased collagen XIII expression (Auvinen 2015). The collagen XIII overexpression in the *Col13a1*^{oe} mice has been obtained as previously described, namely by inserting a transgene construct containing a predicted *Col13a1* promoter including nucleotides −984 to −231 of the 5′ -flanking sequences, the first exon and part of the intron 1 cloned in front of the rest of a collagen XIII cDNA containing exons 2-41 (Peltonen *et al.* 1997, Ylönen *et al.* 2005). This collagen XIII

cDNA was further tailed with an HA-tag, sequences for transcription termination and the SV40 Poly-A sequence (Ylönen *et al.* 2005). In the case of bone and cartilage, this predicted collagen XIII promoter has been shown to correspond to the endogenous gene expression in such tissues (Ylönen *et al.* 2005). However, our results from muscle tissue suggest that this promoter does not drive transgenic collagen XIII expression to the NMJs and instead promotes its expression in fibroblast like-cells and at the MTJs. Nevertheless, this line has brought us valuable information about the roles of these cells and MTJs regarding neuromuscular integrity as well as different requirements for proper transcriptional regulation in different tissues.

The connective tissue of adult muscles consists of a small number of fibroblasts embedded in the ECM that surrounds individual muscle fibers, muscle fiber bundles and entire anatomical muscles (Gillies & Lieber 2011). In contrast, developing embryonal connective tissue in muscles harbors many fibroblasts surrounded by relatively little ECM (Mathew *et al.* 2011). It is known that the development of the connective tissue and muscles are tightly coordinated both temporally and spatially. Furthermore, the role of muscle connective tissue fibroblasts and their precursors in the muscle development was studied by creating the transcription factor Tcf4 null mice. Normally, Tcf4 is strongly expressed in muscle connective tissue fibroblasts in the developing and adult muscles regulating their signaling properties. Specific deletion of Tcf4 from the fibroblasts led to decreased levels of MyHC-β/slow myofibers in multiple muscles at P0, but interestingly this phenomenon persisted only in the slow fiber-rich soleus muscle in adults. Furthermore, myoblast and fibroblast transwell experiments revealed fibroblasts to secrete Tcf4-independent signals generally promoting muscle maturation and formation of more multinucleate myofibers compared to single myoblast cultures. Moreover, the ablation of Tcf4 in fibroblasts in regenerating muscles leads to premature satellite cell differentiation, depletion of the early pool of satellite cells and smaller regenerated myofibers (Murphy *et al.* 2011). All in all, muscle connective tissue fibroblasts are important for the correct myogenesis and muscle regeneration (Mathew *et al.* 2011, Murphy *et al.* 2011). Unfortunately, only limited data exist about the fibroblasts in the development and maturation of the neuromuscular synapses.

The diaphragm muscle of the *Col13a1*^{oe} mice clearly exhibited aberrant muscle morphology with smaller muscle fibers and decreased muscle width accompanied with widened hemidiaphragm length. It was the only muscle that histologically harbored clear signs of myasthenia and decreased muscle mass at P28 and P84 as

a sign of muscle atrophy or immaturity. In addition, a defect in the muscle maturation appears more likely as the number of centrally located nuclei in the diaphragm of the *Col13a1*^{oe} mice was not increased as an indication of muscle regeneration. The NMJ defects at the diaphragms resembled to some extent those in the collagen XIII knock-out animals. Interestingly, the weight of the diaphragm was unaltered by the lack of collagen XIII and the knock-out mice only harbored smaller muscle fibers. This leads to the conclusion that aberrant NMJs in the overexpression of collagen XIII are not enough to explain the muscle phenotype seen in the diaphragm of these animals. Collagen XIII overexpression in the aforesaid diaphragmic fibroblast-like cells in the *Col13a1*^{oe} mice is so drastic that it may interfere with the normal behavior and function of these cells in myogenesis. Interestingly, collagen XIII overexpression in osteoblasts of the *Col13a1*^{oe} mice also changes the fate of these cells by hindering their differentiation and at the same time promoting their proliferation, finally leading to massive bone over-growth (Ylönen *et al.* 2005). Furthermore, MyoD, a muscle-specific transcription factor, leading to aberrant AChR cluster and nerve pattern, is also needed for the myoblast differentiation and suggesting that altered muscle development can lead to altered NMJ development (Wang *et al.* 2003). This could also be the case with overexpression of collagen XIII.

6.7 Collagen XIII overexpression at the MTJ

The MTJ is a strong force-bearing junction connecting muscle fiber cytoskeleton to intracellular proteins linked to sarcolemmal transmembrane proteins that in turn are connected to the ECM of the tendon (Charvet *et al.* 2012). The main sarcolemmal transmembrane proteins include DGC and α7β1 integrin that can bind to the BM component, laminin α2β1γ1 (Charvet *et al.* 2012, Welser *et al.* 2009). In addition, utrophin, a large cytoskeletal protein homologous to dystrophin, has been shown to aggregate with DGC similarly to dystrophin (Grady *et al.* 1997). Both dystrophin and α7β1 integrin are expressed synaptically and extrasynaptically at the muscle fiber sarcolemma and concentrated at the MTJs and costamers (Charvet *et al.* 2012, Mayer *et al.* 1997, Pratt *et al.* 2015). Unlike dystrophin and α7β1 integrin, utrophin is only localized in the adult mouse muscle at the MTJs and NMJs, however during development and muscle damage utrophin becomes localized extrajunctionally (Welser *et al.* 2009). Lack of dystrophin in humans results in Duchenne muscular dystrophy characterized by severely impaired mobility leading patients to a wheelchair by their teens and premature death from cardiopulmonary

failure in their early twenties. In mice, loss of dystrophin produces a milder phenotype without lethality, but progressive muscle damage, weakness, inflammation, necrosis and fibrosis accompanied by NMJ and MTJ abnormalities. Postsynaptic endplates of such mice are fragmented and less covered by AChVs (Pratt *et al.* 2015). Furthermore, presynaptic axons exhibit increased intra-terminal and extra- terminal branching. Mice lacking α7β1 integrin show myopathic pattern with muscle fiber size variation, necrosis, centrally located nuclei, fibrosis and hypertrophy as well as splitting of the muscle fibers (Mayer *et al.* 1997). In addition, loss of α7β1 integrin produces reduced folding of the MTJ without clear defects at the NMJ (Mayer *et al.* 1997). Mice lacking utrophin exhibit a mild form of myasthenia with reduced sarcolemmal folding and AChR density at the NMJ (Grady *et al.* 1997). Furthermore, crossbred mice with different combinations of the aforesaid sarcolemmal molecules have suggested these three complexes to have overlapping roles in providing structural and functional integrity to the skeletal muscle (Deconinck *et al.* 1997, Rooney *et al.* 2006, Welser *et al.* 2009). All in all, compromised subsarcolemmal linkage to the ECM of the muscle and MTJs can lead to muscle weakness and wasting.

We did not study the ultrastructure of the MTJs in the overexpression of collagen XIII but detected under light microscopy the collagen XIII immunoreactivity to be enhanced and extending from the head of the muscle fibers to the tendon area. Moreover, we detected fibroblast-like cells, possibly representing tenocytes, to overexpress collagen XIII at the tendons. Previously, our group has shown muscle fiber size variation, fuzzy BM pattern (with immunofluorescent staining of collagen IV, dystrophin-dystroglycan receptor complex and laminin α2β1γ1) and loosely attached muscle fibers in mice expressing N-terminally altered collagen XIII (Kvist *et al.* 2001). Ultrastructurally, the muscles of such mice showed disorganization and vacuolization of myofilaments and z-bands. Furthermore, a fuzzy and disorganized sarcolemma and the adjacent BM were particularly evident at the MTJ of these mice. These results suggest collagen XIII to participate in stabilizing structures of costamers and MTJs. Moreover, we have detected by immunohistochemical means and a LacZ-reporter mouse line that collagen XIII normally locates in adult muscles only at the NMJs and MTJs (Latvanlehto *et al.* 2010). Furthermore, not even transgenic overexpression was detected at the adult muscle fiber sarcolemma. Nevertheless, in this present thesis work we have detected some sarcolemmal/endomysial immunoreactivity of collagen XIII in the wild-type and *Col13a1*^{oe} embryos. In addition, and supporting this finding, previous *in situ* hybridization of human fetal

tissues at gestational week 15-19 have pointed to collagen XIII expression at the developing endomysium (Sandberg *et al.* 1989). However, further elucidation of embryonal collagen XIII expression and its possible roles in stabilizing the costamers and muscle fibers remains for future work. Nonetheless, we propose that a greatly increased amount of collagen XIII at the tendons and MTJs seen in the *Col13a1*^{oe} mice can affect the force-bearing and mechanical properties of such structures and indirectly lead to aberrant muscle integrity. Supporting this idea, we found both diaphragm and soleus muscles to exhibit reduced muscle mass and marked extra accumulation of collagen XIII at the tendons. Lamentably, there is no information on the AChR cluster and nerve patterning in the dystrophin, α7β1 or utrophin deficient mice to reveal if such genetic modifications could result in a similar widened receptor pattern being observed in the overexpression of collagen XIII.

6.8 Comparison of the NMJ phenotypes in *Col13a1*$^{-/-}$, *Col13a1*$^{tm/tm}$ and *Col13a1*^{oe} mice.

Comparison of the NMJ phenotypes in the mouse lines used in this thesis work is represented in Table 3. Some results on the *Col13a1*$^{-/-}$ mice have been published previously (Latvanlehto *et al.* 2010).

Table 3. Comparison of the NMJ phenotypes in *Col13a1*$^{-/-}$, *Col13a1*$^{tm/tm}$ and *Col13a1*^{oe} mice.

Phenotypes	*Col13a1*$^{-/-}$	*Col13a1*$^{tm/tm}$	*Col13a1*^{oe}
AChR clusters			
Size at P84	↓	↑	↓
Fragmentation at	nc	↑	↓ (dia)
Dispersion and	↑	nc	↑ (immaturity)
Synaptic changes			
AChE diffusion	↑	nc	nc
AChR cluster	not widened	not widened	widened
Motor axons and			
Adhesion of nerve	↓	nc	↓
Schwann cell	↑	nc	↑
Terminal	↓	↑	nc
Schwann cell and	↑	nc	nc
Nerve pattern	not widened	not widened	widened
Nerve terminals			
Active zone	↓	↑	nc
Synaptic vesicle	↓	↑	nc
Endocytosis	↓	↑	na
Synaptic transmission			
Spontaneus	↓	nc	nc
Spontaneus	↓	↑	nc
Sucrose-induced	↓	↑	↑
EPP amplitude	↓	↑	↓
Muscle findings			
Fiber size at P84	↓ (dia, sol)	↓(dia)	↓(dia)
Internal nuclei at	↑(sol)	↑(dia)	nc
Atrophy at P84	↑(sol)	nc	↑ (dia, sol)
Fiber type	↑(sol)	nc	na
Strength by grid	↓	nc	na

nc=no change, na=not assessed, ↑=increased and↓=decreased

7 Conclusion and future perspectives

This work has provided new insights into the roles of collagen XIII in the neuromuscular and musculoskeletal system. We have shown that lack of collagen XIII in mice and humans results in a similar myasthenic syndrome rendering the collagen XIII knock-out mice as a good study model for CMS19. Furthermore, analysis of mice harboring genetic modification to prevent shedding of collagen XIII resulting in the existence of only the transmembrane collagen XIII have suggested distinct functions of the two forms of collagen XIII. More specifically, transmembrane collagen XIII was discovered to be essential for adhesion of the muscle and nerve and, indirectly we conclude that lack of the shed collagen XIII leads to defective stabilization of the NMJ and hence to a fragmented postsynaptic apparatus and aberrantly increased neurotransmission. Importantly, this current study revealed novel interaction between collagen XIII and ColQ, the collagenous anchor of AChE, both *in vitro* and *in vivo*. In addition, findings of the collagen XIII overexpression mice highlighted the importance of correct localization and amount of collagen XIII at the neuromuscular biology, and raised intriguing questions about the roles of the fibroblast-like cells overexpressing collagen XIII in the neuromuscular development. All in all, based on this thesis work collagen XIII is an important postsynaptic plasma membrane and synaptic BL component of the NMJ with both antero- and retrograde effects.

The identified binding of collagen XIII with ColQ could possibly explain the anterograde effects of collagen XIII on AChR clustering and stabilization, and we furthermore hypothesize retrograde effects to result from interactions with another binding partner(s) at the BL or at the presynaptic plasma membrane. In any future investigation, it would be interesting to study the possible links between synaptic laminins, VDCCs and AZ-components with collagen XIII by assessing embryonal and postnatal expression and protein levels in collagen XIII knock-out mice. Furthermore, it would be of great interest to determine if a lack of collagen XIII influences the maturational shift in the VDCCs postnatally. On the other hand, presynaptic integrins could serve as direct collagen XIII receptors and this is supported by the findings of collagen XIII binding with α1β1 (Nykvist *et al.* 2000) and α11β1 integrins (Tu 2004). Interestingly, the α1 integrin subunit has been localized to preterminal structures, possibly both, in the tShCs and preterminal motor neuron with yet unknown function at the NMJ (Martin *et al.* 1996). Co-staining with antibodies against the α1 integrin subunit and collagen XIII at the NMJs of the collagen XIII modified mouse models could bring more information

of possible interaction. It would be also interesting to crossbreed mice exhibiting only the transmembrane collagen XIII with α1 integrin subunit deficient mice (Gardner *et al.* 1996) and also to study adhesion of the muscle and nerve. α11β1 integrin is mainly expressed by fibroblasts and mesenchymal stem cells, but its possible roles at the NMJ and *in vivo* interaction with collagen XIII have not been elucidated and remain to be resolved in the future (Zeltz & Gullberg 2016). Furthermore, assessment of another interesting integrin, α3β1, shown to interact, for example, with endostatin, a proteolytically released fragment of collagen XVIII (Su *et al.* 2012), could offer an insight into possible laminin-mediated or straight effects in the lack of collagen XIII. We also hypothesize shed collagen XIII to stabilize the BL based on the observed *in vitro* interactions with nidogen-2, collagen IV and perlecan. Thus, immunostainings with the corresponding antibodies could also validate the alleged interaction *in vivo*. In addition, further electron microscopy of the BMs and BLs at the NMJs and muscles of the mice expressing only the transmembrane collagen XIII and wild-type controls could be done in order to see possible ultrastructural changes in such structures. We also consider the possibility that collagen XIII could serve as a postsynaptic receptor by itself, hence collagen XIII has been localized to focal adhesions of human skin fibroblasts (Hägg *et al.* 2001). To study this idea in the future, one could engineer a genetically modified mouse exhibiting an altered intracellular part of collagen XIII to reveal its down-stream effects on the muscle cell.

The phenotypical findings in the overexpression of collagen XIII were intriguing and somewhat hard to interpret. The NMJs of such mice resembled in many ways the junctions seen in the lack of collagen XIII, but the diaphragm muscle morphology, AChR cluster and nerve patterning differed greatly between these mouse lines. Furthermore, unlike in bone and cartilage, the predicted collagen XIII promoter did not drive the transgene expression to the NMJs, mimicking the location of endogenous collagen XIII, and instead led to mild perijunctional expression and clear overexpression of collagen XIII in fibroblast-like cells and at the MTJs suggesting different regulatory elements for the synaptic and extrasynaptic collagen XIII expression. We consider it possible that the observed collagen XIII overexpressing fibroblast-like cells influence deleteriously muscle development and NMJ patterning. In future, more immunostainings (for example with an antibody against Tcf4) could reveal the identity of these cells. Moreover, expression and protein levels of the myogenic regulatory factors, MyHC-isoforms and AChR subunits could be assessed embryonally and postnatally to follow their temporal changes in the overexpression of collagen XIII and scout for possible

changes. Furthermore, levels of Cdk5 and localization of nestin would be interesting to see in the neuromuscular system of collagen XIII overexpression mice. Moreover, motoneuron survival could be increased in the overexpression of collagen XIII or collagen XIII could serve as an attractant for the growing nerves. Further *in vivo* and *in vitro* studies of the issue would be of great value. Furthermore, excess collagen XIII at the MTJs could negatively affect the force-bearing properties of such structures and lead indirectly to impairment of the NMJ and muscle integrity. To test this idea, the first steps would include ultrastructural analysis of the MTJs in such mice and possibly testing mechanically the stiffness of tendon and muscle. We also detected NMJs without collagen XIII immunoreactivity in collagen XIII overexpression mice, possibly explaining the immaturity and altered function of the NMJs similar to collagen XIII deficiency and postulated it to result from the association of transgene polypeptides with endogenous ones forming unstable and undetectable heterotrimers. To test this idea in the future, collagen XIII deficient mice could be crossbred with collagen XIII overexpression mice and the collagen XIII expression at the NMJs of such mice could be studied. On the other hand, we also detected increased transgene collagen XIII immunoreactivity in the vicinity of some NMJs and despite the lack of a precise co-localization with AChR clusters such aberrant expression could have deleterious effects on the structure and function of the NMJ. Of interest is also the role of the complex alternative splicing reported for collagen XIII and it would be interesting to test whether such a splice variant specificity exists in muscle tissue.

Our validation of the collagen XIII knock-out mice as a disease model for CMS19 opens the door for the testing of new pharmaceutical treatments to ease the symptoms or even cure the disease. To date, fortunately, only a few human patients have been recognized as suffering from CMS19, hence the novel characterization of the disease. Thus, after clinicians have agreed that collagen XIII is one cause of CMS, the number of patients can inevitably be elevated. In addition to symptoms arising from the neuromuscular system, CMS19 patients harbored skeletal abnormalities, including facial dysmorphism and barrel chest, thus also suggesting a role for collagen XIII in human bone formation (Logan *et al.* 2015). Supporting this idea, our group has already shown collagen XIII to strongly enhance bone formation in collagen XIII overexpression mice (Ylönen *et al.* 2005). However, it remains for future studies to further elucidate the collagen XIII modified mice with regard to skeletal tissues and thus to possibly gain an even better understanding of the phenotypic alterations in CMS19. Taking into consideration the important role of collagen XIII at the NMJ and collagen XIII autoantibodies in Graves' disease

correlating with a more active type of ophthalmopathy, it would also be interesting to test collagen XIII autoantibodies in autoimmune mediated neuromuscular diseases, such as the seronegative and positive MG, and assess if collagen XIII autoantibodies exist that would influence the severity of the disease. Furthermore, it would be interesting to study the clinical information about those patients suffering from Graves' disease and scout possible neuromuscular symptoms. Interestingly, novel therapeutic approaches are provided in the form of *in vivo* postnatal genome editing by delivering virally gene-editing components to cure the effects of splice-site mutations in neuromuscular diseases (Kemaladewi *et al.* 2017, Long *et al.* 2016). It would be interesting to also test this methodology in the case of CMS19 by introducing the specific human mutations into the mice and to test the outcome and possible advantageous effects of genome editing of such mutations. Moreover, in this thesis work we detected collagen XIII to be embryonally expressed at the NMJs and possible at the sarcolemma/BM of muscle fibers and its overexpression to lead to a widened nerve pattern in the diaphragm muscles. It remains for future studies to shed light on the embryonal role of collagen XIII in neuromuscular development.

Altogether, we have fortified the roles of collagen XIII at the NMJ and proven both its forms to be essential for the correct assembly and function of the neuromuscular system.

List of references

Ackermann F, Waites CL & Garner CC (2015) Presynaptic active zones in invertebrates and vertebrates. EMBO Rep 16(8): 923-938.

Arikawa-Hirasawa E, Rossi SG, Rotundo RL & Yamada Y (2002) Absence of acetylcholinesterase at the neuromuscular junctions of perlecan-null mice. Nat Neurosci 5(2): 119-123.

Auvinen A (2015) Modelling the roles of collagen XIII in cardiac integrity and function, and in cutaneus wound healing. Juvenes Print.

Banyard J, Bao L, Hofer MD, Zurakowski D, Spivey KA, Feldman AS, Hutchinson LM, Kuefer R, Rubin MA & Zetter BR (2007) Collagen XXIII expression is associated with prostate cancer recurrence and distant metastases. Clin Cancer Res 13(9): 2634-2642.

Banyard J, Bao L & Zetter BR (2003) Type XXIII collagen, a new transmembrane collagen identified in metastatic tumor cells. J Biol Chem 278(23): 20989-20994.

Bayes A, Collins MO, Croning MD, van de Lagemaat LN, Choudhary JS & Grant SG (2012) Comparative study of human and mouse postsynaptic proteomes finds high compositional conservation and abundance differences for key synaptic proteins. PLoS One 7(10): e46683.

Berrih-Aknin S, Frenkian-Cuvelier M & Eymard B (2014) Diagnostic and clinical classification of autoimmune myasthenia gravis. J Autoimmun 48-49: 143-148.

Bonnans C, Chou J & Werb Z (2014) Remodelling the extracellular matrix in development and disease. Nat Rev Mol Cell Biol 15(12): 786-801.

Brandon EP, Lin W, D'Amour KA, Pizzo DP, Dominguez B, Sugiura Y, Thode S, Ko CP, Thal LJ, Gage FH & Lee KF (2003) Aberrant patterning of neuromuscular synapses in choline acetyltransferase-deficient mice. J Neurosci 23(2): 539-549.

Burden SJ, Yumoto N & Zhang W (2013) The role of MuSK in synapse formation and neuromuscular disease. Cold Spring Harb Perspect Biol 5(5): a009167.

Carlson SS, Valdez G & Sanes JR (2010) Presynaptic calcium channels and alpha3-integrins are complexed with synaptic cleft laminins, cytoskeletal elements and active zone components. J Neurochem 115(3): 654-666.

Cartaud A, Strochlic L, Guerra M, Blanchard B, Lambergeon M, Krejci E, Cartaud J & Legay C (2004) MuSK is required for anchoring acetylcholinesterase at the neuromuscular junction. J Cell Biol 165(4): 505-515.

Chal J & Pourquie O (2017) Making muscle: skeletal myogenesis *in vivo* and *in vitro*. Development 144(12): 2104-2122.

Charvet B, Ruggiero F & Le Guellec D (2012) The development of the myotendinous junction. A review. Muscles Ligaments Tendons J 2(2): 53-63.

Chen F, Liu Y, Sugiura Y, Allen PD, Gregg RG & Lin W (2011) Neuromuscular synaptic patterning requires the function of skeletal muscle dihydropyridine receptors. Nat Neurosci 14(5): 570-577.

Choi BJ, Imlach WL, Jiao W, Wolfram V, Wu Y, Grbic M, Cela C, Baines RA, Nitabach MN & McCabe BD (2014) Miniature neurotransmission regulates Drosophila synaptic structural maturation. Neuron 82(3): 618-634.

Choi HY, Liu Y, Tennert C, Sugiura Y, Karakatsani A, Kroger S, Johnson EB, Hammer RE, Lin W & Herz J (2013) APP interacts with LRP4 and agrin to coordinate the development of the neuromuscular junction in mice. Elife 2: e00220.

Clark KA, McElhinny AS, Beckerle MC & Gregorio CC (2002) Striated muscle cytoarchitecture: an intricate web of form and function. Annu Rev Cell Dev Biol 18: 637-706.

Climie AR (1973) Muscle biopsy: technic and interpretation. Am J Clin Pathol 60(6): 753-770.

Connors BW & Long MA (2004) Electrical synapses in the mammalian brain. Annu Rev Neurosci 27: 393-418.

Court FA, Gillingwater TH, Melrose S, Sherman DL, Greenshields KN, Morton AJ, Harris JB, Willison HJ & Ribchester RR (2008) Identity, developmental restriction and reactivity of extralaminar cells capping mammalian neuromuscular junctions. J Cell Sci 121(Pt 23): 3901-3911.

Dale HH, Feldberg W & Vogt M (1936) Release of acetylcholine at voluntary motor nerve endings. J Physiol 86(4): 353-380.

Daley WP, Peters SB & Larsen M (2008) Extracellular matrix dynamics in development and regenerative medicine. J Cell Sci 121(Pt 3): 255-264.

Darabid H, Perez-Gonzalez AP & Robitaille R (2014) Neuromuscular synaptogenesis: coordinating partners with multiple functions. Nat Rev Neurosci 15(11): 703-718.

De Bellis A, Sansone D, Coronella C, Conte M, Iorio S, Perrino S, Battaglia M, Bellastella G, Wall JR, Bellastella A & Bizzarro A (2005) Serum antibodies to collagen XIII: a further good marker of active Graves' ophthalmopathy. Clin Endocrinol (Oxf) 62(1): 24-29.

DeChiara TM, Bowen DC, Valenzuela DM, Simmons MV, Poueymirou WT, Thomas S, Kinetz E, Compton DL, Rojas E, Park JS, Smith C, DiStefano PS, Glass DJ, Burden SJ & Yancopoulos GD (1996) The receptor tyrosine kinase MuSK is required for neuromuscular junction formation *in vivo*. Cell 85(4): 501-512.

Deconinck AE, Rafael JA, Skinner JA, Brown SC, Potter AC, Metzinger L, Watt DJ, Dickson JG, Tinsley JM & Davies KE (1997) Utrophin-dystrophin-deficient mice as a model for Duchenne muscular dystrophy. Cell 90(4): 717-727.

Deenen JC, Horlings CG, Verschuuren JJ, Verbeek AL & van Engelen BG (2015) The Epidemiology of Neuromuscular Disorders: A Comprehensive Overview of the Literature. J Neuromuscul Dis 2(1): 73-85.

Denker A, Bethani I, Krohnert K, Korber C, Horstmann H, Wilhelm BG, Barysch SV, Kuner T, Neher E & Rizzoli SO (2011) A small pool of vesicles maintains synaptic activity *in vivo*. Proc Natl Acad Sci U S A 108(41): 17177-17182.

Dennis J, Meehan DT, Delimont D, Zallocchi M, Perry GA, O'Brien S, Tu H, Pihlajaniemi T & Cosgrove D (2010) Collagen XIII induced in vascular endothelium mediates alpha1beta1 integrin-dependent transmigration of monocytes in renal fibrosis. Am J Pathol 177(5): 2527-2540.

Desaki J & Uehara Y (1981) The overall morphology of neuromuscular junctions as revealed by scanning electron microscopy. J Neurocytol 10(1): 101-110.

Deschenes MR, Kressin KA, Garratt RN, Leathrum CM & Shaffrey EC (2016) Effects of exercise training on neuromuscular junction morphology and pre- to post-synaptic coupling in young and aged rats. Neuroscience 316: 167-177.

Deschenes MR, Tenny KA & Wilson MH (2006) Increased and decreased activity elicits specific morphological adaptations of the neuromuscular junction. Neuroscience 137(4): 1277-1283.

Dudai Y, Herzberg M & Silman I (1973) Molecular structures of acetylcholinesterase from electric organ tissue of the electric eel. Proc Natl Acad Sci U S A 70(9): 2473-2476.

Dudai Y, Silman I, Kalderon N & Blumberg S (1972) Purification by affinity chromatography of acetylcholinesterase from electric organ tissue of the electric eel subsequent to tryptic treatment. Biochim Biophys Acta 268(1): 138-157.

Ellman GL, Courtney KD, Andres V,Jr & Feather-Stone RM (1961) A new and rapid colorimetric determination of acetylcholinesterase activity. Biochem Pharmacol 7: 88-95.

Emes RD & Grant SG (2012) Evolution of synapse complexity and diversity. Annu Rev Neurosci 35: 111-131.

Engel AG, Shen XM, Selcen D & Sine SM (2015) Congenital myasthenic syndromes: pathogenesis, diagnosis, and treatment. Lancet Neurol 14(5): 461-4422(15)00010-1. Epub 2015 Mar 26.

Feng G, Krejci E, Molgo J, Cunningham JM, Massoulie J & Sanes JR (1999) Genetic analysis of collagen Q: roles in acetylcholinesterase and butyrylcholinesterase assembly and in synaptic structure and function. J Cell Biol 144(6): 1349-1360.

Feng Z & Ko CP (2007) Neuronal glia interactions at the vertebrate neuromuscular junction. Curr Opin Pharmacol 7(3): 316-324.

Fox MA, Ho MS, Smyth N & Sanes JR (2008) A synaptic nidogen: developmental regulation and role of nidogen-2 at the neuromuscular junction. Neural Develop 3: 24.

Fox MA, Sanes JR, Borza DB, Eswarakumar VP, Fassler R, Hudson BG, John SW, Ninomiya Y, Pedchenko V, Pfaff SL, Rheault MN, Sado Y, Segal Y, Werle MJ & Umemori H (2007) Distinct target-derived signals organize formation, maturation, and maintenance of motor nerve terminals. Cell 129(1): 179-193.

Frantz C, Stewart KM & Weaver VM (2010) The extracellular matrix at a glance. J Cell Sci 123(Pt 24): 4195-4200.

Franzke CW, Bruckner P & Bruckner-Tuderman L (2005) Collagenous transmembrane proteins: recent insights into biology and pathology. J Biol Chem 280(6): 4005-4008.

Gardner H, Kreidberg J, Koteliansky V & Jaenisch R (1996) Deletion of integrin alpha 1 by homologous recombination permits normal murine development but gives rise to a specific deficit in cell adhesion. Dev Biol 175(2): 301-313.

Gautam M, Noakes PG, Moscoso L, Rupp F, Scheller RH, Merlie JP & Sanes JR (1996) Defective neuromuscular synaptogenesis in agrin-deficient mutant mice. Cell 85(4): 525-535.

Gilhus NE, Skeie GO, Romi F, Lazaridis K, Zisimopoulou P & Tzartos S (2016) Myasthenia gravis - autoantibody characteristics and their implications for therapy. Nat Rev Neurol 12(5): 259-268.

Gilhus NE & Verschuuren JJ (2015) Myasthenia gravis: subgroup classification and therapeutic strategies. Lancet Neurol 14(10): 1023-1036.
Gillies AR & Lieber RL (2011) Structure and function of the skeletal muscle extracellular matrix. Muscle Nerve 44(3): 318-331.
Gopinath B, Adams CL, Musselman R, Tani J & Wall JR (2007) Antibodies against calsequestrin and type XIII collagen are good markers for chronic upper eyelid retraction. Ocul Immunol Inflamm 15(2): 81-88.
Gordon MK & Hahn RA (2010) Collagens. Cell Tissue Res 339(1): 247-257.
Grady RM, Merlie JP & Sanes JR (1997) Subtle neuromuscular defects in utrophin-deficient mice. J Cell Biol 136(4): 871-882.
Gregg RG, Messing A, Strube C, Beurg M, Moss R, Behan M, Sukhareva M, Haynes S, Powell JA, Coronado R & Powers PA (1996) Absence of the beta subunit (cchb1) of the skeletal muscle dihydropyridine receptor alters expression of the alpha 1 subunit and eliminates excitation-contraction coupling. Proc Natl Acad Sci U S A 93(24): 13961-13966.
Ha JC & Richman DP (2015) Myasthenia gravis and related disorders: Pathology and molecular pathogenesis. Biochim Biophys Acta 1852(4): 651-657.
Hägg P, Rehn M, Huhtala P, Väisänen T, Tamminen M & Pihlajaniemi T (1998) Type XIII collagen is identified as a plasma membrane protein. J Biol Chem 273(25): 15590-15597.
Hägg P, Väisänen T, Tuomisto A, Rehn M, Tu H, Huhtala P, Eskelinen S & Pihlajaniemi T (2001) Type XIII collagen: a novel cell adhesion component present in a range of cell-matrix adhesions and in the intercalated discs between cardiac muscle cells. Matrix Biol 19(8): 727-742.
Hantai D, Nicole S & Eymard B (2013) Congenital myasthenic syndromes: an update. Curr Opin Neurol 26(5): 561-568.
Hashimoto T, Wakabayashi T, Watanabe A, Kowa H, Hosoda R, Nakamura A, Kanazawa I, Arai T, Takio K, Mann DM & Iwatsubo T (2002) CLAC: a novel Alzheimer amyloid plaque component derived from a transmembrane precursor, CLAC-P/collagen type XXV. EMBO J 21(7): 1524-1534.
Haucke V, Neher E & Sigrist SJ (2011) Protein scaffolds in the coupling of synaptic exocytosis and endocytosis. Nat Rev Neurosci 12(3): 127-138.
Heikkinen A, Tu H & Pihlajaniemi T (2012) Collagen XIII: a type II transmembrane protein with relevance to musculoskeletal tissues, microvessels and inflammation. Int J Biochem Cell Biol 44(5): 714-717.
Hirokawa N, Niwa S & Tanaka Y (2010) Molecular motors in neurons: transport mechanisms and roles in brain function, development, and disease. Neuron 68(4): 610-638.
Howard JF,Jr (2013) Electrodiagnosis of disorders of neuromuscular transmission. Phys Med Rehabil Clin N Am 24(1): 169-192.
Hulsbrink R & Hashemolhosseini S (2014) Lambert-Eaton myasthenic syndrome - diagnosis, pathogenesis and therapy. Clin Neurophysiol 125(12): 2328-2336.

Huntwork S & Littleton JT (2007) A complexin fusion clamp regulates spontaneous neurotransmitter release and synaptic growth. Nat Neurosci 10(10): 1235-1237.

Joyce NC, Oskarsson B & Jin LW (2012) Muscle biopsy evaluation in neuromuscular disorders. Phys Med Rehabil Clin N Am 23(3): 609-631.

Juvonen M, Pihlajaniemi T & Autio-Harmainen H (1993) Location and alternative splicing of type XIII collagen RNA in the early human placenta. Lab Invest 69(5): 541-551.

Karlsson C, Dehne T, Lindahl A, Brittberg M, Pruss A, Sittinger M & Ringe J (2010) Genome-wide expression profiling reveals new candidate genes associated with osteoarthritis. Osteoarthritis Cartilage 18(4): 581-592.

Karmouch J, Dobbertin A, Sigoillot S & Legay C (2013) Developmental consequences of the ColQ/MuSK interactions. Chem Biol Interact 203(1): 287-291.

Karnowsky MJ & Roots L (1964) A "Direct-Coloring" Thiocholine Method for Cholinesterases. J Histochem Cytochem 12: 219-221.

Kemaladewi DU, Maino E, Hyatt E, Hou H, Ding M, Place KM, Zhu X, Bassi P, Baghestani Z, Deshwar AG, Merico D, Xiong HY, Frey BJ, Wilson MD, Ivakine EA & Cohn RD (2017) Correction of a splicing defect in a mouse model of congenital muscular dystrophy type 1A using a homology-directed-repair-independent mechanism. Nat Med .

Kierszenbaum AL & Tres LL (2015) Muscle tissue. In: Anonymous Philadelphia, PA, Saunders: 217.

Koch M, Veit G, Stricker S, Bhatt P, Kutsch S, Zhou P, Reinders E, Hahn RA, Song R, Burgeson RE, Gerecke DR, Mundlos S & Gordon MK (2006) Expression of type XXIII collagen mRNA and protein. J Biol Chem 281(30): 21546-21557.

Koenen M, Peter C, Villarroel A, Witzemann V & Sakmann B (2005) Acetylcholine receptor channel subtype directs the innervation pattern of skeletal muscle. EMBO Rep 6(6): 570-576.

KrauseNeto W & and Gama E (2013) The process of aging and neuromuscular junction morphology of limb muscles: a systematic review. J Morphol Sci 30: 213-218.

Kummer TT, Misgeld T & Sanes JR (2006) Assembly of the postsynaptic membrane at the neuromuscular junction: paradigm lost. Curr Opin Neurobiol 16(1): 74-82.

Kvist AP, Latvanlehto A, Sund M, Eklund L, Väisänen T, Hägg P, Sormunen R, Komulainen J, Fässler R & Pihlajaniemi T (2001) Lack of cytosolic and transmembrane domains of type XIII collagen results in progressive myopathy. Am J Pathol 159(4): 1581-1592.

Kvist AP, Latvanlehto A, Sund M, Horelli-Kuitunen N, Rehn M, Palotie A, Beier D & Pihlajaniemi T (1999) Complete exon-intron organization and chromosomal location of the gene for mouse type XIII collagen (col13a1) and comparison with its human homologue. Matrix Biol 18(3): 261-274.

Latvanlehto A, Fox MA, Sormunen R, Tu H, Oikarainen T, Koski A, Naumenko N, Shakirzyanova A, Kallio M, Ilves M, Giniatullin R, Sanes JR & Pihlajaniemi T (2010) Muscle-derived collagen XIII regulates maturation of the skeletal neuromuscular junction. J Neurosci 30(37): 12230-12241.

Latvanlehto A, Snellman A, Tu H & Pihlajaniemi T (2003) Type XIII collagen and some other transmembrane collagens contain two separate coiled-coil motifs, which may function as independent oligomerization domains. J Biol Chem 278(39): 37590-37599.

Lebbink RJ, de Ruiter T, Adelmeijer J, Brenkman AB, van Helvoort JM, Koch M, Farndale RW, Lisman T, Sonnenberg A, Lenting PJ & Meyaard L (2006) Collagens are functional, high affinity ligands for the inhibitory immune receptor LAIR-1. J Exp Med 203(6): 1419-1425.

Lebbink RJ, de Ruiter T, Kaptijn GJ, Bihan DG, Jansen CA, Lenting PJ & Meyaard L (2007) Mouse leukocyte-associated Ig-like receptor-1 (mLAIR-1) functions as an inhibitory collagen-binding receptor on immune cells. Int Immunol 19(8): 1011-1019.

Legay C & Mei L (2017) Moving forward with the neuromuscular junction. J Neurochem .

Li Y, Lee Y & Thompson WJ (2011) Changes in aging mouse neuromuscular junctions are explained by degeneration and regeneration of muscle fiber segments at the synapse. J Neurosci 31(42): 14910-14919.

Liang CL & Han S (2013) Neuromuscular junction disorders. PM R 5(5 Suppl): S81-8.

Liu Y, Padgett D, Takahashi M, Li H, Sayeed A, Teichert RW, Olivera BM, McArdle JJ, Green WN & Lin W (2008) Essential roles of the acetylcholine receptor gamma-subunit in neuromuscular synaptic patterning. Development 135(11): 1957-1967.

Logan CV, Cossins J, Rodriguez Cruz PM, Parry DA, Maxwell S, Martinez-Martinez P, Riepsaame J, Abdelhamed ZA, Lake AV, Moran M, Robb S, Chow G, Sewry C, Hopkins PM, Sheridan E, Jayawant S, Palace J, Johnson CA & Beeson D (2015) Congenital Myasthenic Syndrome Type 19 Is Caused by Mutations in COL13A1, Encoding the Atypical Non-fibrillar Collagen Type XIII alpha1 Chain. Am J Hum Genet 97: 878-885.

Long C, Amoasii L, Mireault AA, McAnally JR, Li H, Sanchez-Ortiz E, Bhattacharyya S, Shelton JM, Bassel-Duby R & Olson EN (2016) Postnatal genome editing partially restores dystrophin expression in a mouse model of muscular dystrophy. Science 351(6271): 400-403.

Lorenzoni PJ, Scola RH, Kay CS & Werneck LC (2012) Congenital myasthenic syndrome: a brief review. Pediatr Neurol 46(3): 141-148.

Lu J & Lichtman JW (2007) Imaging the neuromuscular junction over the past centuries. Sheng Li Xue Bao 59(6): 683-696.

Lwebuga-Mukasa JS, Lappi S & Taylor P (1976) Molecular forms of acetylcholinesterase from Torpedo californica: their relationship to synaptic membranes. Biochemistry 15(7): 1425-1434.

Määttä M, Väisänen T, Väisänen MR, Pihlajaniemi T & Tervo T (2006) Altered expression of type XIII collagen in keratoconus and scarred human cornea: Increased expression in scarred cornea is associated with myofibroblast transformation. Cornea 25(4): 448-453.

Mak AC, Tang PL, Cleveland C, Smith MH, Kari Connolly M, Katsumoto TR, Wolters PJ, Kwok PY & Criswell LA (2016) Brief Report: Whole-Exome Sequencing for Identification of Potential Causal Variants for Diffuse Cutaneous Systemic Sclerosis. Arthritis Rheumatol 68(9): 2257-2262.

Martin PT, Kaufman SJ, Kramer RH & Sanes JR (1996) Synaptic integrins in developing, adult, and mutant muscle: selective association of alpha1, alpha7A, and alpha7B integrins with the neuromuscular junction. Dev Biol 174(1): 125-139.

Mathew SJ, Hansen JM, Merrell AJ, Murphy MM, Lawson JA, Hutcheson DA, Hansen MS, Angus-Hill M & Kardon G (2011) Connective tissue fibroblasts and Tcf4 regulate myogenesis. Development 138(2): 371-384.

Mayer U, Saher G, Fassler R, Bornemann A, Echtermeyer F, von der Mark H, Miosge N, Poschl E & von der Mark K (1997) Absence of integrin alpha 7 causes a novel form of muscular dystrophy. Nat Genet 17(3): 318-323.

Mohseni P, Sung HK, Murphy AJ, Laliberte CL, Pallari HM, Henkelman M, Georgiou J, Xie G, Quaggin SE, Thorner PS, Eriksson JE & Nagy A (2011) Nestin is not essential for development of the CNS but required for dispersion of acetylcholine receptor clusters at the area of neuromuscular junctions. J Neurosci 31(32): 11547-11552.

Morris OC, Schebitz Walter K, Telemo E & Hintschich C (2016) Overexpression of collagen XIII in extraocular fat affected by active thyroid-associated ophthalmopathy: A crucial piece of the puzzle? Orbit 35(4): 227-232.

Mouw JK, Ou G & Weaver VM (2014) Extracellular matrix assembly: a multiscale deconstruction. Nat Rev Mol Cell Biol 15(12): 771-785.

Murphy MM, Lawson JA, Mathew SJ, Hutcheson DA & Kardon G (2011) Satellite cells, connective tissue fibroblasts and their interactions are crucial for muscle regeneration. Development 138(17): 3625-3637.

Myllyharju J & Kivirikko KI (2004) Collagens, modifying enzymes and their mutations in humans, flies and worms. Trends Genet 20(1): 33-43.

Nishimune H (2012) Molecular mechanism of active zone organization at vertebrate neuromuscular junctions. Mol Neurobiol 45(1): 1-16.

Nishimune H, Sanes JR & Carlson SS (2004) A synaptic laminin-calcium channel interaction organizes active zones in motor nerve terminals. Nature 432(7017): 580-587.

Nishimune H, Stanford JA & Mori Y (2014) Role of exercise in maintaining the integrity of the neuromuscular junction. Muscle Nerve 49(3): 315-324.

Nishimune H, Valdez G, Jarad G, Moulson CL, Muller U, Miner JH & Sanes JR (2008) Laminins promote postsynaptic maturation by an autocrine mechanism at the neuromuscular junction. J Cell Biol .

Nykvist P, Tu H, Ivaska J, Kapyla J, Pihlajaniemi T & Heino J (2000) Distinct recognition of collagen subtypes by alpha(1)beta(1) and alpha(2)beta(1) integrins. Alpha(1)beta(1) mediates cell adhesion to type XIII collagen. J Biol Chem 275(11): 8255-8261.

Oguri M, Kato K, Yokoi K, Yoshida T, Watanabe S, Metoki N, Yoshida H, Satoh K, Aoyagi Y, Nozawa Y & Yamada Y (2010) Assessment of a polymorphism of SDK1 with hypertension in Japanese Individuals. Am J Hypertens 23(1): 70-77.

Okada K, Inoue A, Okada M, Murata Y, Kakuta S, Jigami T, Kubo S, Shiraishi H, Eguchi K, Motomura M, Akiyama T, Iwakura Y, Higuchi O & Yamanashi Y (2006) The muscle protein Dok-7 is essential for neuromuscular synaptogenesis. Science 312(5781): 1802-1805.

Patton BL, Cunningham JM, Thyboll J, Kortesmaa J, Westerblad H, Edstrom L, Tryggvason K & Sanes JR (2001) Properly formed but improperly localized synaptic specializations in the absence of laminin alpha4. Nat Neurosci 4(6): 597-604.

Peltonen S, Hentula M, Hägg P, Yla-Outinen H, Tuukkanen J, Lakkakorpi J, Rehn M, Pihlajaniemi T & Peltonen J (1999) A novel component of epidermal cell-matrix and cell-cell contacts: transmembrane protein type XIII collagen. J Invest Dermatol 113(4): 635-642.

Peltonen S, Rehn M & Pihlajaniemi T (1997) Alternative splicing of mouse alpha1(XIII) collagen RNAs results in at least 17 different transcripts, predicting alpha1(XIII) collagen chains with length varying between 651 and 710 amino acid residues. DNA Cell Biol 16(2): 227-234.

Peng HB, Xie H, Rossi SG & Rotundo RL (1999) Acetylcholinesterase clustering at the neuromuscular junction involves perlecan and dystroglycan. J Cell Biol 145(4): 911-921.

Perlman RL (2016) Mouse models of human disease: An evolutionary perspective. Evol Med Public Health 2016(1): 170-176.

Perrot R & Eyer J (2009) Neuronal intermediate filaments and neurodegenerative disorders. Brain Res Bull 80(4-5): 282-295.

Pette D & Staron RS (2000) Myosin isoforms, muscle fiber types, and transitions. Microsc Res Tech 50(6): 500-509.

Pihlajaniemi T & Tamminen M (1990) The alpha 1 chain of type XIII collagen consists of three collagenous and four noncollagenous domains, and its primary transcript undergoes complex alternative splicing. J Biol Chem 265(28): 16922-16928.

Plomp JJ, Morsch M, Phillips WD & Verschuuren JJ (2015) Electrophysiological analysis of neuromuscular synaptic function in myasthenia gravis patients and animal models. Exp Neurol 270: 41-54.

Porter LF, Galli GG, Williamson S, Selley J, Knight D, Elcioglu N, Aydin A, Elcioglu M, Venselaar H, Lund AH, Bonshek R, Black GC & Manson FD (2015) A role for repressive complexes and H3K9 di-methylation in PRDM5-associated brittle cornea syndrome. Hum Mol Genet 24(23): 6565-6579.

Pratt SJ, Valencia AP, Le GK, Shah SB & Lovering RM (2015) Pre- and postsynaptic changes in the neuromuscular junction in dystrophic mice. Front Physiol 6: 252.

Punga AR & Ruegg MA (2012) Signaling and aging at the neuromuscular synapse: lessons learnt from neuromuscular diseases. Curr Opin Pharmacol 12(3): 340-346.

Raez MB, Hussain MS & Mohd-Yasin F (2006) Techniques of EMG signal analysis: detection, processing, classification and applications. Biol Proced Online 8: 11-35.

Ricard-Blum S (2011) The collagen family. Cold Spring Harb Perspect Biol 3(1): a004978.

Rodriguez Cruz PM, Palace J & Beeson D (2014) Inherited disorders of the neuromuscular junction: an update. J Neurol 261(11): 2234-2243.

Rogers RS & Nishimune H (2017) The role of laminins in the organization and function of neuromuscular junctions. Matrix Biol 57-58: 86-105.

Rooney JE, Welser JV, Dechert MA, Flintoff-Dye NL, Kaufman SJ & Burkin DJ (2006) Severe muscular dystrophy in mice that lack dystrophin and alpha7 integrin. J Cell Sci 119(Pt 11): 2185-2195.

Rosenthal N & Brown S (2007) The mouse ascending: perspectives for human-disease models. Nat Cell Biol 9(9): 993-999.

Ross JA, Webster RG, Lechertier T, Reynolds LE, Turmaine M, Bencze M, Jamshidi Y, Cetin H, Muntoni F, Beeson D, Hodilvala-Dilke K & Conti FJ (2017) Multiple roles of integrin-alpha3 at the neuromuscular junction. J Cell Sci 130(10): 1772-1784.

Sahli E & Gunduz K (2017) Thyroid-associated Ophthalmopathy. Turk J Ophthalmol 47(2): 94-105.

Sakai K & Miyazaki J (1997) A transgenic mouse line that retains Cre recombinase activity in mature oocytes irrespective of the cre transgene transmission. Biochem Biophys Res Commun 237(2): 318-324.

Samuel MA, Valdez G, Tapia JC, Lichtman JW & Sanes JR (2012) Agrin and synaptic laminin are required to maintain adult neuromuscular junctions. PLoS One 7(10): e46663.

Sandberg M, Tamminen M, Hirvonen H, Vuorio E & Pihlajaniemi T (1989) Expression of mRNAs coding for the alpha 1 chain of type XIII collagen in human fetal tissues: comparison with expression of mRNAs for collagen types I, II, and III. J Cell Biol 109(3): 1371-1379.

Sandberg-Lall M, Hagg PO, Wahlstrom I & Pihlajaniemi T (2000) Type XIII collagen is widely expressed in the adult and developing human eye and accentuated in the ciliary muscle, the optic nerve and the neural retina. Exp Eye Res 70(4): 401-410.

Sanes JR (2003) The basement membrane/basal lamina of skeletal muscle. J Biol Chem 278(15): 12601-12604.

Sanes JR & Lichtman JW (1999) Development of the vertebrate neuromuscular junction. Annu Rev Neurosci 22: 389-442.

Sanes JR & Lichtman JW (2001) Induction, assembly, maturation and maintenance of a postsynaptic apparatus. Nat Rev Neurosci 2(11): 791-805.

Schiaffino S & Reggiani C (2011) Fiber types in mammalian skeletal muscles. Physiol Rev 91(4): 1447-1531.

Schiaffino S, Rossi AC, Smerdu V, Leinwand LA & Reggiani C (2015) Developmental myosins: expression patterns and functional significance. Skelet Muscle 5: 22-015-0046-6. eCollection 2015.

Schwander M, Shirasaki R, Pfaff SL & Muller U (2004) Beta1 integrins in muscle, but not in motor neurons, are required for skeletal muscle innervation. J Neurosci 24(37): 8181-8191.

Schweitzer R, Zelzer E & Volk T (2010) Connecting muscles to tendons: tendons and musculoskeletal development in flies and vertebrates. Development 137(17): 2807-2817.

Serini G & Gabbiani G (1999) Mechanisms of myofibroblast activity and phenotypic modulation. Exp Cell Res 250(2): 273-283.

Sewry CA & Wallgren-Pettersson C (2017) Myopathology in congenital myopathies. Neuropathol Appl Neurobiol 43(1): 5-23.

Shang XR, Song JY, Liu FH, Ma J & Wang HJ (2015) GWAS-Identified Common Variants With Nonalcoholic Fatty Liver Disease in Chinese Children. J Pediatr Gastroenterol Nutr 60(5): 669-674.

Shen XM, Selcen D, Brengman J & Engel AG (2014) Mutant SNAP25B causes myasthenia, cortical hyperexcitability, ataxia, and intellectual disability. Neurology 83(24): 2247-2255.

Shi L, Fu AK & Ip NY (2012) Molecular mechanisms underlying maturation and maintenance of the vertebrate neuromuscular junction. Trends Neurosci 35(7): 441-453.

Shi Y, Ivannikov MV, Walsh ME, Liu Y, Zhang Y, Jaramillo CA, Macleod GT & Van Remmen H (2014) The lack of CuZnSOD leads to impaired neurotransmitter release, neuromuscular junction destabilization and reduced muscle strength in mice. PLoS One 9(6): e100834.

Shows TB, Tikka L, Byers MG, Eddy RL, Haley LL, Henry WM, Prockop DJ & Tryggvason K (1989) Assignment of the human collagen alpha 1 (XIII) chain gene (COL13A1) to the q22 region of chromosome 10. Genomics 5(1): 128-133.

Sigoillot SM, Bourgeois F, Karmouch J, Molgo J, Dobbertin A, Chevalier C, Houlgatte R, Leger J & Legay C (2016) Neuromuscular junction immaturity and muscle atrophy are hallmarks of the ColQ-deficient mouse, a model of congenital myasthenic syndrome with acetylcholinesterase deficiency. FASEB J 30(6): 2382-2399.

Sigoillot SM, Bourgeois F, Lambergeon M, Strochlic L & Legay C (2010) ColQ controls postsynaptic differentiation at the neuromuscular junction. J Neurosci 30(1): 13-23.

Singhal N & Martin PT (2011) Role of extracellular matrix proteins and their receptors in the development of the vertebrate neuromuscular junction. Dev Neurobiol 71(11): 982-1005.

Slater CR (2008) Structural factors influencing the efficacy of neuromuscular transmission. Ann N Y Acad Sci 1132: 1-12.

Slater CR (2015) The functional organization of motor nerve terminals. Prog Neurobiol 134: 55-103.

Snellman A, Keranen MR, Hägg PO, Lamberg A, Hiltunen JK, Kivirikko KI & Pihlajaniemi T (2000a) Type XIII collagen forms homotrimers with three triple helical collagenous domains and its association into disulfide-bonded trimers is enhanced by prolyl 4-hydroxylase. J Biol Chem 275(12): 8936-8944.

Snellman A, Tu H, Väisänen T, Kvist AP, Huhtala P & Pihlajaniemi T (2000b) A short sequence in the N-terminal region is required for the trimerization of type XIII collagen and is conserved in other collagenous transmembrane proteins. EMBO J 19(19): 5051-5059.

Souza PV, Batistella GN, Lino VC, Pinto WB, Annes M & Oliveira AS (2016) Clinical and genetic basis of congenital myasthenic syndromes. Arq Neuropsiquiatr 74(9): 750-760.

Spillane J, Beeson DJ & Kullmann DM (2010) Myasthenia and related disorders of the neuromuscular junction. J Neurol Neurosurg Psychiatry 81(8): 850-857.

Spivey KA, Banyard J, Solis LM, Wistuba II, Barletta JA, Gandhi L, Feldman HA, Rodig SJ, Chirieac LR & Zetter BR (2010) Collagen XXIII: a potential biomarker for the detection of primary and recurrent non-small cell lung cancer. Cancer Epidemiol Biomarkers Prev 19(5): 1362-1372.

Spivey KA, Chung I, Banyard J, Adini I, Feldman HA & Zetter BR (2012) A role for collagen XXIII in cancer cell adhesion, anchorage-independence and metastasis. Oncogene 31(18): 2362-2372.

Stalberg E (1980) Clinical electrophysiology in myasthenia gravis. J Neurol Neurosurg Psychiatry 43(7): 622-633.

Su J, Stenbjorn RS, Gorse K, Su K, Hauser KF, Ricard-Blum S, Pihlajaniemi T & Fox MA (2012) Target-derived matricryptins organize cerebellar synapse formation through alpha3beta1 integrins. Cell Rep 2(2): 223-230.

Subramanian A & Schilling TF (2015) Tendon development and musculoskeletal assembly: emerging roles for the extracellular matrix. Development 142(24): 4191-4204.

Sugiura Y, Chen F, Liu Y & Lin W (2011) Electrophysiological characterization of neuromuscular synaptic dysfunction in mice. Methods Mol Biol 793: 391-400.

Sugiura Y & Lin W (2011) Neuron-glia interactions: the roles of Schwann cells in neuromuscular synapse formation and function. Biosci Rep 31(5): 295-302.

Sund M, Väisänen T, Kaukinen S, Ilves M, Tu H, Autio-Harmainen H, Rauvala H & Pihlajaniemi T (2001a) Distinct expression of type XIII collagen in neuronal structures and other tissues during mouse development. Matrix Biol 20(4): 215-231.

Sund M, Ylönen R, Tuomisto A, Sormunen R, Tahkola J, Kvist AP, Kontusaari S, Autio-Harmainen H & Pihlajaniemi T (2001b) Abnormal adherence junctions in the heart and reduced angiogenesis in transgenic mice overexpressing mutant type XIII collagen. EMBO J 20(18): 5153-5164.

Sussman JL, Harel M, Frolow F, Varon L, Toker L, Futerman AH & Silman I (1988) Purification and crystallization of a dimeric form of acetylcholinesterase from Torpedo californica subsequent to solubilization with phosphatidylinositol-specific phospholipase C. J Mol Biol 203(3): 821-823.

Tahkola J, Rasanen J, Sund M, Makikallio K, Autio-Harmainen H & Pihlajaniemi T (2008) Cardiac dysfunction in transgenic mouse fetuses overexpressing shortened type XIII collagen. Cell Tissue Res 333(1): 61-69.

Tanaka T, Wakabayashi T, Oizumi H, Nishio S, Sato T, Harada A, Fujii D, Matsuo Y, Hashimoto T & Iwatsubo T (2014) CLAC-P/Collagen Type XXV Is Required for the Intramuscular Innervation of Motoneurons during Neuromuscular Development. J Neurosci 34(4): 1370-1379.

Theocharis AD, Skandalis SS, Gialeli C & Karamanos NK (2016) Extracellular matrix structure. Adv Drug Deliv Rev 97: 4-27.

Tikka L, Elomaa O, Pihlajaniemi T & Tryggvason K (1991) Human alpha 1 (XIII) collagen gene. Multiple forms of the gene transcripts are generated through complex alternative splicing of several short exons. J Biol Chem 266(26): 17713-17719.

Tintignac LA, Brenner HR & Ruegg MA (2015) Mechanisms Regulating Neuromuscular Junction Development and Function and Causes of Muscle Wasting. Physiol Rev 95(3): 809-852.

Tu H (2004) Type XIII collagen: structural and functional characterization of the ectodomain and identification of the binding ligands.

Tu H, Huhtala P, Lee HM, Adams JC & Pihlajaniemi T (2015) Membrane-associated collagens with interrupted triple-helices (MACITs): evolution from a bilaterian common ancestor and functional conservation in C. elegans. BMC Evol Biol 15(1): 281-015-0554-3.

Tu H, Sasaki T, Snellman A, Gohring W, Pirilä P, Timpl R & Pihlajaniemi T (2002) The type XIII collagen ectodomain is a 150-nm rod and capable of binding to fibronectin, nidogen-2, perlecan, and heparin. J Biol Chem 277(25): 23092-23099.

Tuomisto A, Sund M, Tahkola J, Latvanlehto A, Savolainen ER, Autio-Harmainen H, Liakka A, Sormunen R, Vuoristo J, West A, Lahesmaa R, Morse HC,3rd & Pihlajaniemi T (2008) A mutant collagen XIII alters intestinal expression of immune response genes and predisposes transgenic mice to develop B-cell lymphomas. Cancer Res 68(24): 10324-10332.

Vainzof M, Ayub-Guerrieri D, Onofre PC, Martins PC, Lopes VF, Zilberztajn D, Maia LS, Sell K & Yamamoto LU (2008) Animal models for genetic neuromuscular diseases. J Mol Neurosci 34(3): 241-248.

Väisänen MR, Väisänen T & Pihlajaniemi T (2004) The shed ectodomain of type XIII collagen affects cell behaviour in a matrix-dependent manner. Biochem J 380(Pt 3): 685-693.

Väisänen MR, Väisänen T, Tu H, Pirilä P, Sormunen R & Pihlajaniemi T (2006) The shed ectodomain of type XIII collagen associates with the fibrillar fibronectin matrix and may interfere with its assembly *in vitro*. Biochem J 393(Pt 1): 43-50.

Väisänen T, Väisänen MR, Autio-Harmainen H & Pihlajaniemi T (2005) Type XIII collagen expression is induced during malignant transformation in various epithelial and mesenchymal tumours. J Pathol 207(3): 324-335.

Vaittinen S, Lukka R, Sahlgren C, Rantanen J, Hurme T, Lendahl U, Eriksson JE & Kalimo H (1999) Specific and innervation-regulated expression of the intermediate filament protein nestin at neuromuscular and myotendinous junctions in skeletal muscle. Am J Pathol 154(2): 591-600.

Valdez G, Tapia JC, Kang H, Clemenson GD,Jr, Gage FH, Lichtman JW & Sanes JR (2010) Attenuation of age-related changes in mouse neuromuscular synapses by caloric restriction and exercise. Proc Natl Acad Sci U S A 107(33): 14863-14868.

Vaquer G, Riviere F, Mavris M, Bignami F, Llinares-Garcia J, Westermark K & Sepodes B (2013) Animal models for metabolic, neuromuscular and ophthalmological rare diseases. Nat Rev Drug Discov 12(4): 287-305.

Veit G, Zimina EP, Franzke CW, Kutsch S, Siebolds U, Gordon MK, Bruckner-Tuderman L & Koch M (2007) Shedding of collagen XXIII is mediated by furin and depends on the plasma membrane microenvironment. J Biol Chem 282(37): 27424-27435.

Veit G, Zwolanek D, Eckes B, Niland S, Kapyla J, Zweers MC, Ishada-Yamamoto A, Krieg T, Heino J, Eble JA & Koch M (2011) Collagen XXIII, novel ligand for integrin alpha2beta1 in the epidermis. J Biol Chem 286(31): 27804-27813.

Wang ZZ, Washabaugh CH, Yao Y, Wang JM, Zhang L, Ontell MP, Watkins SC, Rudnicki MA & Ontell M (2003) Aberrant development of motor axons and neuromuscular synapses in MyoD-null mice. J Neurosci 23(12): 5161-5169.

Watanabe H, Fujisawa T & Holstein TW (2009) Cnidarians and the evolutionary origin of the nervous system. Dev Growth Differ 51(3): 167-183.

Weatherbee SD, Anderson KV & Niswander LA (2006) LDL-receptor-related protein 4 is crucial for formation of the neuromuscular junction. Development 133(24): 4993-5000.

Welser JV, Rooney JE, Cohen NC, Gurpur PB, Singer CA, Evans RA, Haines BA & Burkin DJ (2009) Myotendinous junction defects and reduced force transmission in mice that lack alpha7 integrin and utrophin. Am J Pathol 175(4): 1545-1554.

Wu H, Xiong WC & Mei L (2010) To build a synapse: signaling pathways in neuromuscular junction assembly. Development 137(7): 1017-1033.

Xiao Q, Hu X, Wei Z & Tam KY (2016) Cytoskeleton Molecular Motors: Structures and Their Functions in Neuron. Int J Biol Sci 12(9): 1083-1092.

Xie W, Stribley JA, Chatonnet A, Wilder PJ, Rizzino A, McComb RD, Taylor P, Hinrichs SH & Lockridge O (2000) Postnatal developmental delay and supersensitivity to organophosphate in gene-targeted mice lacking acetylcholinesterase. J Pharmacol Exp Ther 293(3): 896-902.

Yang Y, Coleman M, Zhang L, Zheng X & Yue Z (2013) Autophagy in axonal and dendritic degeneration. Trends Neurosci 36(7): 418-428.

Ylönen R, Kyrönlahti T, Sund M, Ilves M, Lehenkari P, Tuukkanen J & Pihlajaniemi T (2005) Type XIII collagen strongly affects bone formation in transgenic mice. J Bone Miner Res 20(8): 1381-1393.

Yoshida T, Kato K, Yokoi K, Oguri M, Watanabe S, Metoki N, Yoshida H, Satoh K, Aoyagi Y, Nozawa Y & Yamada Y (2010) Association of genetic variants with hemorrhagic stroke in Japanese individuals. Int J Mol Med 25(4): 649-656.

Yumoto N, Kim N & Burden SJ (2012) Lrp4 is a retrograde signal for presynaptic differentiation at neuromuscular synapses. Nature 489(7416): 438-442.

Yurchenco PD (2011) Basement membranes: cell scaffoldings and signaling platforms. Cold Spring Harb Perspect Biol 3(2): 10.1101/cshperspect.a004911.

Zeltz C & Gullberg D (2016) The integrin-collagen connection - a glue for tissue repair? J Cell Sci 129(6): 1284.

Original publications

I Härönen H, Zainul Z, Tu H, Naumenko N, Sormunen R, Miinalainen I, Shakirzyanova A, Oikarainen T, Abdullin A, Martin P, Santoleri S, Koistinaho J, Silman I, Giniatullin R, Fox M. A, Heikkinen A, Pihlajaniemi T (2017) Collagen XIII secures pre- and postsynaptic integrity of the neuromuscular synapse. Hum. Mol. Gen. 1;26(11):2076-2090

II Härönen H, Zainul Z, Naumenko N, Sormunen R, Miinalainen I, Shakirzyanova A, Santoleri S, Giniatullin R, Pihlajaniemi T, Heikkinen A. Correct expression and localization of collagen XIII is crucial for the normal formation and function of the neuromuscular system. Manuscript.

Original publications are not included in the electronic version of the dissertation.

1432. Vihanninjoki, Kyösti (2017) The Heidelberg Retina Tomograph in the diagnosis of glaucoma

1433. Männistö, Jaana (2017) The effects of termination of pregnancy on future reproduction

1434. Hulkko, Anja (2017) The association of lifetime antipsychotic and other psychiatric medications with cognition in schizophrenia : the Northern Finland Birth Cohort 1966 Study

1435. Ramsay, Hugh (2017) Predictors of psychosis risk and neurocognitive deficits

1436. Kuitunen, Hanne (2017) DLBCL, primary and secondary central nervous system involvement, treatment and prophylaxis

1437. Filatova, Svetlana (2017) Incidence of schizophrenia and associations of schizophrenia and schizotypy with early motor developmental milestones

1438. Käräjämäki, Aki (2017) Non-alcoholic fatty liver disease (NAFLD) : perspectives to etiology, complications and lipid metabolism

1439. Mikkola, Reija (2017) Determinants and clinical implications of bleeding related to coronary artery bypass surgery

1440. Hagnäs, Magnus (2018) The association of cardiorespiratory fitness, physical activity and ischemic ECG findings with coronary heart disease-related deaths among men

1441. Huhtaniska, Sanna (2018) The association between antipsychotic and benzodiazepine use with brain morphology and its changes in schizophrenia

1442. Sundquist, Elias (2018) The role of tumor microenvironment on oral tongue cancer invasion and prognosis

1443. Keto, Jaana (2018) The middle-aged smoker in health care : primary health care use, cardiovascular risk factors, and physician's help in quitting

1444. Tiisanoja, Antti (2018) Sedative load and oral health among community-dwelling older people

1445. Alaraudanjoki, Viivi (2018) Erosive tooth wear and associated factors in Northern Finland Birth Cohort 1966

1446. Sinikumpu, Suvi-Päivikki (2018) Skin diseases and their association with systemic diseases in the Northern Finland Birth Cohort 1966

1447. Nortunen, Simo (2018) Stability assessment of isolated lateral malleolar supination-external rotation-type ankle fractures

Book orders:
Granum: Virtual book store
http://granum.uta.fi/granum/

UNIVERSITY OF OULU P.O. Box 8000 FI-90014 UNIVERSITY OF OULU FINLAND

ACTA UNIVERSITATIS OULUENSIS

UNIVERSITY of OULU
OULUN YLIOPISTO

ISBN 978-952-62-1800-7 (Paperback)
ISBN 978-952-62-1801-4 (PDF)
ISSN 0355-3221 (Print)
ISSN 1796-2234 (Online)